Continuous Robotic Filament Winding for Tensile Applications

Reducing the material usage by creating an interaction based connection

Master Thesis

Lars de Vries

Delft University of Technology

Continuous Robotic Filament Winding for Tensile Applications

Reducing the material usage by creating an interaction based connection

by

Lars de Vries

Chair:	Dr. Roel Schipper	Delft university of technology
Committee member:	Dr. Stijn Brancart	Delft university of technology
Guidance:	Dr. Robin Oval	École nationale des ponts et chaussées
	Dr. Mariana Popescu	Massachusetts Institute of Technology

Project Duration:	November, 2024 - Oktober, 2025
Faculty:	Faculty of Civil engineering, Delft

Cover: Robotic winding setup
Style: TU Delft Report Style, with modifications by Daan Zwaneveld

Preface

What began as a curiosity about parametric design became my research over the past year. This thesis marks the end of the master's degree at the Delft University of Technology. I had the opportunity to explore a novel approach to filament winding techniques, creating an interaction-based system. This allowed me to explore and test a new method, including the creation of prototypes to evaluate whether the design guidelines and setup worked.

I could not have done this without all my supervisors. Starting with Robin Oval, who helped me especially in the beginning by forming the roadmap of this research and explaining the possibilities in an abstract field of research. After the plan was mapped out, Roel Schipper provided valuable support in structuring the report and improving its readability. I am glad that I could drop by both daily supervisors to help me with all kinds of problems that occurred during the research. Furthermore, I would like to thank Mariana Popescu and Stijn Brancart for being available when needed and providing feedback during my master's thesis.

Besides my supervisors, there are more people relevant to this research. I would like to especially thank Hugo Schravesande for helping me with transforming the designs into working prototypes. Moreover, I would like to thank everyone who gave feedback on the report or with whom I discussed certain aspects of the research. Finally, artificial intelligence was used to check this document in British spelling and grammar.

Lars de Vries
Delft, October 2025

Abstract

With the rising urgency of building more sustainably and emitting less carbon dioxide into the atmosphere, optimising material use is becoming increasingly relevant. Globally, the civil engineering sector contributes to 8 % of total CO_2 emissions through cement production. In addition to reinforced concrete, it is estimated that 40 % of these emissions originate from steel reinforcement. By optimising reinforced concrete elements, material waste can be reduced by up to 40 %, while still meeting the required strength capacity. Due to the use of standard-sized steel bars and conservative detailing, this often results in significant oversizing of reinforcement. However, optimising reinforcement requires a change from using standardised steel reinforcement bars, mats, and cages towards long filament fibres. For example, when reviewing floors or walls with an open space, such as a door opening, around these locations the reinforcement net cannot continue its path, and the reinforcement needs to be strengthened locally. In these cases, the long filament fibres are capable of being placed in less fixed shapes and can be adjusted on a local scale to improve the strength. These filaments can be made from impregnated glass or carbon fibres, which harden over time.

Besides reducing the oversizing of steel, filament winding could also be made interaction-based, meaning that the winding is not limited to a fixed scaffolding point but can also intertwine with earlier wound filaments, reducing the material of these scaffolding elements. This led to the central question: *How can material usage be reduced in both the filament and the scaffolding by using a construction process of continuous robotic winding?* This research focuses on the topology and sequencing of tensile wound structures using automated robotic filament winding with a nylon rope. This study introduces a novel approach to filament winding by changing rope intersections into functional support points, replacing the need for traditional fixed scaffolding.

To create interactions, the separate winding layers must be connected to each other. This is achieved by transforming the concept of Reidemeister moves from knot theory into either back-and-forth or looped connections. To allow interactions to become connections, the 2D winding plane is combined with a 3D workspace. Additionally, scaling up the external scaffolding increases the number of possible intersection points that can be used to form interactions. In this research, scaffolding does not refer to the conventional way of supporting a structure, but the term is used to indicate fixed attachment points around which the fibre can be wound. These scaffolding supports are used to allow the wound structure to be created, but the shape of these supports can differ for each setup.

The research first identifies the design guidelines needed to create an interaction-based winding system. First of all, repeating patterns must be avoided, as they act like pulley systems and relocate nodes unpredictably. It is recommended to wind perpendicular to a single spanned rope, allowing a margin of 10 degrees. This prevents the nylon rope, which is used during this research, from sliding off and creating undesired topologies. Furthermore, connections help resist nodal movement and ensure all ropes are integrated into the interaction. For the winding sequence, it is preferable to begin winding between fixed supports to build resistance in the system before introducing interaction-based knots. Finally, straight-line winding is preferred over angled winding between fixed supports. Using these guidelines, a final design was developed based on a certain topology with spanned ropes. This reduced the number of scaffolding supports by 33 %, from 12 to 8, while keeping the same topology. In contrast, the rope length increased by only 2 %, from 6.42 m to 6.56 m. Another key observation is the nodal displacement in the interaction-based system. The average vector deviation amounted to 1.6 cm, which is 6.3 % of the distance between the supports. An additional winding resulted in a slight deviation, meaning that the system becomes stiffer and the nodes begin to behave like fixed supports.

In conclusion, the use of interaction-based methods enables a reduction in scaffolding material by replacing internal supports with rope intersections. Although this approach results in a slight increase in filament length, the difference is minimal. By minimising nodal displacement and improving the autonomy of the robotic arm to avoid collisions, continuous filament winding has significant potential to be applied effectively to non-fixed support setups based on interactions.

Contents

List of Figures

List of Tables

Nomenclature

The nomenclature is used to provide the definition of words, which will be used within this research.

List of definition

Term	Explanation
Autonomous process	Without human interference during the process
Centre point	The geometric centre of the grid layout
Connection	A method used to join ropes together
Continuous winding	One long fibre wound without interruptions
Coreless winding	Winding between discrete points in space without a solid core
Filament	A long fibre material which will be wound around the supports (carbon, glass or bio-fibres)
Fixed support	A scaffolding point at a fixed location
Interaction	Two ropes creating a connection
Intersection	Two ropes cross paths
Knot	Tangling or tying something together
Middle point	The midpoint of a rope connection
Node	Any point within the grid
Non-fixed support	An interaction point created by at least two ropes
Scaffolding	Construction parts used during the winding process
Spanned rope	Earlier wound ropes in the system
Support	A scaffolding point to wound rope around
Topology	The connectivity how the design should look like

1 Introduction

The introduction will be used to provide context for this research. It will start by explaining the relevance of change within the manufacturing of reinforced concrete by using fibres instead of conventional steel reinforcement. In addition, the filament winding process will be explained, followed by some filament-built structures, ending with the possibilities of change within the conventional way of using reinforcement in concrete.

1.1. Reinforced Concrete in Constructions

The construction industry has a long-standing tradition of building structures using conventional methods, in which reinforced concrete is a commonly used material. While reinforced concrete has proven to be a reliable and durable solution, it also has significant environmental drawbacks. Globally, the civil engineering sector contributes approximately 8% of total carbon emissions through cement production [16]. Furthermore, ”The amount of CO_2 emissions that construction can influence is significant, accounting for almost 47% of total CO_2 emissions of the UK” [28].

On the other hand, ”The fluidity of concrete offers the opportunity to economically create structures of almost any shape, yet reinforced concrete structures are rarely optimised and, as a result, as much as 40% of the concrete in a typical building can be wasted” [21]. By optimising the reinforced concrete element, including the casting moulds, material waste can be reduced by up to 40%, while still meeting the required strength capacity according to design standards [12].

1.2. Oversizing in Reinforcement

It is estimated that 40% of emissions originate from steel reinforcement, with the remaining 60% attributed to the concrete itself [13]. Steel reinforcement, in particular, has a major impact on total emissions. The lack of structural optimisation frequently leads to excessive material use. In reinforced concrete specifically, the use of standard-size steel bars and conservative detailing often results in gross oversizing of reinforcement [21]. This inefficiency could be addressed through the use of strut-and-tie models, which can guide the layout of tensile reinforcement more effectively across various structural elements [14]. Conventional reinforcement encounters several ”problems” in terms of material efficiency, which are shown in Figure 1.1. For instance, when a door opening or floor saving is created, a lot of extra reinforcement is used around these empty spaces to guarantee the strength, given the standardised shapes and sizes of both the reinforcement bars and nets. This also occurs in column-based buildings like parking garages, where, for example, a radial layout could be interesting to explore to resist the punching shear. All these patterns and sizes should be optimised to reduce the material waste of overdesigning.

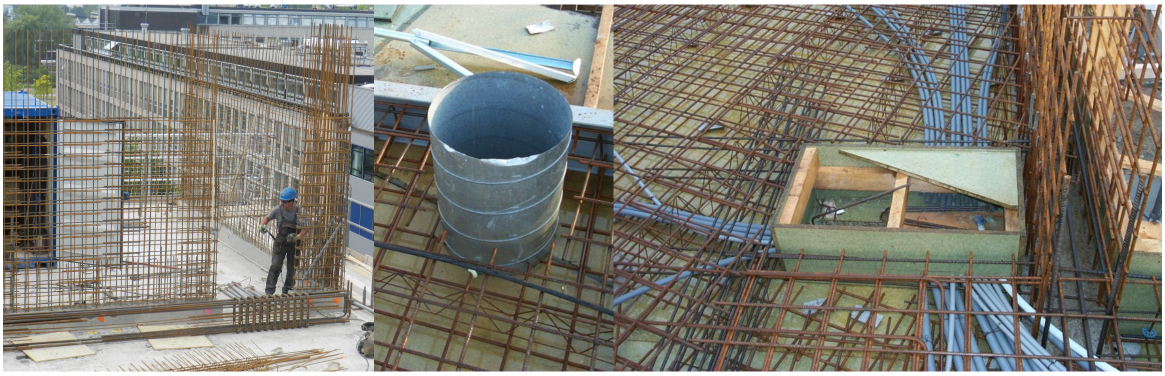

(a) Door opening **(b)** Ventilation pipe **(c)** Floor saving

Figure 1.1: Different examples of placed reinforcement

”However, these optimised layouts are not affordable, or even feasible, without significant post-rationalisation to build such reinforcement from stiff bar elements. Extreme rationalisation resorts to the use of standardised reinforcement bars, mats, and cages, which require a higher amount of material and energy to produce. Therefore, deviating from standardised steel reinforcement sizes leads to increased costs. However, the use of advanced fabrication strategies and additive manufacturing, combined with robotics, provides an opportunity to automate the fabrication of complex optimised layouts of reinforced concrete structures using flexible filament materials” [14].

By using both long filament fibres and an automated process, these costs can be reduced, making it an attractive method for manufacturing new reinforcement for concrete elements. Furthermore, combining long-filament and short-fibre reinforcement can provide the required material properties. Whereas short fibres are directly added to the concrete mix, long filaments require specific fabrication strategies [13]. Given the pressing challenges to reduce rising greenhouse gas emissions, alongside sustainability goals set by the United Nations, it is essential to critically evaluate conventional construction practices and explore opportunities for optimisation. This is especially relevant in light of the growing demand for more sustainable and structurally complex buildings.

1.3. Filament Winding

Currently, these optimised layouts are not widely used because the associated costs are higher than those of oversizing. This is due to both labour and material constraints. Steel reinforcement bars are mostly available in standard sizes, and as designs become more complex, reinforcement workers require more time to assemble the reinforcement, increasing both labour costs and project duration. On the other hand, by automating the filament winding process, robotic arms can operate continuously, 24 hours a day, taking over the tasks traditionally performed by reinforcement workers. As a result, the role of these workers would shift from manual placement to overseeing and managing the automated process.

Furthermore, filament winding presents considerable potential to reduce material overuse by enabling more efficient layouts. Traditional steel reinforcement often exhibits oversizing rates between 300% and 450%, whereas filament reinforcement typically has oversizing rates between 20% and 30%. Despite this, the impact-to-performance ratio of steel and carbon fibres is quite similar, measured respectively at 4.6×10^{-3} kgCO_2e/kg/MPa for steel and 4.8×10^{-3} kgCO_2e/kg/MPa for carbon fibres [13]. The structural strength of the fibre can be tailored by weaving it back and forth multiple times, increasing the number of strands between the same nodes, whereas steel reinforcement bars are less flexible in size. These fibres are supplied from a coil, allowing continuous delivery throughout the process and reducing cut-off waste. In addition, fibre-reinforced concrete is already gaining popularity and is being used in shotcrete for tunnel linings [8]. In conclusion, reinforced concrete could be replaced by continuous filament winding using robotic arms, offering a more efficient and potentially more sustainable approach to construction.

1.3.1. Filament Winding Materials

Before the filament can be used, it must be prepared, as shown in Figure 1.2. The process begins with the (composite) fibre creels, which are guided to the tensioning system (A, B, C). After the fibres are placed under tension, they are directed via a roller system to the resin bath (D, E, F). Once the fibres have passed through the resin bath, they are bundled together and prepared for use (G, H, I). These can, for example, be used to create pressure tanks by winding the fibre around a mandrel (J). In addition to the resin bath method (wet winding), it is also possible to use either dry winding, where the fibre is cured in an oven to gain strength, or a pre-impregnated fibre [30]. Both methods begin with a fibre that behaves like a string and displaces under an applied force. Once the resin has dried, or the fibres have been cured in the oven, the material becomes hardened, enabling it to carry compressive forces.

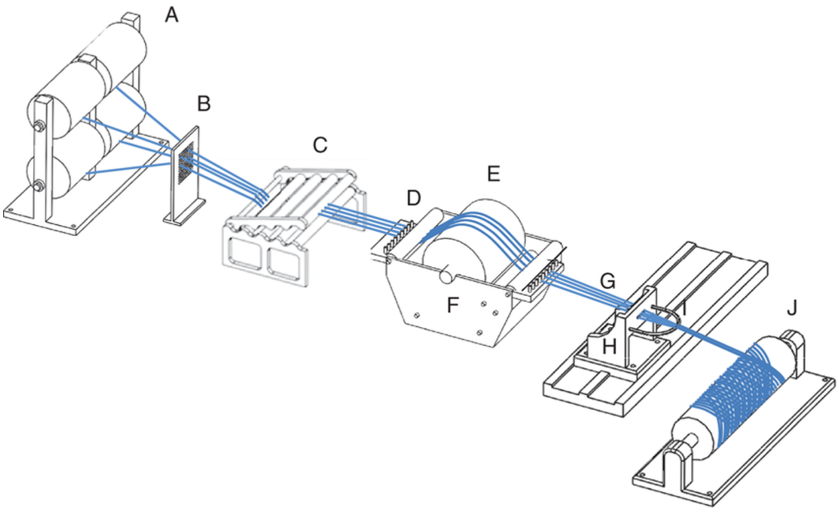

Figure 1.2: Schematic illustration of the conventional wet filament winding process [15]

A wide range of materials can be used as fibres, including carbon, aramid (Kevlar), and glass fibre-reinforced polymers (C/GFRP), as well as biofibres. C/GFRP is often combined with a specific resin. The material properties of these fibres have been explored in several research papers [21, 18, 5, 10, 1]. Biofibres, such as flax fibres, represent a relatively new class of materials with the potential to replace synthetic fibres due to their sustainable characteristics. However, further research is ongoing to fully confirm their potential.

1.3.2. Winding Process

In the process of transitioning from concept to construction, several intermediate steps are required as displayed in Figure 1.3 [21, 18, 5]. Although there are several ways to manufacture these construction using filament fibres, only the workflow for robotic filament winding is shown. This workflow is typically divided into multiple phases [14, 13], incorporating fabrication-informed optimisation and rationalisation.

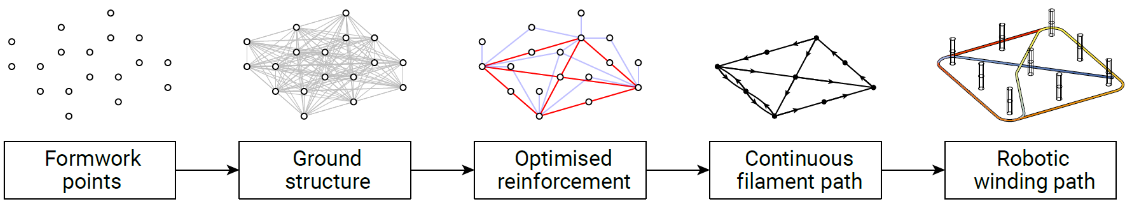

Figure 1.3: Long filament winding workpath [14]

The process begins with identifying the winding points within the framework system, in combination with the desired topology. These winding points refer to the fixed supports around which the rope can be wound, which may also be referred to as scaffolding. Once these points are established, a ground structure is generated by evaluating all possible connections between the support locations, representing all admissible winding passes and rope interactions. The next step is to optimise the layout of this ground structure. This can involve several strategies, such as minimising the total rope length, reducing the number of support interactions, or applying a strut-and-tie approach to ensure structural adequacy under loading conditions. In many cases, a combination of these criteria is used to generate an efficient and fabricable solution.

Once the layout is defined, the tensile paths are rationalised for continuous robotic filament winding. This involves creating a continuous path through Eulerisation of the graph, ensuring that every intermediate node has both an entry and exit, effectively enabling uninterrupted winding. In theory, this results would create an Eulerian circuit, a closed loop that visits every rope segment (edge) exactly once. If the original layout does not permit such a path, certain edges are duplicated to satisfy the even degree condition at each node. The winding sequence should also consider alternating winding directions (for example, clockwise followed by counterclockwise) and ensure that the rope winds around a support to avoid both material build-up and collisions while maintain geometric balance.

Following the definition of the winding path, a trajectory is generated for the robotic system to execute. This trajectory must account for the geometry of the formwork and support elements to avoid clashes and allow consistent fibre placement [6]. Software tools that can be used in this step include Rhino with the Grasshopper, Hal robotics, Karamba3D, or BATS plug-in/extension, and Python-based platforms [3, 32, 20].

1.4. Structures

In addition to its application in reinforcement, the method of filament winding can also be used to create entire structures. This is due to the ability of the material to withstand both tension and compression once it is cured. Throughout history, various projects have laid the groundwork for understanding the structural behaviour of these constructions.

Figure 1.4: Olympic Stadium in Munich (1)

A notable example is the design of the Olympic Stadium in Munich (Figure 1.4 & 1.5), constructed for the 1972 Summer Olympics. Architect Günter Behnisch and structural designer Frei Otto developed a landmark tensile structure that harmonised with the surrounding landscape. A minimal surface form-finding method was used to create a tensile canopy that appears to float above the stadium. The canopy structure consists of steel cables anchored to tall pylons, which handle the compressive and bending forces by transferring them to the foundation. This enabled the designers to span large areas both efficiently and elegantly [20]. The tensile forces in the canopy are managed by the steel cables spanning between anchor points, while PVC-coated polyester panels fixed to the cable network complete the enclosure [4, 11]. This structure illustrates the effective use of form and material to combine compression and tension in an integrated system.

Figure 1.5: Olympic Stadium in Munich (2) [31][1]

Recent developments in Filament winding techniques have already led to the construction of several built structures. One of the first large-scale prototypes was the BUGA Fibre Pavilion, which was temporarily located at the Federal Garden Show (BUGA) in Heilbronn, Germany. This pavilion utilised a fibre winding technique to fabricate its structural elements, allowing composite components to act as load-bearing elements. These components are fabricated using coreless filament winding. This is a technique where fibre filaments (impregnated with resin) are wound freely between two scaffolds by a robotic arm. These scaffolding could either be fixed or rotate depending on the needs. In the contrary, coreless fibre winding does not make use of something to wind around, like a mandrel. The coreless winding techinique allows the structure be be build using less materials and be more flexible within the creation of a structural element.

[1]This source only hold for the most right picture

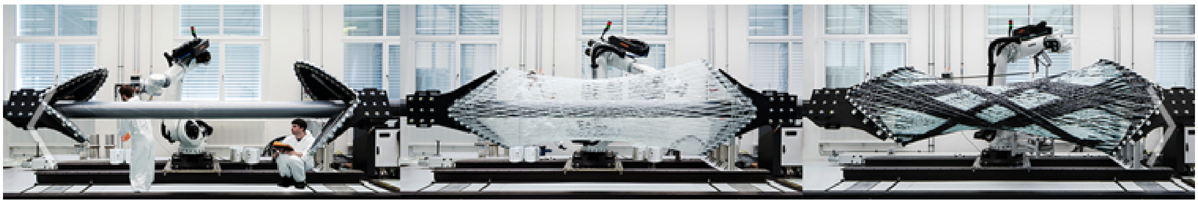

Figure 1.6: Winding an element for the BUGA Fibre Pavilion [25]

The structural elements of the BUGA Pavilion were made from carbon and glass fibre-reinforced plastics. Figure 1.6 shows the winding of an element, where Figure 1.7 shows the structure. These elements were capable of withstanding tension, compression and bending forces. This represented a significant shift from earlier structural concepts, which often used nets suspended across intermediate supports to carry loads. In contrast, these wound components were fabricated by laying fibres between metal end-pieces. Once wound, the fibres were impregnated with a thermoset resin and cured in an oven to achieve the required structural performance. “The most prominent advantage resulting from this is a low weight per built floor area that is roughly estimated to be five times lighter than conventional steel structures with a similar span” [10].

Figure 1.7: BUGA Fibre Pavilion [25]

A second example is the Maison Fibre project, which explored multi-storey construction using hybrid slabs made from fibre-polymer composites and laminated veneer lumber (Figure 1.8). The fibres in this system were used to redirect internal forces to the perimeter of the slab, allowing the thickness of the glued timber to be reduced and optimising overall material use [5]. This demonstrated the potential of filament winding in applications based on 2D geometries.

Figure 1.8: Maison Fibre [24]

Figure 1.9: LivMatS Pavilion [23]

The third project is the LivMatS Pavilion, which is the first building to use a fully load-bearing structure made entirely from robotically wound flax fibre (Figure 1.9). The choice of flax, which is a natural, fully renewable, and regionally sourced material in Central Europe, introduces a highly sustainable alternative to synthetic fibres [23].

Together, these three projects illustrate the technical viability and growing potential of filament winding in structural applications. The BUGA Pavilion demonstrated the feasibility of using winding to form structural elements; Maison Fibre proved its applicability in planar 2D construction; and the LivMatS Pavilion highlighted the potential of using sustainable, bio-based materials in place of conventional carbon and glass fibres [5].

1.5. Weaving Change into Concrete Logic

Filament winding is becoming increasingly relevant in the field of digital fabrication. It enables the creation of complex geometries while aiming to optimise the material-to-strength ratio. In particular, the precision of robotic arms allows for the fabrication of intricate shapes directly from digital design tools, enabling more efficient and custom-tailored structural solutions.

Filaments and long fibres have already proven effective in industries such as automotive, or aviation manufacturing processes. Their application in the construction industry could reduce material waste by minimising the oversizing of concrete reinforcement or by improving material efficiency in long-span structures [5]. In addition, the construction of such structures often requires significant amounts of scaffolding. This process involves considerable time and material use, whereas the use of rope intersection points within a wound structure remains largely unexplored. Beside reducing the material waste, by creating connections through fibre interactions the need for scaffolding could be reduced and structural autonomy during construction will be increased.

Fibre winding also offers the potential to replace traditional steel reinforcement and reduce reinforcement waste through improved efficiency [14, 21]. Robotic filament winding supports this transition by allowing continuous operation, eliminating manual assembly time, and improving consistency. Furthermore, using materials such as carbon and glass fibres allow the conventional steel reinforcement to be replaced. Moreover, bio-fibre filament has the potential to become a more environmentally friendly alternative compared to the other fibres. Companies are already showcasing the use of this technology in applications such as beams, trusses, pressure vessels, pipe fittings, and car parking canopies [2].

The filament winding method is already integrated into various industries. However, optimising the process, by reducing the dependency on scaffolding and improving material efficiency, can significantly boost construction sustainability. This research is particularly relevant due to its potential to lower environmental impact through better material use, both in the final design and throughout the prototyping phase [14].

2
Research problem

This chapter is used to state the main research question, including the sub-questions. In addition, the objective and the scope are stated, including the boundaries of the research, which will make sure the research keeps focus on the main goal.

2.1. Research Question

The main research question is:

> *How can material usage be reduced in both the filament and the scaffolding by using a construction process of continuous robotic winding?*

To answer this question, the research is divided into three sub-questions, focusing on the strategy, mechanical guidelines, and path creation for these topologies:

1. In what way can coreless winding techniques reduce the need for scaffolding?
2. Which considerations need to be taken into account when creating interaction-based windings around non-fixed support points?
3. How can the robotic path be planned to create tensile filament winding geometries?

2.2. Research Objectives

This research project aims to explore a novel approach to robotic filament winding, striving for optimal patterns leading to a minimisation of scaffolding. To achieve this, a way of interaction-based windings with already spanned filament will be considered, combining it with a robotic trajectory. All considerations will be performed and tested, making use of prototypes to validate the research.

2.3. Research Scope

Within the scope, some limitations and descriptions will be clarified. To start with the scaffolding, which could be seen as some kind of support to keep the wound materials in place where they are meant to stay. By aiming to use an interaction-based method, these supports might become unnecessary because the tensile material will stay in the desired topology even without the use of a support. This should result in a reduction of the scaffolding, leading to less material used within the total construction process. In this research, scaffolding does not refer to the conventional way of supporting a structure, but the term is used to indicate fixed attachment points around which the fibre can be wound. These scaffolding supports are used to allow the wound structure to be created. It can be compared with a tennis racket. Without the frame, the fibres cannot be wound in tension and stay in place. This frame acts as scaffolding for the fibres to be supported. Although these supports (scaffolding points) can be designed in different shapes depending on the design, the main goal is to keep the wound filament in the predetermined fixed position.

Because the research focuses mainly on topology and sequence, it was decided to limit the study to the winding process specifically, the step of moving from a given topology towards a sequence that defines the path for the robotic arm. This was done with the aim of investigating the potential of interactions. To ensure that material waste is kept to a minimum and that all safety aspects are considered, the material was simplified to a nylon rope with a diameter of 1 mm. This rope is expected to behave in a similar way to long filament fibres, because after winding, these filament fibres initially behave flexibly, assumed to behave comparably with the selected rope. The key difference arises later in the process, when carbon and glass fibres gradually stiffen due to chemical curing, eventually becoming capable of withstanding compressive forces. In contrast, the rope remains flexible and does not undergo this transformation. The rope can therefore replace the filament (before curing), as both materials behave in the same way in terms of flexibility. In addition, the diameter of the long filament strands determines the permissible corner radius, although this can be adjusted depending on the required specifications, allowing it to loop around an earlier wound rope.

Furthermore, the form-finding methods will be presented in the research but are left out of the design process. This is because creating the interaction between the fibres is the first step needed to reduce the scaffolding. Once the interactions are established, new equilibriums occur, which depend on the created connections between the filaments. Due to time limitations, investigating these interactions by means of connections became the main priority. This resulted in the fact that coordinate predictions using form-finding methods remain a topic for future exploration.

Finally, limited sizes should be used for the prototypes. The work field is bounded by the robotic arm, which could reach all locations with its full potential within a range of 0.5 m × 0.5 m from where the robotic arm is attached to the workspace. The full potential means that it has six degrees of freedom in terms of rotations of the arm. The tip of the winding tool has three degrees of freedom in translations and three in rotation. Beyond these distances, the robotic arm reaches its limitations within the degree of freedom for its movement, meaning that not all movements can be made. Depending on the necessary movements, some points can be reached with fewer degrees of freedom in the robotic arm. This robotic arm also has a limited weight capacity of five kilograms. In addition, only one arm will be available for prototyping, limiting both the options of enlarging the reach and passing the fibre from one arm to the arm of a second robot.

2.4. Roadmap of the Report

The report consists of several chapters, each building towards the development and evaluation of an interaction-based filament winding method. It begins with a section on graphical conventions and definitions that are frequently used throughout the report to make the document easier to follow (Chapter 3). This is followed by a vision centred on reducing material use during automated robotic manufacturing, from which the concept of creating interactions is introduced as a potential solution (Chapter 4). The potential of connections is then described, alongside an exploration of possible concepts for achieving them (Chapter 5). Once a suitable method of connecting the materials is identified, both the software to generate the robotic trajectory and the hardware for winding the rope around the setup are developed (Chapter 6). The next stage focuses on testing boundary conditions and evaluating which approaches work best, leading to the formulation of a final design (Chapter 7). This final design is then used to compare the current practice of winding with the newly developed interaction-based method. Finally, the two approaches are assessed in the discussion and conclusion chapters, which also present recommendations and suggestions for future research (Chapters 8, 9 & 10).

3

Graphical Conventions and Definitions

This chapter before reading the report is to explain how certain figures are created and some definitions will be explained both in words and by giving an example

In general, most figures are set up in the same way. They are created within a frame consisting of several lines. There are two types of line styles used: a solid line and a dotted line. These indicate the position of the rope. When both line styles are present, the solid line represents the rope in the foreground, while the dotted line indicates a rope placed behind. Occasionally, a dotted grey line refers to an earlier wound rope. Colours are used to help understanding the sequence of wound ropes. When several lines are present, it may be unclear which direction the rope continues. In such cases, the colour should be followed. For example, an arrow will end at another arrow of the same colour, or the rope may change colour during the process to indicate that the sequence continues with a distinct colour.

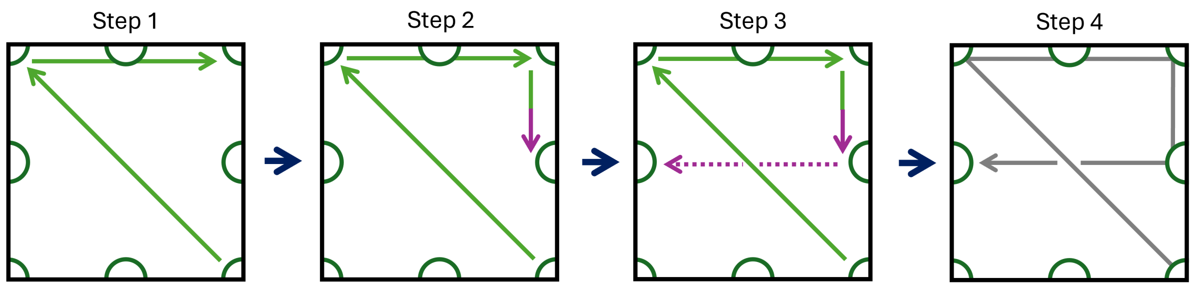

Figure 3.1: Explanation of the stepwise view of self created figures

Finally, the sequence itself can be important. It is shown by placing several images next to each other, representing small steps. This makes the steps easier to follow. This method is illustrated in Figure 3.1. Step 1 shows the first part of the rope being wound. In step 2, the rope continues, but in the image, the rope changes colour (from green to purple). This change helps to visualise the winding sequence. Step 3 continues the same rope but passes underneath an already cast rope (shown as a dotted line), indicating depth in a 2D representation. Step 4 shows the final wound rope, which represents the completed result. These four steps form a sequence demonstrating how the winding is carried out. The actual winding is shown in Figure 3.2

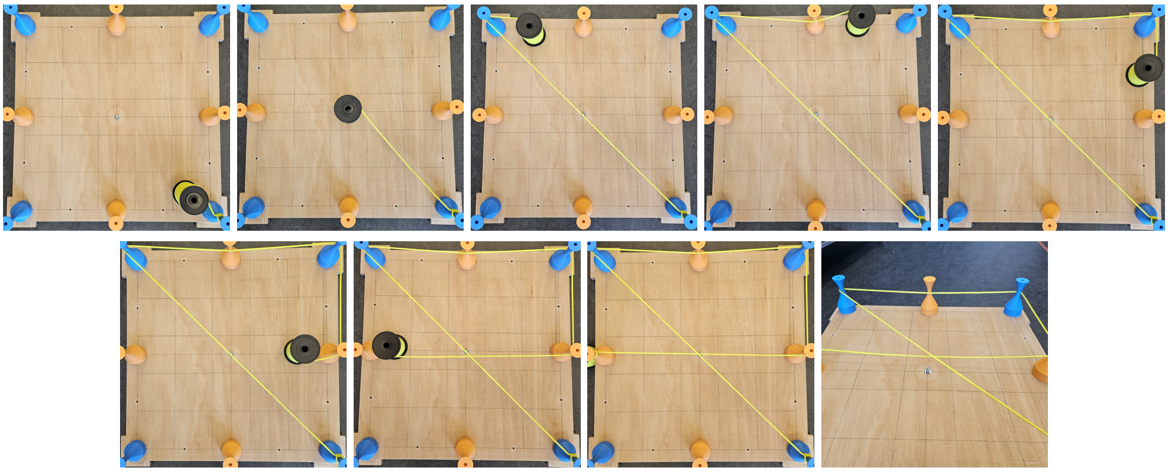

Figure 3.2: Actual example of Figure 3.1 using the board setup

Beside the figures there are also some main definitions within the research. These are explained both in words and in a schematic overview. Figure 3.3 shows the oveview and Figure 3.4 shows the actual windings. These definitions are also stated in the nomenclature. A node refers to any point within the grid and serves as a potential location for interaction or connection. An intersection is defined as a point where two ropes cross paths, although they do not make contact. In contrast, an interaction involves an actual connection between two ropes. A connection specifically refers to one of the defined methods used to join ropes together. Casted or spanned ropes are those that have already been placed in earlier stages of the process and are fixed in position. These ropes can be used to create an interaction with. The centre point represents the geometric centre of the grid layout, whereas the middle point refers to the midpoint of a rope connection and can be interpreted as the central position of that particular interaction.

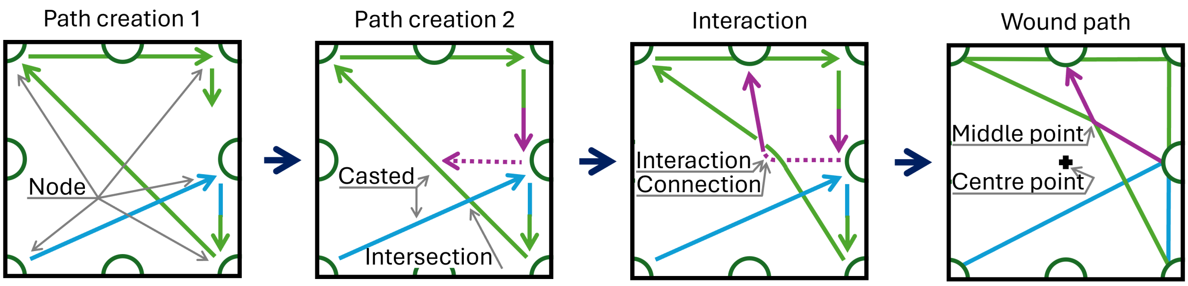

Figure 3.3: Explanation of different definitions

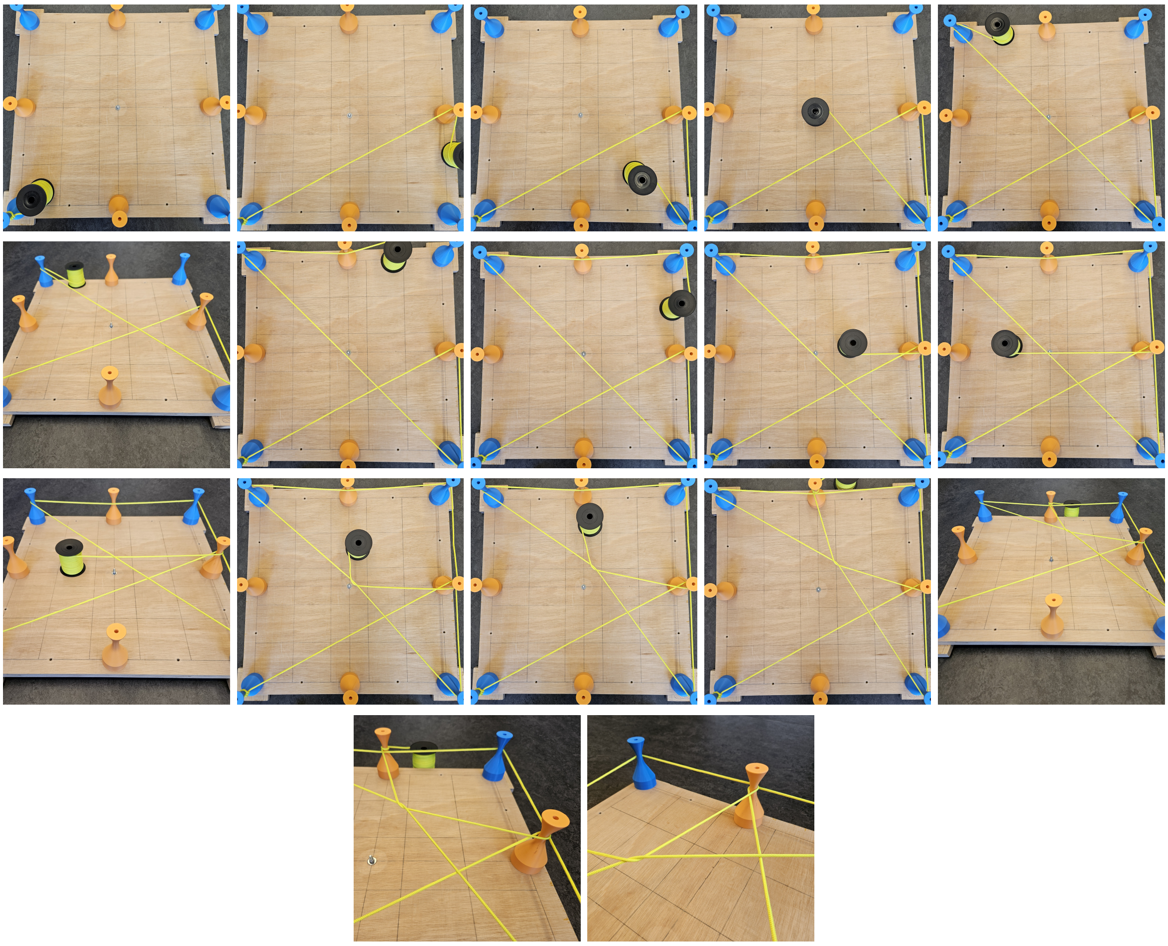

Figure 3.4: Actual example of Figure 3.3 using the board setup

4

Connections between Sublayers

This chapter continues with the possibility of using filament windings, including the research objectives, and combines this with the concept behind creating an interaction within a 2D winding plane by establishing a 3D workspace.

4.1. Winding Workflow

Transforming the desired shape into a manufacturable concept requires a structured fabrication process. This process consists of several steps, with the first four illustrated in Figure 4.1. The process begins with defining the framework points, shown as green dots in the figure. These represent scaffolding points (also referred to as supports), which serve as anchor locations around which the rope can be wound. The ground structure outlines all possible connections between fixed support points. A distinction is made between line types: purple lines indicate shorter connections, while orange lines represent longer ones. Next, the topology defines the intended structure, incorporating intermediate lines between supports to achieve the desired layout. In Figure 4.1, this is exemplified by a cross configuration. If the shape is based on internal force flow within a concrete member, a strut-and-tie model may be used to determine the topology. This could, for example, be done to determine the reinforcement for a wall or floor in which the fibre-wound reinforcement can be simplified into a 2D plane. This allows the method to be tested with a concrete filament-reinforced floor or wall. After the topology has been established, the winding sequence specifies the order in which each rope is placed. Once this order is set, the robotic path can be generated. The process concludes with the actual winding of the rope, resulting in the fabrication of the final structure.

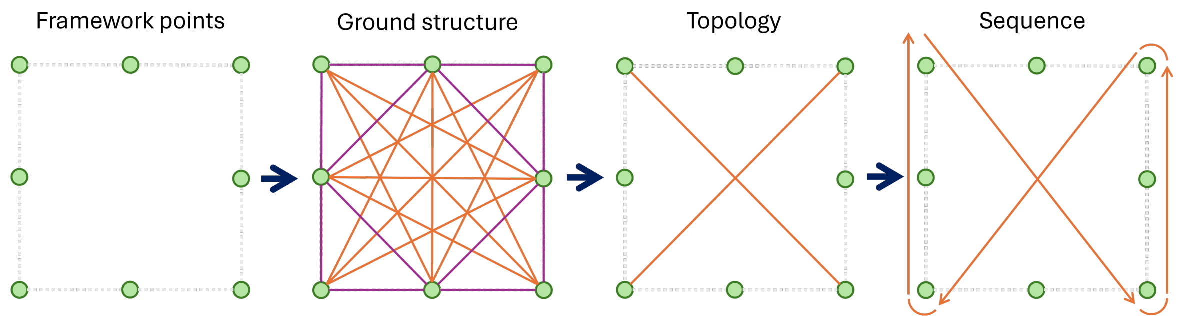

Figure 4.1: Fabrication steps

4.2. Winding Interaction

A possible way to improve material efficiency is to create an interaction. These interactions can be created by using a certain way of connecting the ropes. These connections should be able to replace the function of the support used during construction. Figure 4.2 shows the concept of three stages.

Each of these sub-figures will create a 2D cross, in which the top figure is the topology and the lower figure represents a sequence. Figure 4.2a creates the cross using two lines that pass over each other. Figure 4.2b adds the middle support to reduce the rope length. When comparing both of these setups, a difference can be noted. The setup with the corner points uses four times the length of a diagonal and once the length between the corner supports, whereas when the middle support is added, the rope length reduces by one times the length between the corner supports, thereby achieving the optimal rope pattern without any waste. However, by adding the middle support point, the number of scaffolding points increases from 4 to 5. Figure 4.2c combines both thoughts. This novel approach strives to use the least number of supports and the least amount of filament. However, this does require a new approach to creating a certain connection in the middle to locate the filament in the desired position. In addition, Figure 4.3 displays the sequence of all three options in 3D.

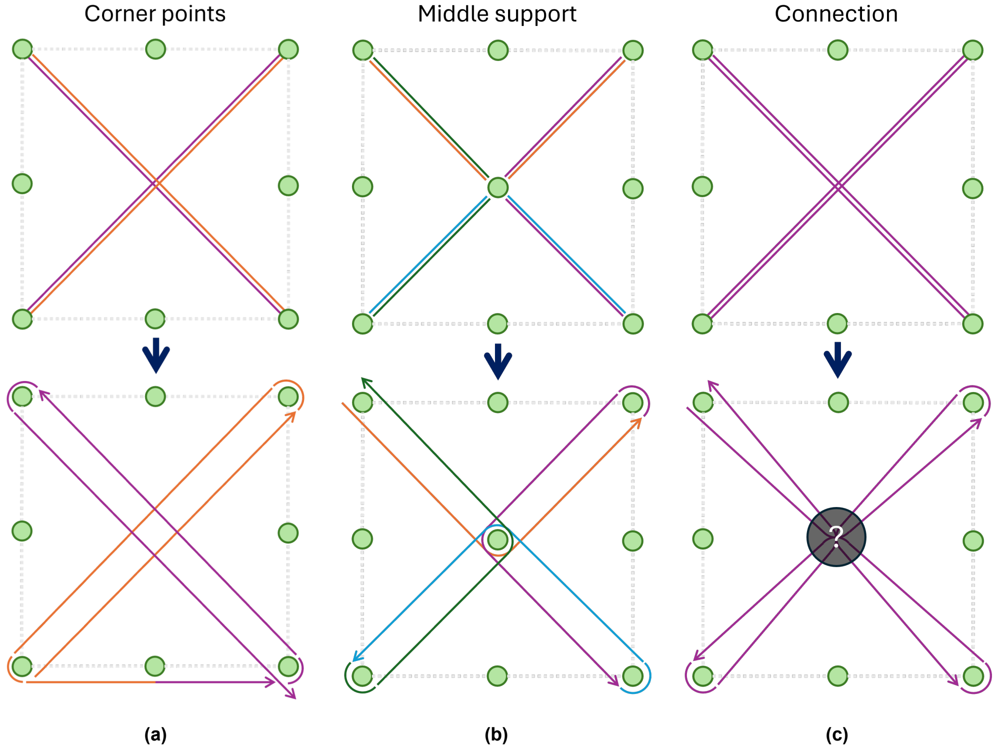

Figure 4.2: Different possibilities of the winding path

The goal is to create a connection in the middle of the framework where the filament interacts. This connection should be able to resolve the question mark shown in Figure 4.2c and 4.3c. Creating such a connection makes it possible to reduce the use of scaffolding needed during construction and the rope length of the design. When implementing this on a larger scale, it could potentially reduce material waste compared to the optimal solution. The difference in material usage can also be expressed in environmental impact using a life cycle assessment.

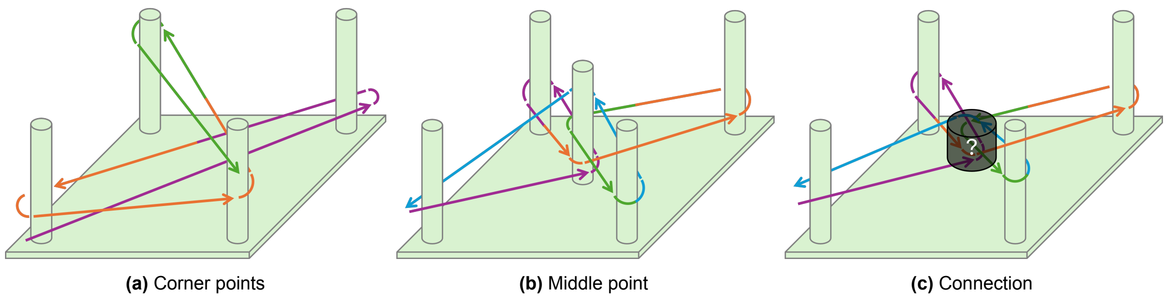

Figure 4.3: 3D view of Figure 4.2

4.3. Winding Layers

Winding the rope works in a similar way to 3D printing in terms of layers. New layers are created on top of the existing ones. However, there is a significant difference between filament printing and rope winding. While filament is heated and bonds with the previously printed material, the rope does not interact with the earlier wound layers. The rope behaves as separate layers, as shown in Figure 4.4. Without any created interaction, the layers will move independently. This means the rope cannot form any non-fixed support locations without changes to the conventional process of filament winding, because to create a possible connection the rope needs to interact with different layers of rope.

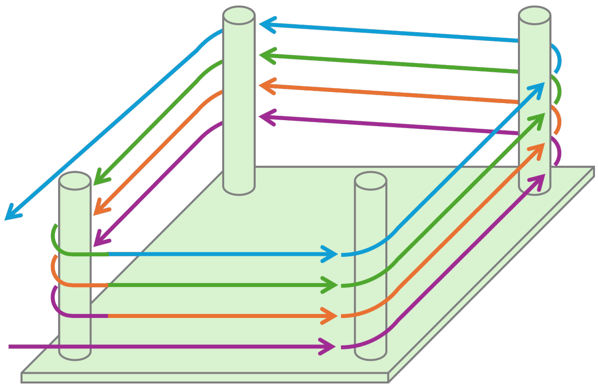

Figure 4.4: Winding in layers

To overcome the problem of separate rope layers, interaction between the ropes should be created to make a connection. The aim is to form an interaction with earlier wound layers/fibres. This would allow the ropes to intertwine with each other, making it possible to create non-fixed supports. This research presents two methods. The first one tests the principle of lifting the support, as shown in Figure 4.5. When lifting the support, the winding head with the new rope becomes the lowest layer, enabling interaction with the layers above. Figure 4.6 shows the second method, which is based on the concept of moving through the plane. By doing so, all previously spanned ropes can be incorporated into an interaction with the aim of creating non-fixed support points.

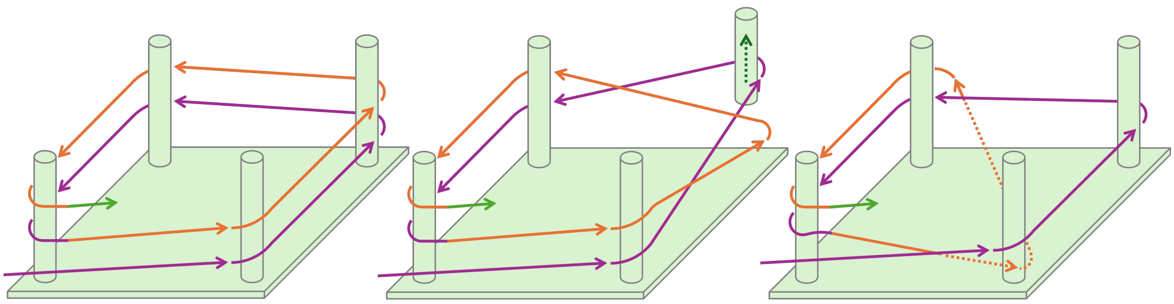

Figure 4.5: Lifting the support to create an interaction (3D)

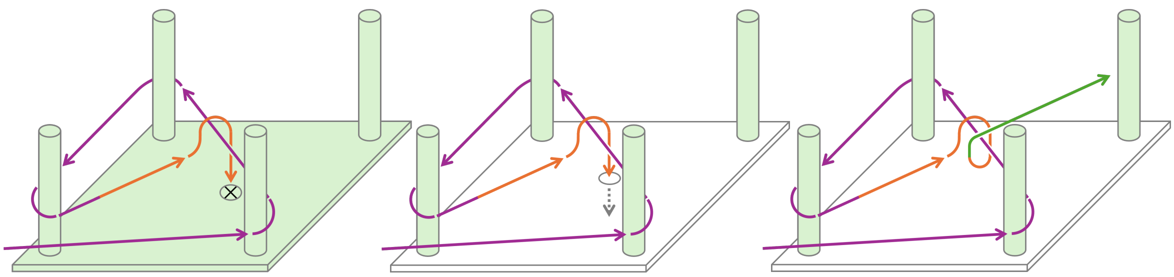

Figure 4.6: Moving through the plane to create an interaction (3D)

4.4. Force Equilibrium

When winding between two fixed supports, the rope forms a straight line between them. These supports cannot move, so the position remains the same. In contrast, when winding around a ”non-fixed” support, created by the interaction of ropes, the connection point is no longer fixed within the surface. Its position may shift from the intended location due to the combined influence of tension and friction in the system. This behaviour is governed by the concept of force equilibrium. This equilibrium occurs when the sum of all forces, both horizontal and vertical, equals zero, and the sum of all moments also equals zero. Figure 4.7 illustrates this equilibrium using Bow’s notation, where force magnitudes and directions are represented visually through connected lines. In Figure 4.7a, all forces are equal, and the ropes form three angles of 120 degrees between them, representing an ”ideal” state of equilibrium. In Figure 4.7b, the forces differ in magnitude, resulting in an equilibrium of unequal angles. This reflects a more realistic scenario, where friction affects the system and shifts the point of equilibrium.

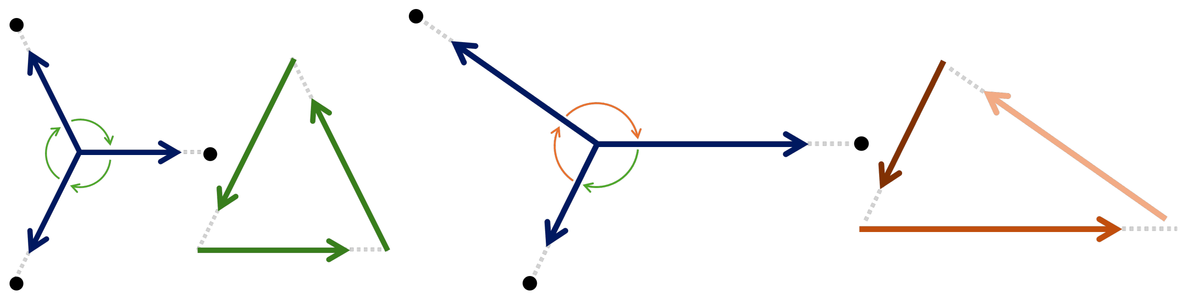

(a) Equal forces

(b) Unequal forces

Figure 4.7: Triangle force equilibrium

When a non-fixed support is used, the location of the connection point may shift. This movement depends on the balance of forces and the amount of friction present in the system. In the absence of friction, and with equal tension across all ropes, the system would naturally settle into the equal-angle configuration seen in Figure 4.7a. However, friction plays a crucial role in practical applications. It can arise from contact between ropes or from how the rope wraps around supports. As more layers are wound, especially with loops or crossovers, the earlier wound sections of rope become less responsive to tension adjustments from the winding head. In these cases, friction increasingly prevents movement, influencing the final position of the connection point. The more rope length, interactions, and supports between the winding head and the rope being spanned, the greater the resistance, and the less likely the point is to move.

4.5. Nodal Displacement due to Interactions

A key step in creating a connection with an already cast fibre is the determination of its geometrical configuration. This can depend on the shape and the forces applied to the tensile materials. There are two types of forces: an external force, which is applied to the structure by adding weight, and an internal force, which is generated by the rope itself. The ”internal” force can arise from winding the fibres and letting them interact with each other, as shown in Figure 4.8. By creating these interactions, the force can shift the equilibrium position of a given node. Greater insight into the location of these nodes can be gained through a form-finding method. The definition of form finding is: ”Finding an (optimal) shape of a [form-active structure] that is in (or approximately) a state of static equilibrium” [29]. This method has previously been used by both Antoni Gaudí, through his hanging chain models, and Heinz Isler, who applied it to hanging membranes. They demonstrated how natural force-flow patterns could be leveraged to design effectively. This could now be used to design more efficiently, both in terms of material use for unstrained gridshells, cable-nets, and tensegrity elements, and the material use within the scaffolding during the construction of these structures [5]. Several form-finding methods are already known [27, 17], but the selection of the most appropriate approach will be explored further in this research.

Figure 4.8 presents two scenarios. In the first (possibility 1), the tension and number of strands in all directions are equal, resulting in uniform forces across all ropes. This leads to an equilibrium between the two purple arrows (the diagonal direction) and the single orange arrow (interaction direction), following Bow’s notation by summing all force vectors. In the second scenario (possibility 2), an additional purple strand is introduced. Although the tension in each rope remains the same, the difference in the number of strands alters the overall force balance. The added strand doubles the total area, which intensively leads to higher resistance in the diagonal direction (purple arrows), while the interaction (orange arrow) direction remains supported by only one rope. As a result, the purple ropes experience less deformation compared to the first scenario. It is important to note that the figure assumes equal tension in all ropes for illustrative purposes. In reality, small variations in tension between ropes will occur, potentially shifting the actual equilibrium point. This figure serves to highlight the influence of force distribution, induced by winding, on the resulting geometry.

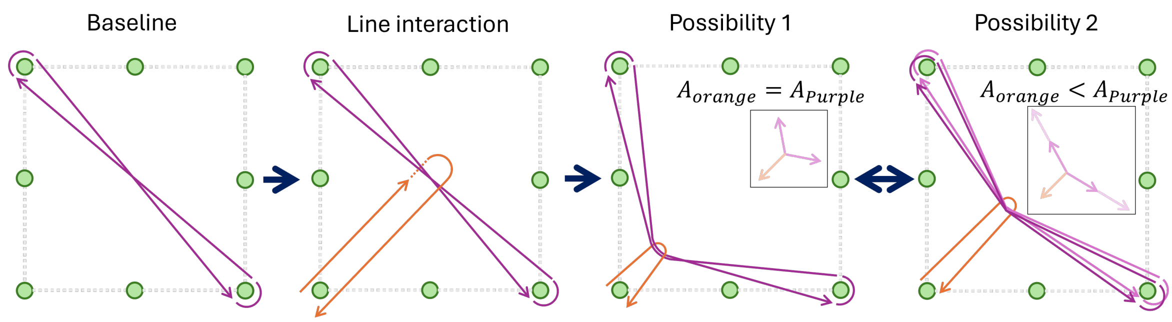

Figure 4.8: Force equilibrium effect of the ropes

Form finding strategies could play an important role for all tensile materials to predict the geometry. This is because rope interaction can result in a different layout of the tensile materials compared to the desired shape. There are several known methods which will be shown in Table 4.1 and 4.2. These methods are retrieved from different sources which will be refered to in the tables. When reviewing the information summerized in the table, the force density method would likely be the best method to explore further. This because the method is material independent making it suitable for more practical purposes. In addition, it is a recommended method to use for exploring new configurations [27].

Table 4.1: Kinematical form finding methods

Kinematical form finding methods: These method are based on defining the geometry of the given tensile structure by maximising the lengths of the struts but keeping the length of the cable's constant. This is often performed in preliminary designs and geometric explorations, where a force equilibrium is less relevant			
	Method:	**Usage:**	**Downside:**
Analytical Approach [27]	This technique involves connecting the bottom and topside polygon, creating a prism by using a rotational angle for the struts between both ends of the prism amplifying the geometry	Conceptual phase where the geometric relationship is important	It does not take the equilibrium of forces into account directly
Non-Linear Optimization [27]	This method uses optimalisation algorithms to adjust the length of the element and aiming to solve all constraints in the model	Complex geometry, to minimize the use of material without compromising the structural integrity	Unfeasibe for larger systems, due to the increase of constrains (equations) for each element
Dynamic equilibrium [27][29]	It is an iterative process which fictitiously applies masses and damping to derive a solution using the steady state equivalent to the static equilibrium ending up into a "relax" state of a spring equilibrium	Membrane and cable net structures, subjected to an external force resulting in a mass spring system	Difficult to determine all necessary parameters for the mass spring system including a time step to achieve a convergence of the model

Table 4.2: Statical form finding methods

Statical form finding methods: These methods are based on determining the possible equilibrium configurations of a tensile structure given a topology (number of nodes and connecting elements between them)			
	Method:	**Usage:**	**Downside:**
Analytical Method [27]	Virtual work and symmetry will be used to approach the equilibrium configurations of the elements with reduced set of equations	Simple structures and validate numerical models	Often incorporates parts of the force density method
Force Density Method [27][17][29]	It uses a formulation of (non)linear equations to find an equilibrium in terms of a force density matrix	Material independent method, recommended for finding new configurations	It determines the tension coefficient using the ratio of force over the length, not having direct control over the length
Energy Minimization [27]	This approach models members assumes them to be a linear elastic spring with the goal to reduce the systems potential energy	Complex systems and stability analysis	The concept is linked to the Force density method
Stiffness matrix method [29]	It uses standard elastic and geometric matrixes while focussing on the topological layout	Structural analysis	It includes material properties leading to more computational time and possible convergence problems and unstable solution

5

Knotted Connection

This chapter examines the intersection of lines to estimate available interaction locations. It also investigates ways to overcome the missing link of creating a connection between intersecting ropes. Such a connection must allow all ropes to connect to each other, enabling the combination of different sublayers.

5.1. Intersection

Filament winding has already been used successfully to construct structures such as the BUGA Fibre Pavilion, LivMatS Pavilion, and Maison Fibre. The Maison Fibre used 2D planes, which is similar to the setup designed here. However, these examples still rely heavily on fixed support points. Each fixed support requires anchorage and an attachment mechanism to a supporting frame. In such setups, every point in the grid that requires a rope connection must include a physical support. By contrast, non-fixed supports eliminate the need for such attachments. This provides a strong case for developing new approaches to filament winding. One such approach involves the use of ”non-fixed” supports, created through interactions between fibres within a 2D winding field. These intersections emerge from spanning two lines between two fixed support points, as shown in the first subfigure in Figure 5.1. If these lines are not aligned (i.e., have different directional vectors), an intersection point is formed. As the number of supports increases, the number of potential intersections grows, creating a range of unique locations (nodes) that can be used to optimise the winding path.

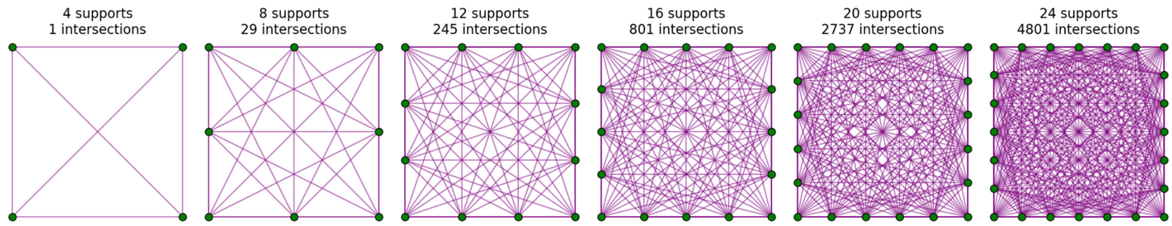

Figure 5.1: Possible interactions based on a square setup[1]

Figure 5.1 illustrates how unique winding paths between fixed supports generate multiple intersection points. This figure is based on a square setup using straight intersection lines. Beside the square, a circular shape has also been used, as shown in Figure 5.2.

[1]The code for this figure was created using (partially) artificial intelligence.

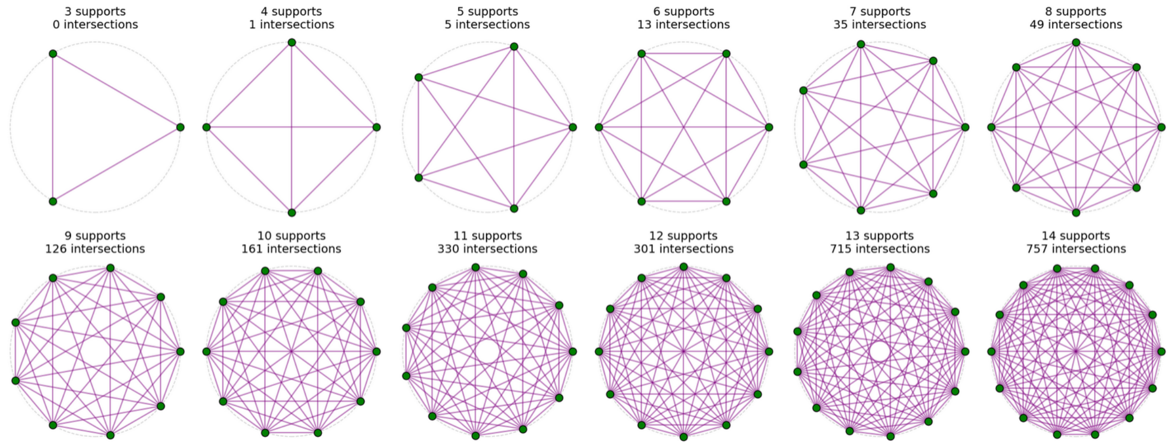

Figure 5.2: Possible interactions based on a circle setup[2]

Figure 5.3 displays the number of supports and interactions for both setups. The number of unique intersections increases exponentially with the number of supports. Therefore, the more fixed-support points used, the more potential intersection points can be determined, enabling the structure to be optimised.

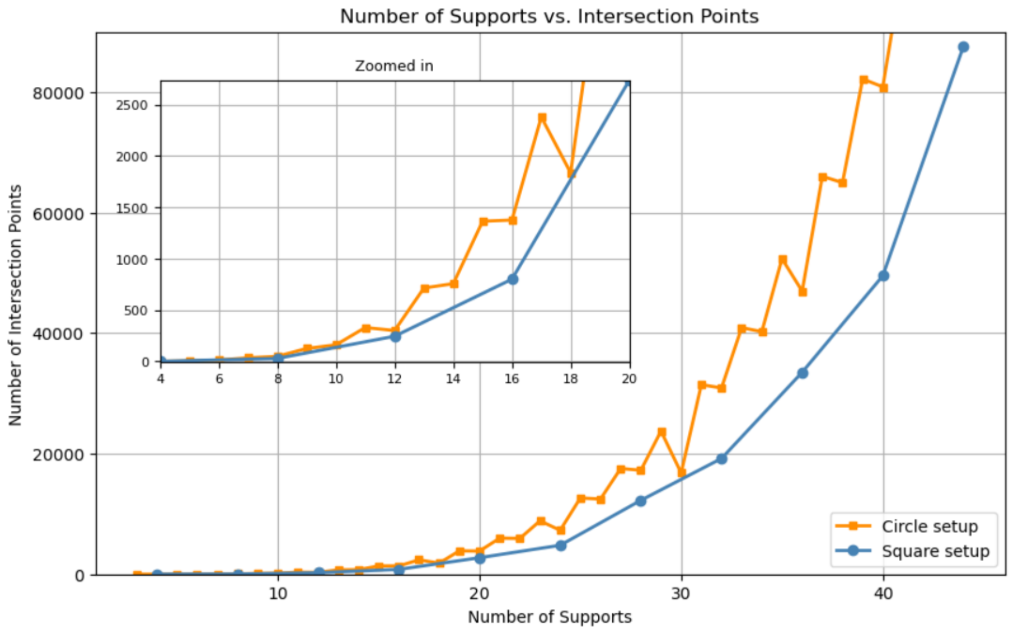

Figure 5.3: Number of unique intersection points (support locations)[3]

Besides straight lines between fixed supports, the system can also use interaction points that function as non-fixed supports. Figure 5.4 illustrates this, beginning with two basic shapes. These shapes are shown only to indicate the outline, with no diagonals in the square to maintain readability. The two shapes are capable of creating six new interaction points (orange circles). When these interaction points are allowed to function as connections, nine new lines can be formed solely between the newly created locations (dotted orange lines). These new lines could potentially generate fifteen additional interaction points. Furthermore, allowing all possible interactions between two points of the base figures increases the number of unique lines even more. Applied on a larger scale, including the possibility that lines could include a kink at a connection location, the exponential growth of possible interaction points and connecting lines allows for almost infinite possibilities, particularly when rope thickness and accuracy are taken into account. In this way, virtually any topology can be created.

[2]The code for this figure was created using (partially) artificial intelligence.
[3]The code for this figure was created using (partially) artificial intelligence.

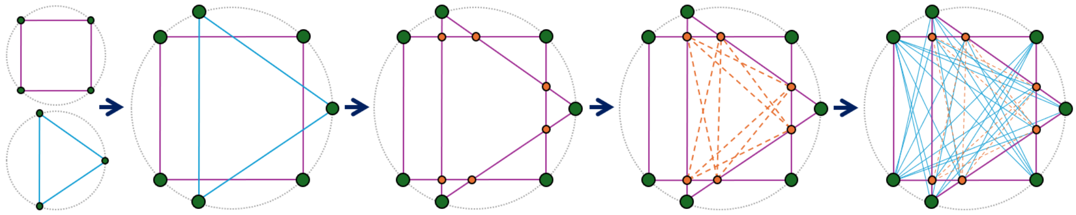

Figure 5.4: Interaction potential[4]

Increasing the number of intersections provides more refined control over the winding pattern. This control can be used to optimise load distribution and nodal spacing in later stages of the design. It is particularly useful when aiming to minimise material usage, whether by replacing traditional rebars with wound fibres or by producing lightweight structural elements such as shells or spatial frameworks.

5.2. Knots

To realise the potential of these intersections, a method for creating meaningful interactions must be established. An interaction point is formed by winding a line around two fixed supports. However, as shown in Figure 4.4, these lines do not interact when winding solely within a 2D plane. To enable such interactions, a 3D workspace is required. The necessity of a 3D workspace arises from the 2D winding plane and the need to move both in and out of the plane to create the connection. These connections must be compatible with continuous robotic filament winding, meaning that the robotic arm should be able to complete the entire path without human intervention. Additionally, a continuous rope needs to be used. While this enables uninterrupted operation, it also introduces the challenge of forming connections without the robotic arm becoming entangled in its own knot. This subsection begins by exploring several knotting strategies aimed at overcoming this challenge.

5.2.1. Maritime Knots

Knots have been used for centuries in the maritime industry to join ropes or secure objects. According to the Cambridge Dictionary, a knot is defined as: "a join made by tying together the ends of a piece or pieces of string, rope, cloth or more." When adapting this concept to continuous filament winding, a challenge arises. Most traditional maritime knots require the rope to pass through itself, as shown in Figure 5.5. If this method were applied in continuous filament winding, the winding head, including the coil of rope, would need to pass through the loop created by the rope itself. However, for the purposes of this study, the definition of a knot can be reinterpreted. A "knot" may be seen as any interaction between the winding rope and an already spanned rope that enables the creation of a new connection. These interactions function as non-fixed supports and may offer a novel means of reducing material usage in traditional support structures. In this context, a knot is defined as a connection made when the winding head loops around or alongside an existing rope, allowing the robotic process to continue seamlessly to the next location.

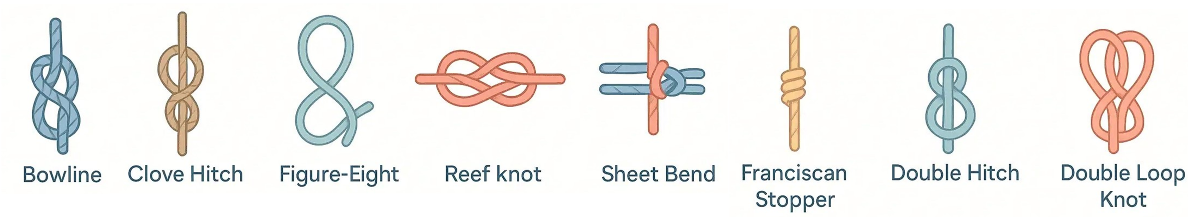

Figure 5.5: Nautical knots examples [26]

[4]The code for this figure was created using (partially) artificial intelligence.

5.2.2. Knot Theory

Having considered the practical use of knots in maritime contexts, the mathematical theory of knots also becomes relevant. Knot theory typically considers a closed loop of rope, which more closely resembles the process of continuous filament winding. The foundation of knot theory is based on the Reidemeister moves. These are a set of transformations that can be applied to a knot without altering its fundamental properties, as shown in Figure 5.6 [9]. These three moves: twist, poke, and slide can determine whether a knot can be untangled into a simple loop. A knot remains a knot if it cannot be reduced to an untangled circle through combinations of these moves. When translating this to the filament winding context, it becomes clear that twisting the rope around itself or moving it underneath and then back over will not create a meaningful connection unless there is an interaction with another rope. Therefore, a twist connection can only be achieved by looping around an existing rope, and the poke move is only applicable when the rope loops alongside another. These rules are illustrated in Figure 5.7.

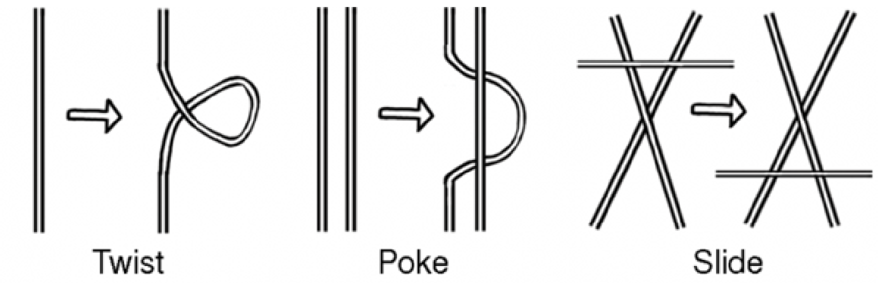

Figure 5.6: Reidemeister moves

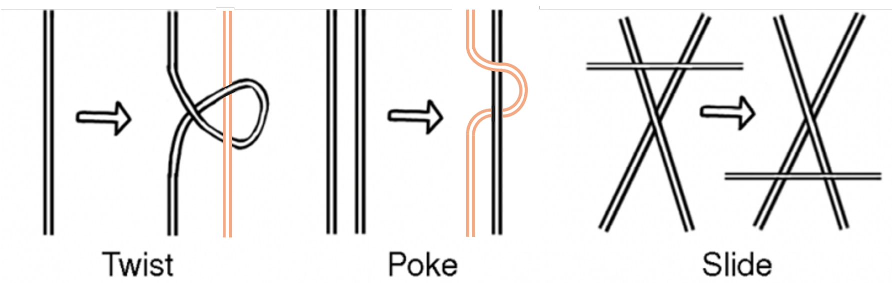

Figure 5.7: Adjusted Reidemeister moves

In this research, a knot refers to a connection formed between an existing rope and the winding rope. This can be achieved by winding around or alongside another rope, but an interaction must occur. Without such interaction, the knot can unfold and will not serve as a connection point. By applying the twist and poke Reidemeister moves in combination with interaction with another rope, a novel approach to the filament winding process is possible. The ropes are spanned in a 2D plane, but to create a connection, a 3D workspace is required. This allows the winding head to move perpendicular to the plane in which the web is formed. In doing so, a twist can be created by winding around the spanned line, and a poke can be achieved by circling alongside the rope.

5.3. Rope Connection

Combining the creation of a knot with the concept of force equilibrium, several connection strategies have been devised. This is because the resistance created by a knot influences the system's ability to maintain equal angles between all spanned ropes, as explained in Chapter 4.4. Several types of knots can be used in the winding process. This research focuses on three specific options, illustrated in Figure 5.8. The first type is suitable when the rope needs to return to the same side of the spanned line it wraps around, typically assuming a 90-degree angle. The second, a loop-around connection, is appropriate when the next anchor point lies on the opposite side of the spanned rope. The third knot type will be further explored for its potential to form a stronger connection that resists sliding. These connections will be evaluated during the testing phase.

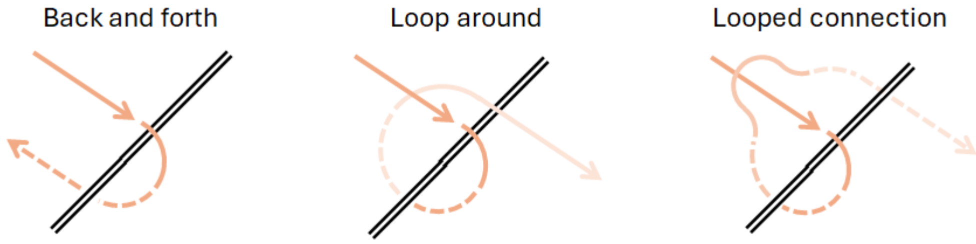

Figure 5.8: Possible interactions to create a connection

All connections are based on the principle of penetrating the winding plane. The adjusted Reidemeister moves allow the fibre to create a connection by winding around an earlier wound fibre. This earlier wound fibre resists the new fibre from twisting or poking back, due to the interaction forming the connection.

Furthermore, the preference for a certain connection also depends on limited space. Some paths to penetrate the winding plane may no longer be available due to earlier wound fibres, as elaborated in Subsection 7.4. Additionally, the choice of rope interaction depends on the position of the robotic winding head. It may approach from the front or rear of the setup, depending on the configuration and the current position of both the robotic head and arm. As visible in Figure 5.8, each connection has its own properties. They respectively penetrate the plane once, twice, or three times. In the loop-around connection, the rope ends on the same side as it started, whereas in the other two it does not. Nevertheless, the more interactions with earlier wound rope, the higher the resistance of the connection. During the creation of these interactions, the preferable connection for each situation will be used, taking all these aspects into consideration.

6 Prototyping

This chapter describes the design steps taken during the prototyping phase. Starting with the general design requirements for all designs. This also includes some additional requirements that became clear during the iterative steps between the designs. This chapter states only considerable iteration leaving out small adjustments. This because the prototypes are not a main project, but a tool to realise and show the final goal. Furthermore, both concepts as shown in Subchapter 4.2 will be investigated. Besides the created hardware, the software will be explained afterwards. This focuses on the robotic arm and the path planning to create the winding pattern. Finally, more visuals of the designs and used code can be found in Appendix A and B.

6.1. Hardware Requirements

Creating prototypes is needed to evaluate the process of filament winding. These prototypes have been used to test and assess part of the research. This resulted in an iterative process due to all uncertainties and the explorative character of the work. The maximum size of the workplane is approximately 0.6 by 0.6 metres, determined by the limited range of the robot when using all degrees of freedom of the arm. The limitation of the free space in between the earlier wound ropes is determined by the path, the design of the supports, and the parameters adjusted in the Grasshopper code. This means that optimizing in terms of minimizing the size of the support and robotic head will increase the winding possibilities due to the bigger free space in between them. The number of nodes is dependent on the minimum distance between two nodes that is needed in order not to restrict or hinder the winding process. This means that the printing head should always be able to wind freely without getting stuck or colliding with other lines which were wound before.

The experimental phase starts with exploring by winding around several supports on the board investigating possible methods to reduce the material use by creating interactions. In addition, the robotic head in combination with the path determination created by using the Grasshopper implementation in Rhino are evaluated. The requirements are stated in Table 6.1. These requirements are for all designs, although during the iterations the mechanisms to achieve the requirements improved. Moreover, some requirements from the list are retrieved from issues during the testing phase. These have a “*” behind the text, meaning that these requirements have been added at a later stage in the design process.

All 3D prints shown in Chapter 6 have been made using PLA filament and are produced using FDM 3D printing.

Table 6.1: Design requirements of all prototypes

Design requirements	
Setup:	
1.	Stays in the intended place
2.	Does not deform
3.	Allows the supports to be attached to it
Supports:	
1.	Attachment to the setup (but also able to take them off)
2.	Support should not move during the winding
3.	Ensuring that the rope remains attached to the support
Winding head:	
1.	Main frame needs to be attached to the robotic arm
2.	Fail safe mechanism in the winding tool (not break immediately)
3.	Automated process
4.	Winding around or through the support
5.	Rope is being guided towards the location (rope distributor)
6.	Prevents the winding head from colliding or getting tangled
7.	Coil with the rope can be taken off
8.	Resistance in the coil is adjustable
9.	Resistance on the rope is adjustable
10.	Keep tension on the rope (pull back) *
11.	Independent direction of the rope distribution *

6.2. Winding Board Setup with the Standing Support

The winding board setup is the first prototype created consists out of 2 components. The support at which the rope is wound around, and the board itself. Furthermore, the winding head is created which allows the robotic arm to wind a rope around the support. The first prototype is created to test possible interactions. This is achieved by lifting the support and winding around, but underneath the former spanned line as explained in Section 4.3. This prototype yielded some limitations, in the sense that manual lifting of the support points was needed, which when using it on large scale, would require a lot of time. In addition, the rope sometimes lost its tension during the winding process. This would result in temporary loss of the rope's tension leading to different nodal locations comparing the the situations before the temporary tensions loss and after regaining the tension. These things were taken into consideration as potential improvements when developing the second prototype.

6.2.1. The Board

The winding board serves as the foundation for the filament winding setup. It defines the grid layout and ensures that all standing supports remain in the desired position. Each position has a designated attachment point on the board, which allows the board to be used in many configurations. These bolts allow the support to be placed on top of it. In addition, the winding board can be secured making sure the board does not move due to the tensile forces exerted by the rope in combination with the robotic arm. The winding board is shown in Figure 6.1 and 6.2.

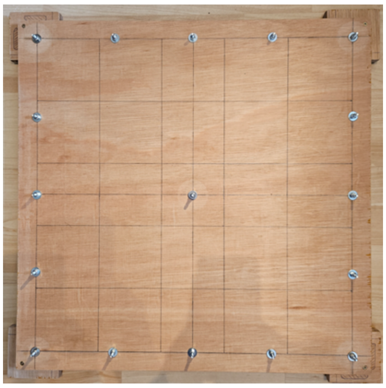

Figure 6.1: Topside board

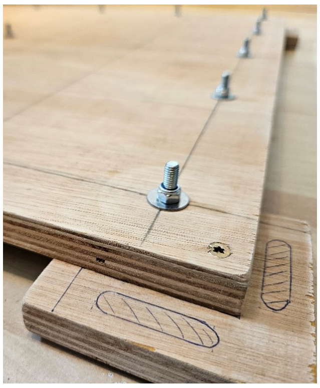

Figure 6.2: Corner of the board

6.2.2. The Standing Supports

The standing supports are designed to guide the rope as it is woven around these supports. They ensure the rope remains in place, both at the top and bottom, preventing it from sliding off during the winding process. In addition, an incline is added in the support to help the rope be more consistent in its position. The support must be shaped in such a way that, even if the rope or winding head lifts slightly above the head, the rope does not slide off the support. Moreover, the support is made as smooth as possible to let the rope slide easiliy allowing for an equal amount of tension at both sides of the support. For practical use, the support should be easy to attach to the setup and sufficiently stiff to avoid bending or flexing. Overall stability is provided through a firm base, ensuring the support remains upright and reliable during fabrication. These standing supports are shown in Figure 6.3 and 6.4. The final design of the supports is shown in Figure 6.18.

Figure 6.3: Standing supports (front view)

Figure 6.4: Standing supports (upside down)

6.2.3. The Dispenser Head

The first prototype is designed to enable controlled winding of the rope around the standing supports. This prototype has the following parts included. The main frame is connected to the robotic arm and is the base of the winding head. Both a coil holder that secures the rope and a directional head which guides the rope are connected to the main frame. The rope is guided from the coil through the distributor head, which ensures it remains aligned and slides toward the intended attachment point. In addition, a fail safe is included in the design to make sure that unwanted forces do not break the winding head or damage other components. This is done by both using a click system in the connection to the winding head and attaching this component with a spring allowing it to move but making sure that the head goes back to the original position after the force is gone. Finally, to make sure that the rope stays in tension during the winding an adjustable resistance is place next to the rope coil. The dispenser head is shown in Figure 6.5 and 6.6.

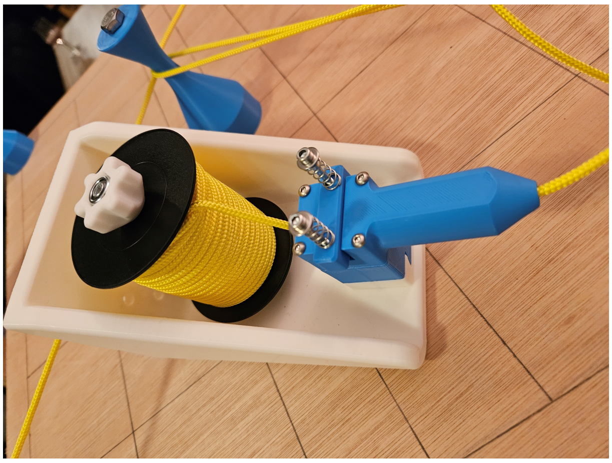

Figure 6.5: Dispenser head (design)

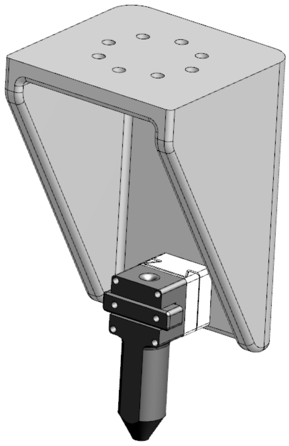

Figure 6.6: Dispenser head (model)

6.3. The Standing Setup

The winding board setup is limited in its possibilities, as the winding head cannot pass through the plane. It is designed with the concept of lifting the supports to create an interaction, which makes it difficult to create connections. Because of this, a new setup is created which, allows the winding to go through the winding plane enabling winding from both sides. This makes it possible to create connections and interaction between the rope. Furthermore, the rope distributor part is depending on the robotic head. This causes more resistance in certain situations, which can be solved by letting the rope distributor move independent from the head. Finally, the size is preferably reduced allowing it to increase the potential of creating more interactions. The standing setup including the ring and standing supports are shown in Figure 6.7 and 6.8.

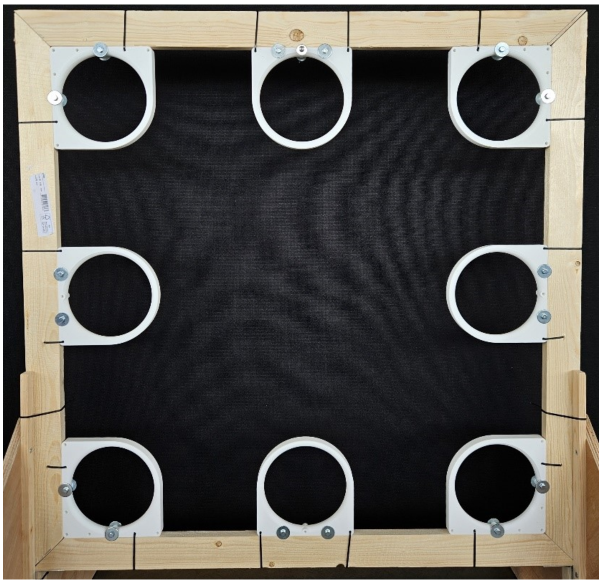

Figure 6.7: Standing setup (Ring supports)

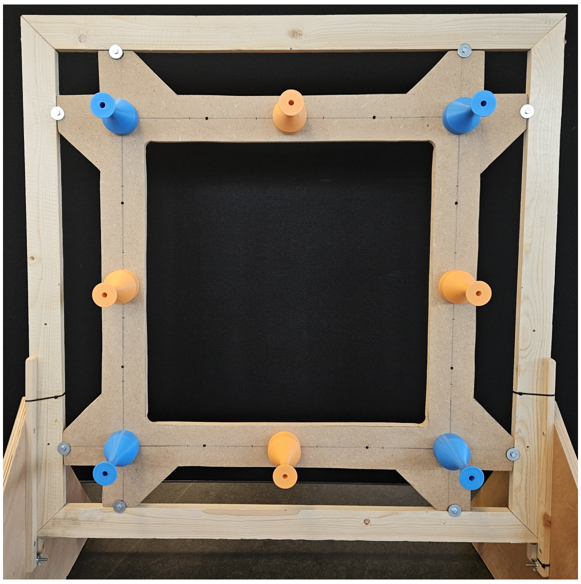

Figure 6.8: Standing setup (Standing supports)

6.3.1. Ring Supports

The ring supports serve as an attachment for the standing setup to wind through and keep the rope in place. The ring supports are designed for both the corner point and the locations in between allowing to determine the location depending on the desired shape. In addition, the rings are stiff enough resisting deformations which could be caused by the tensile forces of the rope. The ring supports are shown in Figure 6.9 and 6.10.

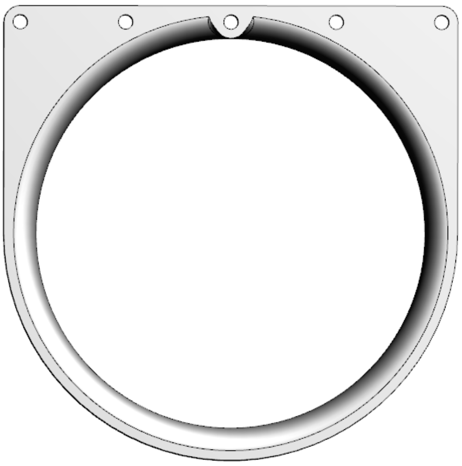

Figure 6.9: Ring support edge

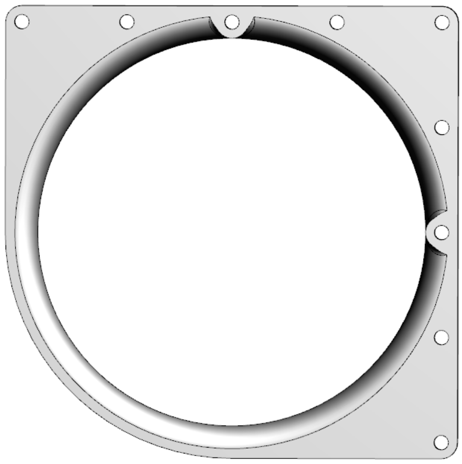

Figure 6.10: Ring support corner

6.3.2. Slide Through Head

The slide-through head is designed to move through the 2D winding plane, enabling the possibility to create connections with earlier wound ropes by using rope interactions. It must be able to move through the ring support while guiding the rope. The coil carrying the rope is replaceable making it possible to change the winding material during the process. The slide through head can be attached and loosened onto the robotic arm by rotating only clockwise. This allows to make the process fully automated when a second robotic arm is included operation from both sides of the winding setup. The slide through head is shown in Figure 6.11. Figure 6.12 shows the collaboration between two robotic arms.

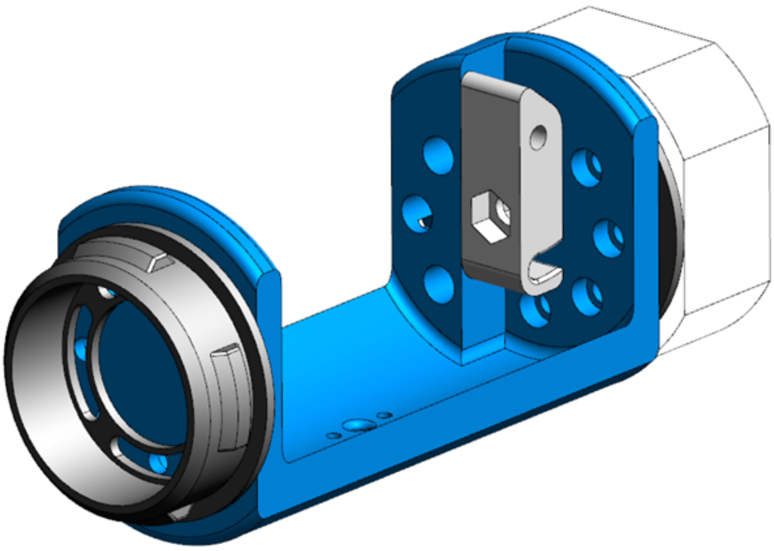

Figure 6.11: Slide through

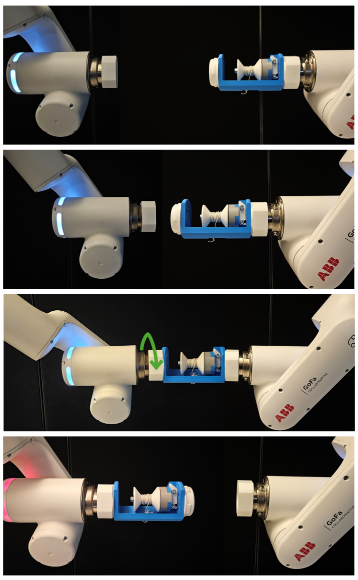

Figure 6.12: Automated process

6.3.3. Penetrating Head

The improved slide-through head features a more compact design, reducing its overall size allowing it to create more interactions in places where the windings are closer to each other. A key enhancement is the independent rotation of the directional guider for the rope, allowing the rope to adjust its path freely without rotating the entire assembly. Additionally, the system now includes adjustable mechanisms for both the pull-back force and the resistance on the coil, providing more precise control over rope tension and keeping the rope in tension during the winding process. The penetrating head is shown in Figure 6.13 and 6.14.

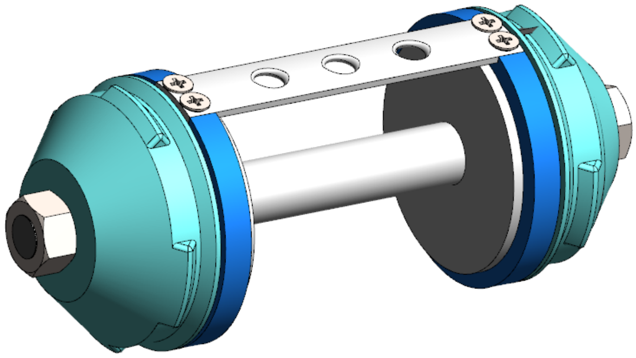

Figure 6.13: Penetrating head (winding coil)

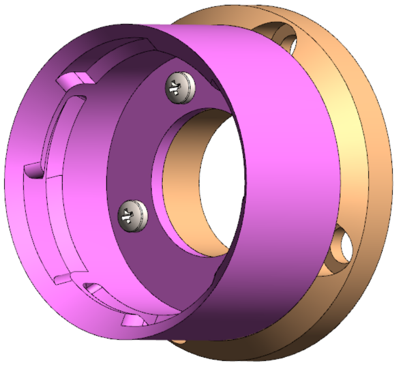

Figure 6.14: Penetrating head (connecting side)

Figure 6.15 shows the exploded view of the penetrating head. This shows all elements used to create the full design.

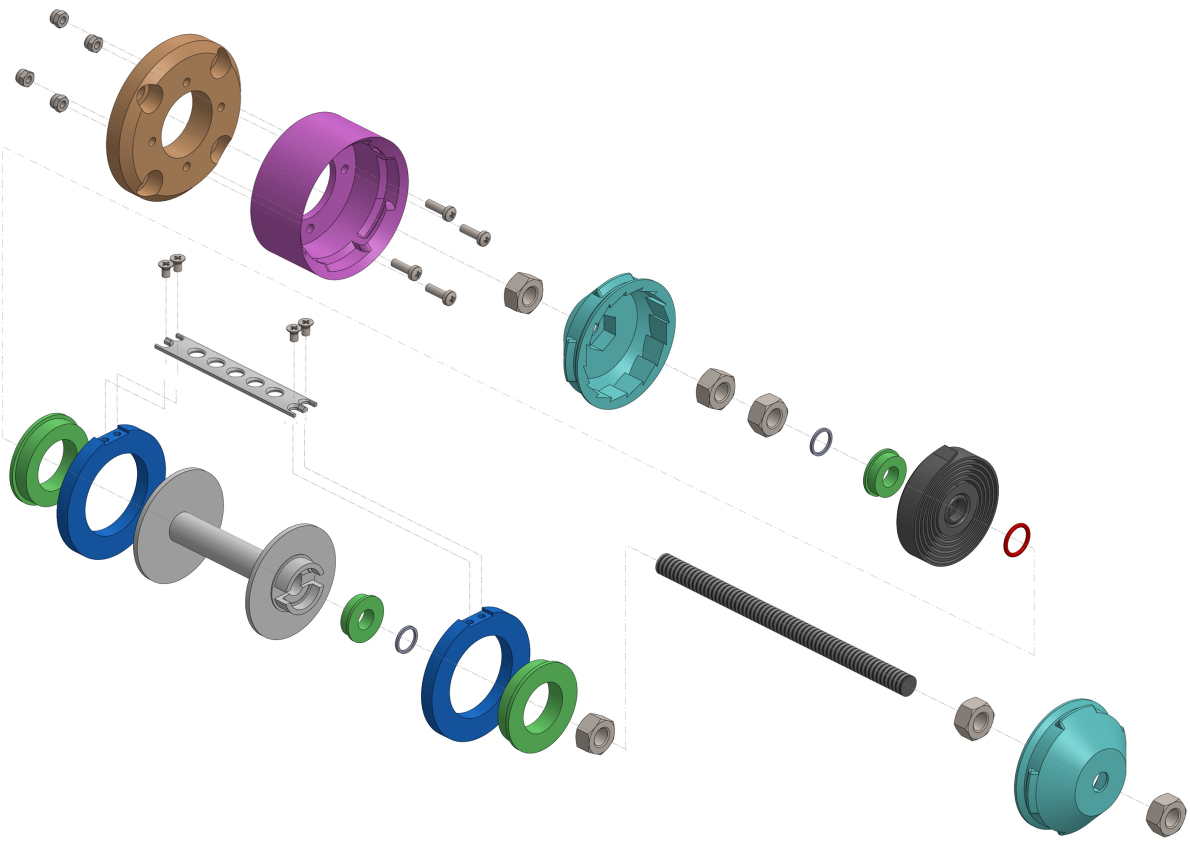

Figure 6.15: Penetrating head (exploded view)

6.3.4. Hourglass Supports

Because the winding head needed to pass through the rings to wind around the support, some problems with the sequence occurred. To prevent this, the supports were changed back to the standing supports of the winding board. However, due to a change in the winding head design, both the supports and code required modifications. This was caused by the shift in the dispenser's position. Instead of being located at the end of the head, which was the case in the previous dispenser, the dispense place was now placed more centrally, with the tip reserved for making connections. As a result, the elevations had to be reduced, and the supports were enlarged to ensure that the rope could still attach to the support and slide off toward the centre. This issue is illustrated in Figure 6.16, where either the bolt at the end of the winding head collided with the rope, or the rope failed to remain on the standing support (even when using the design cap). The improvement is shown in Figure 6.17, where the distance from the outer bolt to the dispensing point is increased. This adjustment allowed the rope to stay attached to the support.

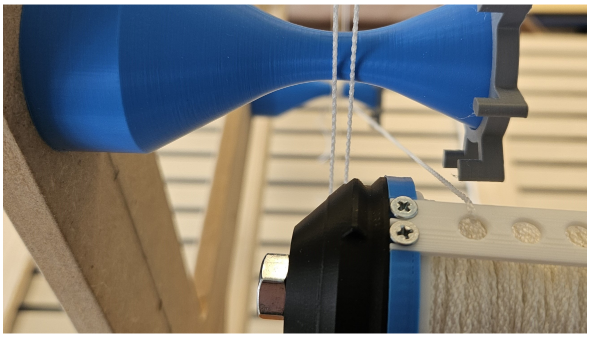

Figure 6.16: First standing support

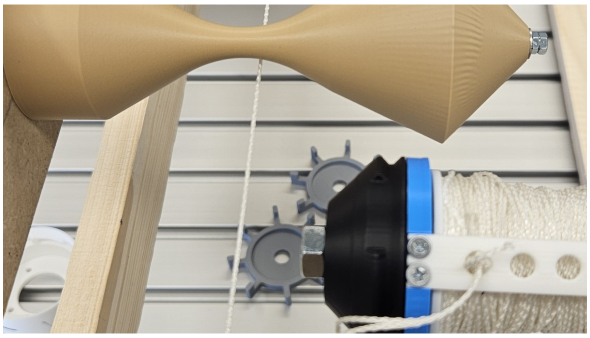

Figure 6.17: Improved standing support

In addition, the curvature of the support also played an important role in the design. Initially, the first (white) support caused the rope to slide off too easily. This resulted in redesigning the support to include a curved radius. The blue supports worked for the board setup, but they became insufficient for the new standing setup. This led to experiments with red supports. All supports are shown in Appendix A.

The first adjustment involved increasing the support height, which successfully kept the rope in place. However, the large diameter at the top created a new problem: the robotic arm could not reach all positions anymore. This required either a change in the setup or further optimisation of the supports. The supports were adjusted by first changing the angle to encourage the rope to slide off from the top of the supports towards the smallest diameter in the middle, followed by completely removing the curvature and using straight edges. This change ensured that the rope no longer rested above the narrowest part of the support, but instead slid directly down to the intended location. This led to the final design as shown in Figure 6.18.

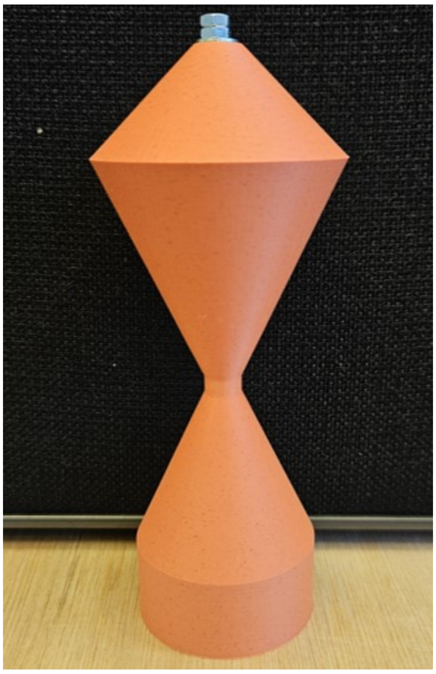

Figure 6.18: Final standing support

6.4. Robotic Path Creation

Beside creating prototypes of the winding board, standing setup, the rope dispenser and the various types of support points, controlling the path of the robotic arm also plays an important role in the process of filament winding. There are some requirements which need to be applied within the code to control the robotic arm. These are stated in Table 6.2.

Table 6.2: Design requirements

Design requirements robotic path	
1.	Guides the robotic head to the intended position
2.	Has a start and end point
3.	Moves around the supports
4.	Avoids collisions with the spanned rope
5.	Adjustable robotic properties
5.	Automated process

These requirements are used to create a workflow for the code. The code to create the robotic path is constructed using Grasshopper, which is a Rhino plug-in. This program allows to set up a parametrically based model. This requires the input of the dimensions, which will be explained in both 6.4.2 and 6.4.3. These dimensions will create the theoretical path. this path will later be combined with the robotic arm parameters. These allows to provide the acceptable deviation and speed of the arm. Everything in between the created path and the final trajectory will be determined by the Hal robotics plug-in inside grasshopper.

This simplified workflow of the code for the trajectory is shown in Figure 6.19. This workflow starts with a grid layout corresponding to the built setup. After that, two paths are created to allow for both movements. These are then combined depending on if the head had to move around the support or through the plane. When these codes are combined a path consisting out of coordinates is created. These coordinates are then used for the robotic arm to create all the needed movements which will allow the robotic arm to move from point to point.

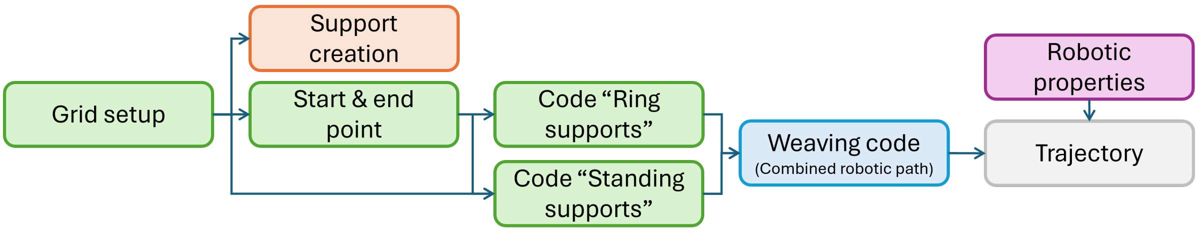

Figure 6.19: Path workflow

Before the prototypes were created, the code was used to determine the maximum dimensions. These dimensions are based on the range where the robotic arm can use all degrees of freedom. Else, the robotic arm will have limitations in moveability resulting in inaccuracies or even skipping parts of the intended path. The path needs to take the supports, winding head and spanned ropes into account, to make sure that collisions will be avoided. The first winding setup is shown in Figure 6.20 and the path creation in Figure 6.21.

6.4.1. Grid Setup

The grid is determined using indexes linked to a coordinate. By linking the coordinates to an index number, the change caused by parametric adjustments will be taken into account automatically. This ensures that the gridlines remain consistent even if the setup location changes. Both axes correspond to a number, ranging from 0 to 5 as shown in Figure 6.22. The index value can be obtained stating at counting the x-axis and afterwards the y-axis. The index number is determined using the following formula:

$$\text{Index\_number} = X_{\text{axis}} + Y_{\text{axis}} \times (X_{\max} + 1)$$

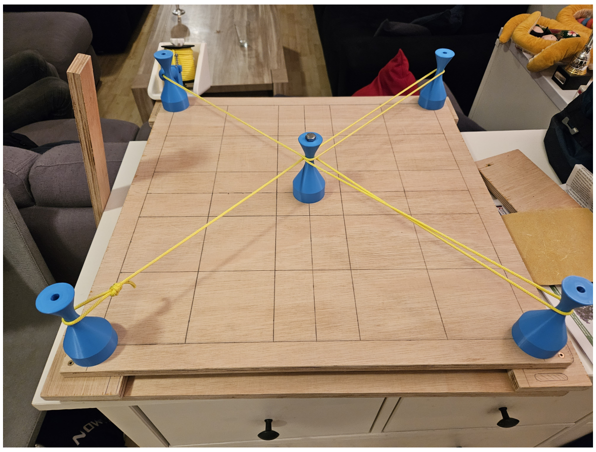

Figure 6.20: Winding setup

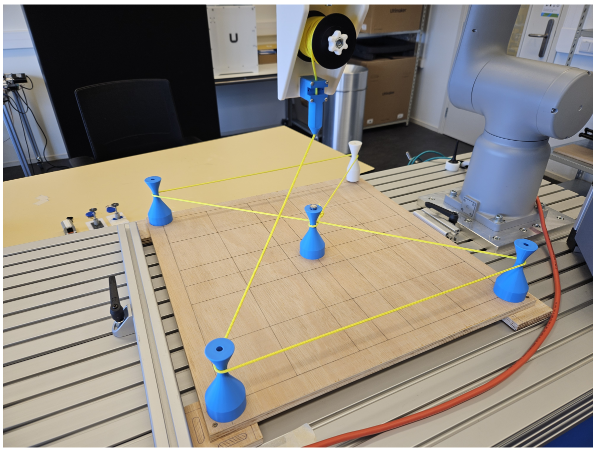

Figure 6.21: Winding path

Where $X_{\max}$ and $Y_{\max}$ represent the highest grid numbers. Additionally, a midpoint is included, corresponding to the highest index number from the grid plus 1, as illustrated in Figure 6.23. The midpoint is determined using the following formula:

$$\text{Middle\_index} = 1 + X_{\max} + Y_{\max} \times (X_{\max} + 1)$$

Figure 6.23 shows the index numbering used for a 3 by 3 grid, which is commonly used in the report. These grid points are used to create line in between the support points. These lines are the bases of the path creation.

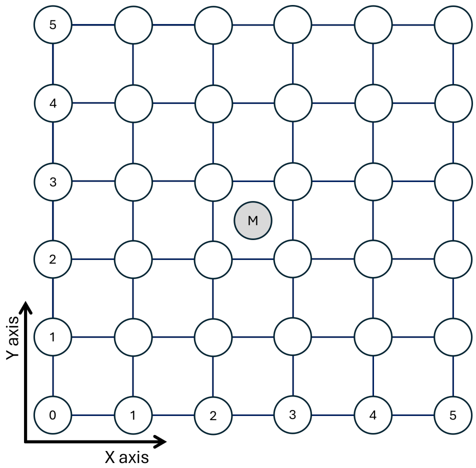

Figure 6.22: Gridpoints with axis numbering

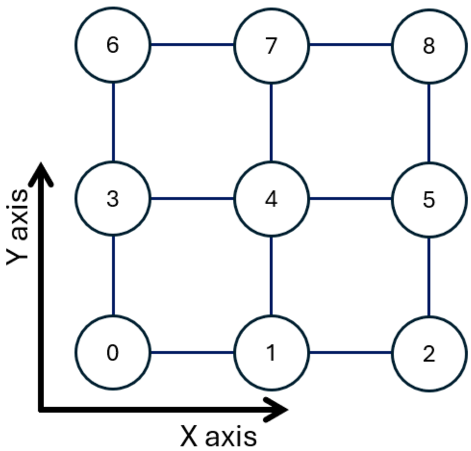

Figure 6.23: Indexpoints for a 3 by 3 grid

6.4.2. Ring Support Code

The ring support code is also called the 'go through code'. This is the code which makes the dispenser penetrate the winding plane of the setup. The ring support code will be used as the ground work for the entire could wich will create the trajectory of the robotic arm. Figure 6.24 shows how the path is created used several parametric aspects. It starts with the two grid points assigned by a certain index. Between these points a line is created. This line is then moved out of plane (1) to prevent the winding head from colliding with the spanned rope. This line is then duplicated and can be moved up and down as well (2). From this line the middle point is selected which can move outwards (3). In addition, both lines (4 & 5) can be scale towards the inside and outside as well.

This creates 7 points in total. These points will be the bases of the ring code path. Both the direct lines in between the points (grey) and a curved line (green) is shown in the winding path subfigure.

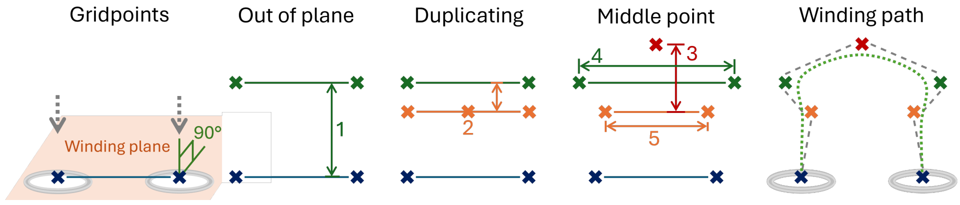

Figure 6.24: Ring path step by step

6.4.3. Standing Support Code

The standing support code is meant to go around a certain point. These grid points are the locations at which the support is attached. There are two kinds of paths to go around the support. Both paths will be explained and are shown in Figure 6.25 & 6.26. The first one is based on an angle bigger than zero, and smaller then 180 degrees. This starts with creating two intersection points between the purple circle and the blue line. Then the middle point of the created line between the intersection points and the grid point (centre point) creates a unity vector direction towards the outside, so the winding goes around the outside of the support. After some geometry is established, the following parametric points can be determined. Two sets of points can move in both directions from the middle support (3 & 5), in addition these points can also be scaled (4 & 6). The last point is the endpoint (2) which moves towards the outside.

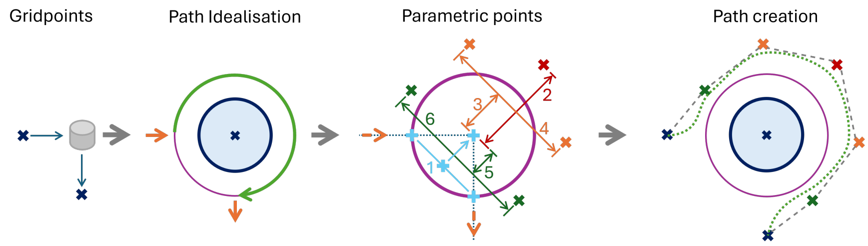

Figure 6.25: Standing support angled corner

The second one is based on angles of 180 degrees. This also makes use of the intersection points. After creating a line between the intersection point including a midpoint the line is being rotated by 90 degrees. This because both sections are parallel making it impossible to use unity vectors. This create points at both sides, in which the correct one will be selected at a later stage. By having a line in between the intersection point and a selected side, the geometry can be used to determine the parametric points. To make sure the height can be controlled correctly it has two points at both sides of the purple circle. These can be moved (7 & 9) and scaled (8 & 10). Finally, the middle point ban be moved outwards (11).

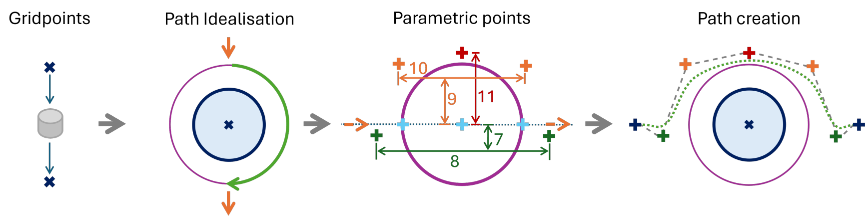

Figure 6.26: Standing support straight line

To chose either the clockwise or counterclockwise direction for the 180 degrees path the length towards the next point is being used. It takes the middle point of the first locations (coordinate lined to the indices) and measures the distance to either of the points. The shortest distance is selected to be the first point, and the longer distance will be the second point.

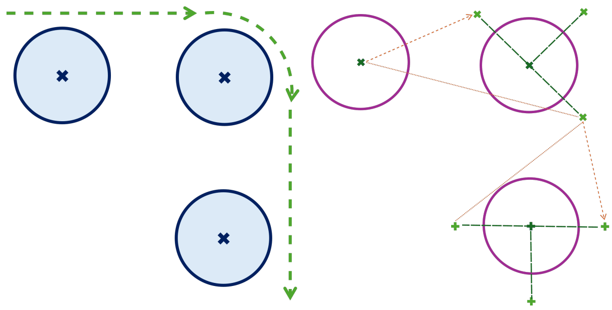

Figure 6.27: Corner path and topology

6.4.4. Weaving and Path Creation

For the final robotic path, both parts of the code need to be combined. The ring code ensures passage through the plane and the creation of connections, while the standing support code prevents the head from colliding with the supports. The combined code setup is shown in Figure 6.28, which focuses more on the weaving of the code. In addition, Figure 6.29 illustrates the schematic differences in direction. It is not linked to a coordinate system, but the axes indicate the direction of movement. For example, if the trajectory moves around a support, it shifts within the winding plane. By contrast, if the trajectory passes through the plane, only one in-plane direction remains while an out-of-plane movement is added. The 3D visuals are shown in Figure 6.30.

The winding begins with the starting coordinate (S), which is assigned in the code. From there, the path runs from midpoint M4 to midpoint M10. Between these points, two options are available: either passing through the plane when a connection is required (base path: 5, 6, 7, 8 & 9), or going around a support to replace the other point (R5, R6, R7, R8 & R9). This selection occurs automatically when one of the outer ring indices is used; otherwise, the middle index number can be replaced with any coordinate within the plane. Finally, once all coordinates have been processed, the sequence finishes at the same coordinate as the start. The Grasshopper code is included in Appendix B, along with all parameters used.

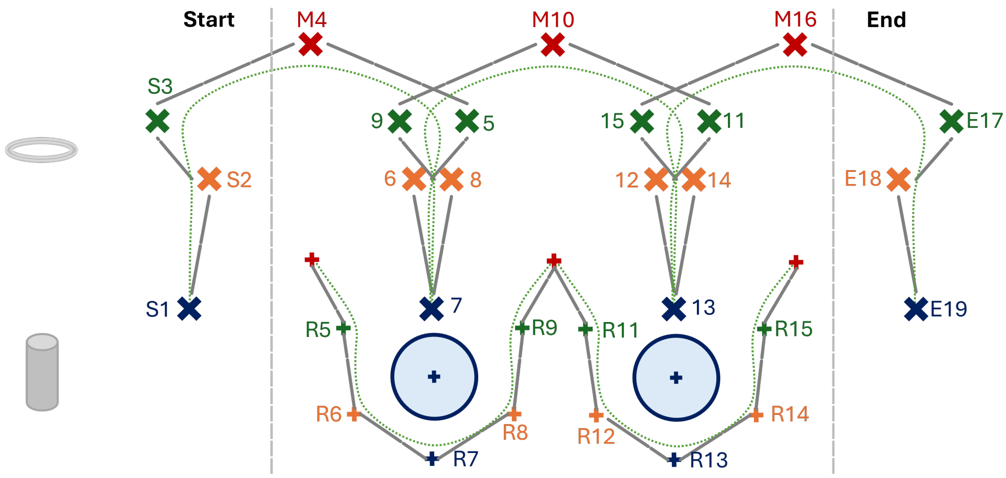

Figure 6.28: Combined path

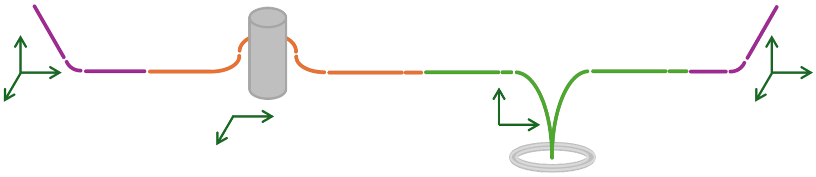

Figure 6.29: Combined path (3D)

When applying this code, a 3D trajectory is created. Figure 6.30a shows a simplified path that the robotic arm could follow. This sequence includes one “go-around” and one “go-through” movement. The colours indicate the direction of movement. Furthermore, Figures 6.30b to 6.30j show the different stages of the Grasshopper code. It begins with the initial movement from the starting point, followed by two “go-around” and one “go-through” movement, ending with a return to the starting location. Finally, note that the red supports in Figure 6.30a are in the same position as in Figures 6.30b to 6.30j.

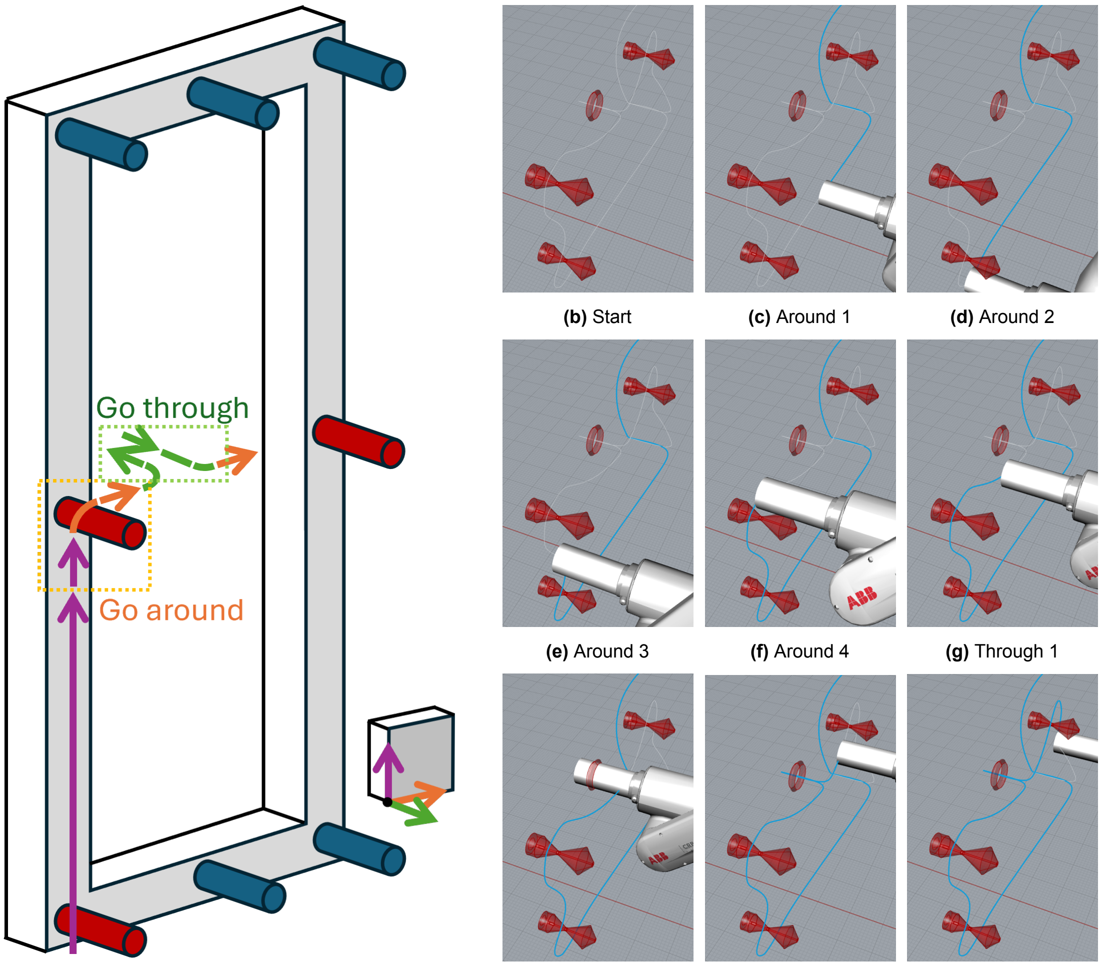

(a) Combined path sketch (3D)
(b) Start
(c) Around 1
(d) Around 2
(e) Around 3
(f) Around 4
(g) Through 1
(h) Through 2
(i) Through 3
(j) End

Figure 6.30: Comparison between 3D sketch and Grasshopper paths

7 Experimenting

In the previous chapters, the setup and theoretical principles for creating connections have been explained. The setup can be used to wind the rope around the supports, and the parametrically designed code generates a sequence that defines the robotic arm's path. When combined with the theory of creating interactions, this should enable the fabrication of specific patterns. However, before these patterns can be manufactured, several aspects of the winding process must be considered. For example, to make sure the nodes will stay in its intended place and and finding out if it is even possible to create an interaction without damaging the shape of the setup. Because of this, the chapter begins with analysing repeating patterns, followed by an exploration of winding angles. The importance of sequencing is then demonstrated, concluding with the practical creation of various connections and topologies. In all these experiments a nylon rope with a diameter of 1 mm is being used. Finally, These results will be analysed and applied in the final design.

7.1. Pulley Effect

When using repeating patterns the pulley effect can occur. The pulley effect influences the nodal position. This shift in position is caused by the increasing number of strands, changing the total force in one direction, affecting the equilibrium. Figure 7.1 shows a decreasing pulling force due to the increase in number of pullies in the system. Additionally, the length of the spanned rope varies between different configurations. To analyse this behaviour, unit vectors are used to represent force directions. This allows an understanding of equilibrium without needing exact force values. A resistance factor is also introduced to account for differences in tension caused by friction. This simulates how previously tensioned ropes resist movement more than newly wound ones. Such resistance can arise from interactions between the rope and either itself or the supports. Predicting the location of the middle node can be seen as a difficult task because of the force dependency. Altough categorizing them can help understand which topologies can be useful, because in these case the point tends to keep its desired position.

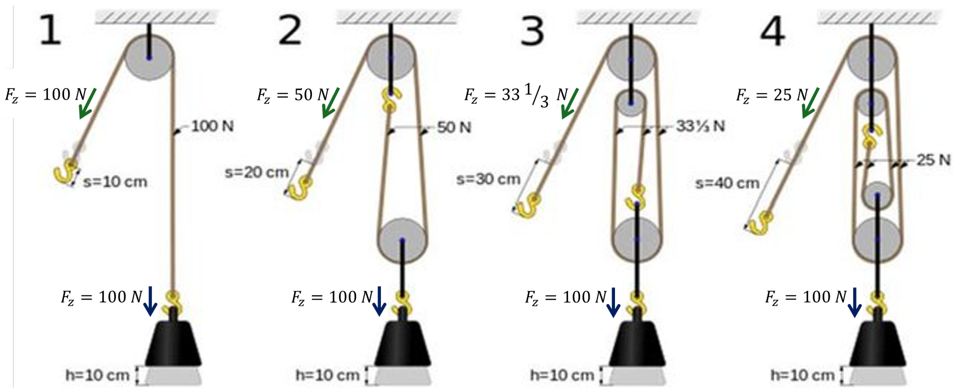

Figure 7.1: Force difference due to the pulley system [22]

During the winding process, the rope length can significantly influence the new equilibrium position, particularly when the pulley effect occurs. This is illustrated in Figure 7.2. The effect begins with a diagonal rope spanned between two fixed supports. A second rope is then wound between one fixed support and the midpoint of the diagonal. This rope weaves back and forth, interacting with the spanned line. The grey line in Figure 7.2 shows the shift in location between the first and second interaction, where the rope has made an additional loop around both the support and the diagonal. Although only one configuration is shown, the test was performed with multiple setups.

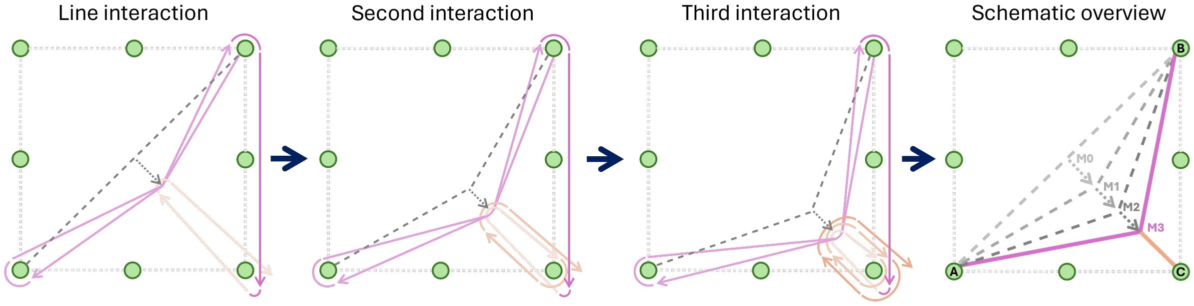

Figure 7.2: Pulley effect on the rope

This interaction has two main consequences. First, the tension in the diagonal increases due to the repeated wrapping of the second rope, which acts like a pulley system. The force applied by the winding head is effectively multiplied as it is distributed over multiple rope segments (individual orange lines). Second, each configuration has a specific geometry where the combined length of both the rope segments, for example from bottom-left to top-right (A to B) and from bottom-right to the central point (C to M), reaches a minimum. At this point, the rope is more likely to shift, making the middle connection point more prone to displacement.

There are three general scenarios based on how this minimum length develops. These are shown in Figure 7.3, 7.4 & 7.5. One out of the three scenarios occur depending on the ratio of the rope length comparing the line between two fixed supports and the interaction line. Ratio of the rope length compares the extremes. In this case the initial state and the final state where point M became the same as point C. All needed points are in between these two, else the point is out of bound for the setup, meaning that it is unreachable. This ratio helps to indicate the stability of a node.

$$\text{Ratio} = \frac{\text{distance of AC} + \text{distance of BC (final state)}}{\text{distance of AB} + \text{distance of CM (initial state)}}$$

Scenario 1: The total rope length continuously decreases until it reaches the end point (for example, the bottom-right support). As the force increases, the rope length keeps decreasing. The middle point slides off or moves immediately towards the support, making it unsuitable due to its instability and unpredictability. In this case the ratio keeps decreasing towards the minimum.

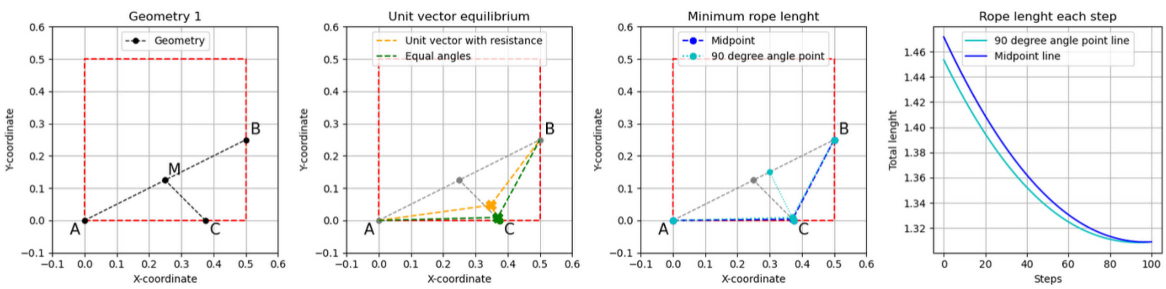

Figure 7.3: Rope lenght scenario 1

Scenario 2: The rope length decreases at first but increases again before reaching the end point. The middle point shifts incrementally towards the support and eventually reaches it after several repetitions. This is because each loop increases the force while the overall rope length continues to reduce compared to the initial state. The ratio will increase, but stays below the ratio of the initial state.

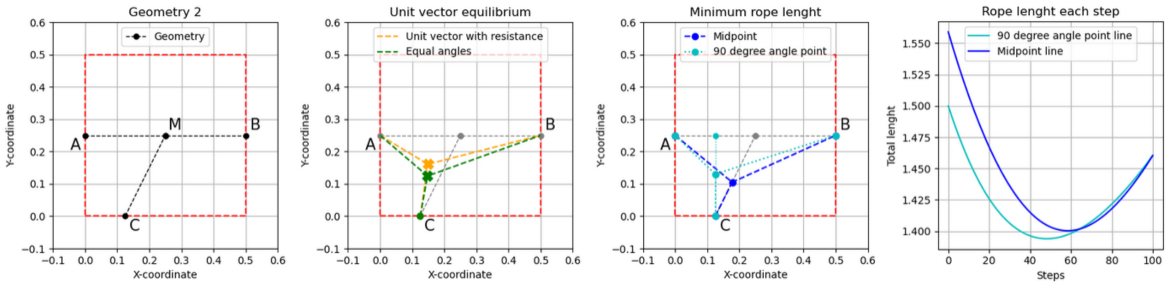

Figure 7.4: Rope lenght scenario 2

Scenario 3: The rope length decreases initially but then increases to a value greater than the original. This may result in a relatively stable point, as the force from the pulley effect exceeds the opposing forces. Movement would require additional rope length, which the high tension in the interaction rope resists. Deformation is then absorbed by the rope's elasticity, resulting in a stable knot. These nodes have a ratio which is higher compared to the initial ratio.

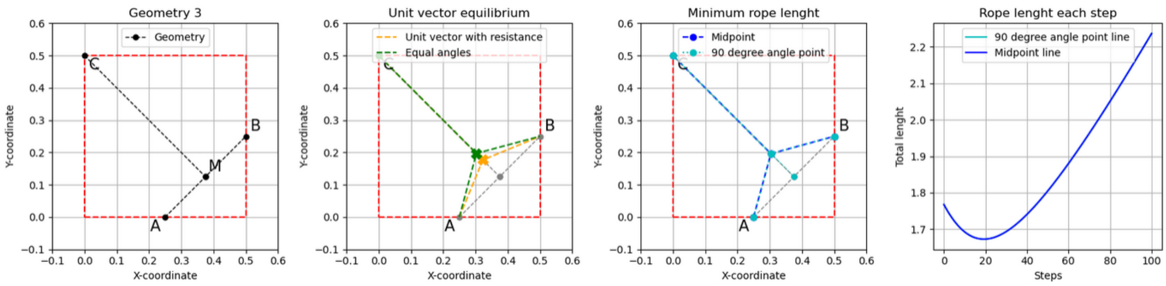

Figure 7.5: Rope lenght scenario 3

Although all three scenarios are possible, this research focuses on topology and sequence. Therefore, the influence of force magnitudes on the prediction of the nodal position is excluded. While the pulley effect can theoretically create a stable knot, the risk of producing unstable nodes outweighs its benefits. This because for every topology, the ratio needs to be determined also taking into account that topologies can shift when new ropes are spanned to exsisting once. For this reason, repeating patterns in combination with non-fixed support points are not recommended.

7.2. Slide Off Angle

This section introduces the influence of friction and tension on the shape stability of a single wound rope connections. Because due to the force, the shape of the connection tends to go towards a new equilibrium. In a situation where the friction does not have any contribution and the force of the rope will be constant over all the ropes, the equal force equilibrium from Figure 4.7 will occur. Nevertheless, friction will play a role within these designs. The friction can be created by the rope interacting with another rope, or the winding around the supports. The larger the friction, the more unevenly the force is distributed. This can be explained by the fact that after the first cable is wound around a support, the tension will be approximately the same in the whole fibre both before and after the support. But after the rope is wound around a second support the part of the rope which is further away from the winding head tends to be less adjustable in tension. Moreover, if a loop is created the tension will become even less influential comparing the part before the loop and after, because the friction is resisting more movement.

7.2.1. Maintaining Equilibrium

In addition to the force equilibrium and friction, the angle at which the rope starts to move also plays an important role. It could for example influence the intended shape by added more lines to each other. This is shown in Figure 7.6. It starts with a diagonal base line. To this diagonal another line is connected creating the first interaction. This interaction has two equal angles at both sides between the green and purple line due to the force equilibrium. After spanning the third orange line to the purple line, the purple line creates an equilibrium with the orange line. In addition, this also effects the first equilibrium between the green diagonal and the purple line. It will create an angle, which could be seen as the slide off angle. As long as the friction resist the rope to slide off, the shape will be the same as the intended position. If it would slide off, the interaction points could move changing the desired location of the interaction, which could result in a slightly different topology. In Figure 7.6, this could result in a movement from the intersection point to the bottom left side. A change in topology by the rope itself is undesired, which should be prevented at all times. The slide-off angle helps indicate the potential risk of nodal movement and should be used to prevent topological shifts during the design of paths.

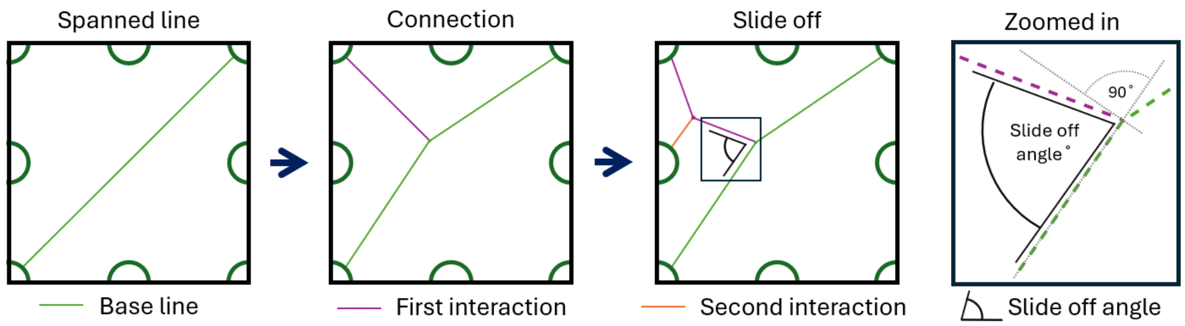

Figure 7.6: Importance of the slide off angle

7.2.2. Sliding Setup

Performing the experiment will start spanning the rope between two fixed supports. This will be done in several direction ensuring that the minimum slides off angle can be found despite the differences in length and direction. The main line is spanned between two fixed supports while ensuring tension independent of the winding head. This will be done for a diagonal line, and two straight lines measuring both from the bottom and topside of these ropes. The robotic path will be created parallel to this spanned rope. This allows the length of the rope to keep increasing due to the movement of the robotic head, to keep the rope in tension. The robotic head moves in small segments of 25 mm with a maximum speed of 25 mm/s, followed by a break of 0.1 seconds between every segment.

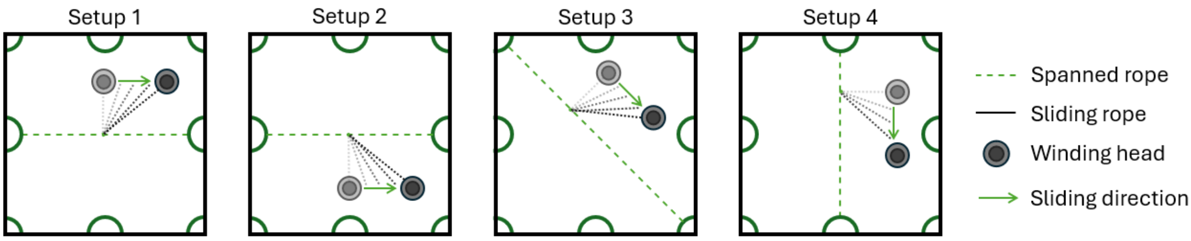

Figure 7.7: Angle evaluation setups

The slide off angle is measured from the original starting point to the winding head just after the rope moved. Meaning that as soon as the rope starts to slide, the interaction points from before it slid away and the final position of the robotic head is used to determine the angle. This help to predict from what angle the interaction between the ropes could possibly move and become unstable. A movement can go from sliding consistently over the rope when a small angle creates the movement, towards a large angle when the interaction suddenly jumps towards the new equilibrium. This test assumes that there will always be tension on the cable. Without tension, there is nothing to resist the movement and the slide off angle is predicted to be close to 0. The method from measuring the angle could be improved in accuracy by using the exact coordinates instead of measuring the angle. Although, it is not needed for this experiment because the experiment only wants to know when the rope starts to slide combining all cases. The angle starts at a 90-degree angle, so perpendicular to the rope and will slowly decrease the angle till it starts to slide off.

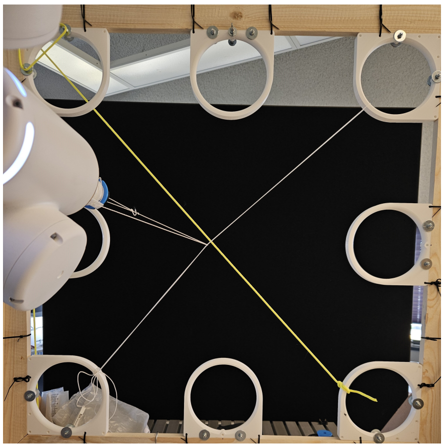

Figure 7.8: Slide off test 1

Figure 7.9: Slide off test 2

7.2.3. Allowable Angle

In total the test is performed 40 times divided over all setups. Each setup is used in both the sliding direction as shown in Figure 7.7 and the opposite sliding direction. This led to the following results. Figure 7.10 shows how many times at which angle the rope connections based on friction started to slide off. Figure 7.11 shows the visual representation of the angle slide off.

These results are are split into two categories. The lowest 90% of the values are coloured orange, the other 10% is coloured yellow. The angle equal 90° when the sliding rope (connecting rope) is spanned perpendicular to the spanned line (first line). When the angle increases, the angle values will decrease. The angle orientation is shown in the zoomed in picture of Figure 7.6. Out of the 40 measurements the first rope started to slide at an angle of 79°, which is an eleven-degree offset of the perpendicular line. The biggest measured angle equals 61°. No bigger angle has been found during testing.

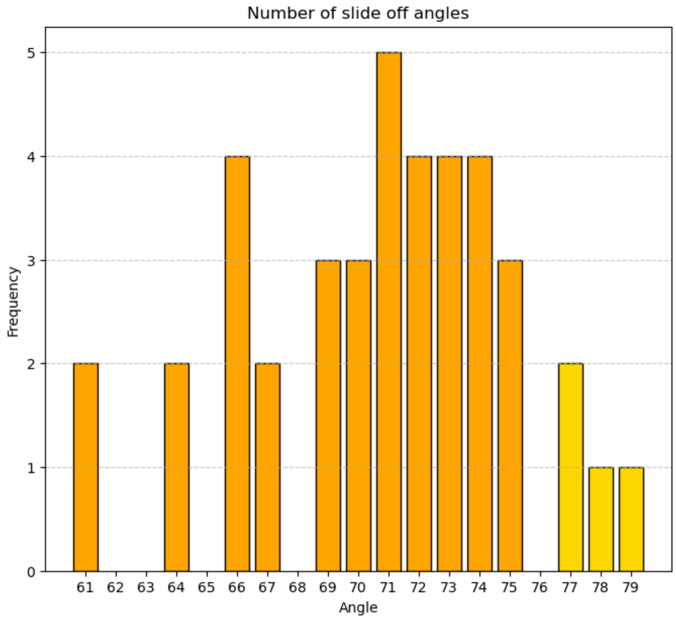

Figure 7.10: Histogram of the slide off results

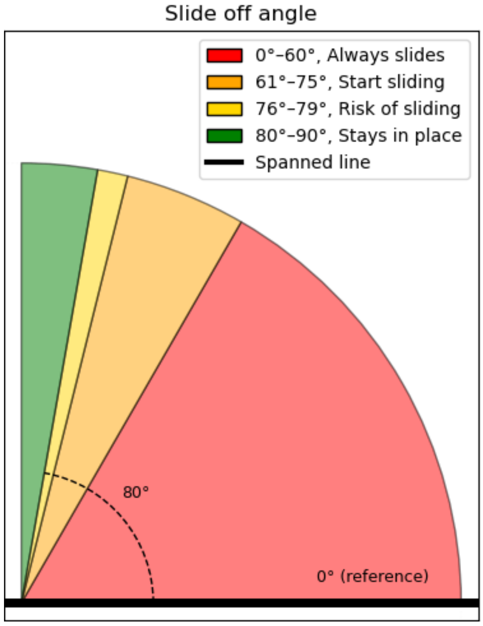

Figure 7.11: Slide off angles

These results are used to determine the maximum allowable angle at which an intersection point can be considered stable. As long as sufficient tension is maintained in the rope, friction between the rope and its surroundings prevents unwanted movement at the interaction points. This friction is essential to the stability of the system. Test results indicate that rope angles can deviate by up to 10° from the perpendicular (90°) before the rope begins to slide. Within this margin, the connection remains stable in position. However, if the angle exceeds this limit, the friction may no longer be enough to prevent the rope from sliding towards a new equilibrium. This unintended movement can shift the location of the intersection point, thereby altering the intended topology of the wound structure, something that must be avoided.

This 80-degree threshold is therefore considered the critical angle, allowing a deviation of 10-degree from the ideal alignment. However, it is only valid if the rope remains under tension to generate friction; without it, the rope is free to move. The main aim of this criterion is to ensure that minor rope adjustments do not result in changes to the location of knots or interactions, which is essential for preserving the designed layout. For this reason, it is recommended to begin winding as close as possible to a 90° angle. The 10° tolerance can then account for small deviations caused by the influence of other connected fibres as shown in Figure 7.6.

7.3. Connecting Sequence

Creating connections through rope interactions requires not only the right topology but also a carefully considered winding sequence. This begins with a blank setup that allows fixed supports to be attached. These supports serve as anchor points around which the rope can be wound. To generate rope interactions, a line must first be spanned between two fixed supports. This enables a second line to connect with the first, forming an interaction point.

When a third rope connects to a junction formed by two independent ropes, the winding sequence plays an important role. This concept is illustrated in Figure 7.12 and Figure 7.14. Both setups shown have a similar topology, but they differ in the winding order. In one setup, the sequence is mirrored compared to the other. This can be seen when looking to the green cross. In the one senario, it starts at the bottom left side 7.14, and in the other at the bottom right side 7.12. This reverses the effect of which rope layer lies further away and which layer lies closer to the new, incoming rope. After the initial cross is formed, a third rope is introduced to establish a connection at the non-fixed support point located at the centre.

Figure 7.12 shows the schematic overview of the first sequence followed by the actual winding setup which is shown in Figure 7.13. This creates a connection where the ropes interact.

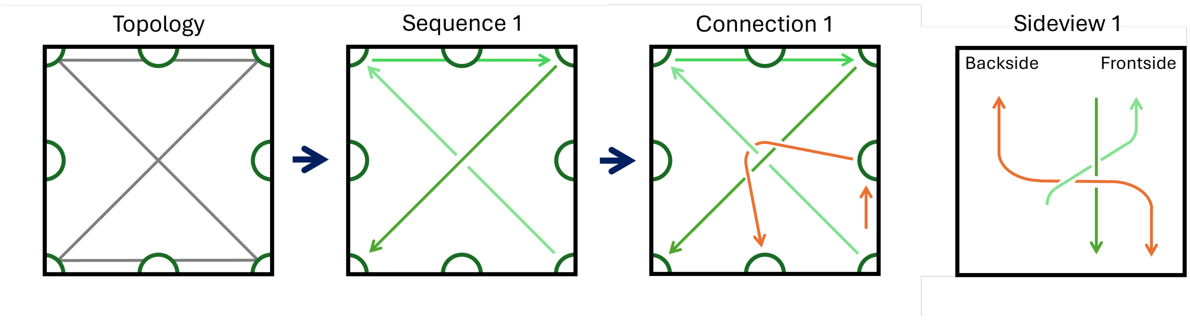

Figure 7.12: Connecting sequence clockwise cross

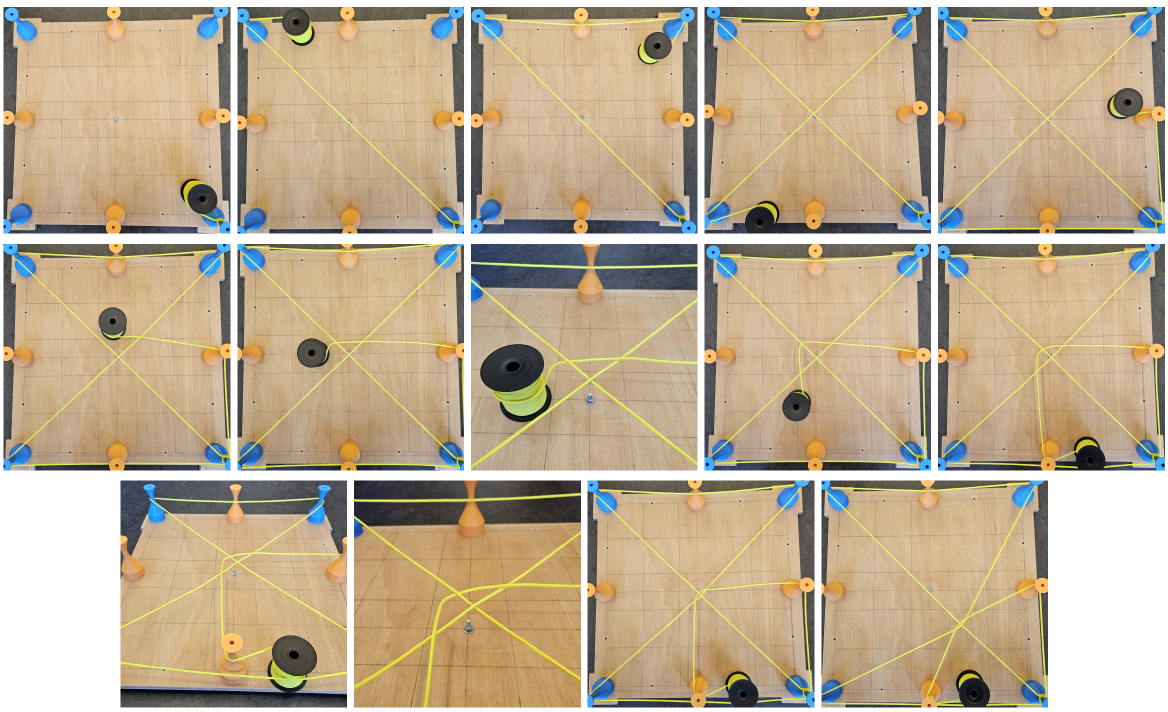

Figure 7.13: Actual example of Figure 7.12

On the other hand, Figure 7.14 shows the schematic overview of the second sequence followed by the actual winding setup which is shown in Figure 7.15. this winding path tries to creates a connection at the location where the ropes intersect, but is unable due to the used sequence.

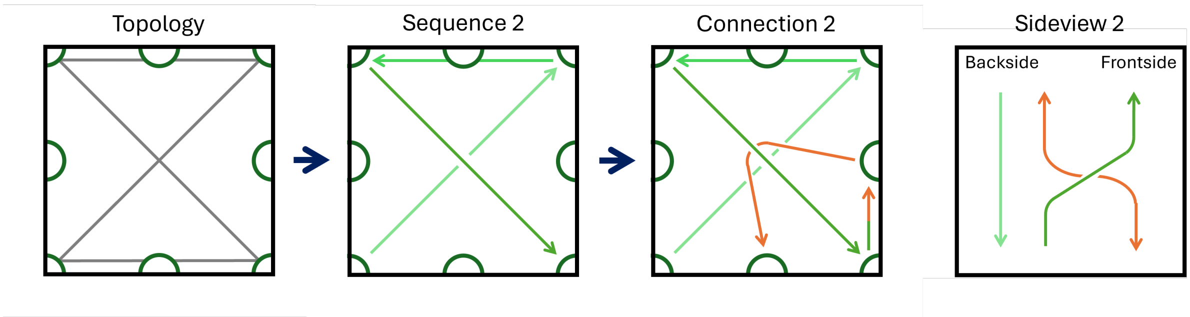

Figure 7.14: Connecting sequence counter-clockwise cross

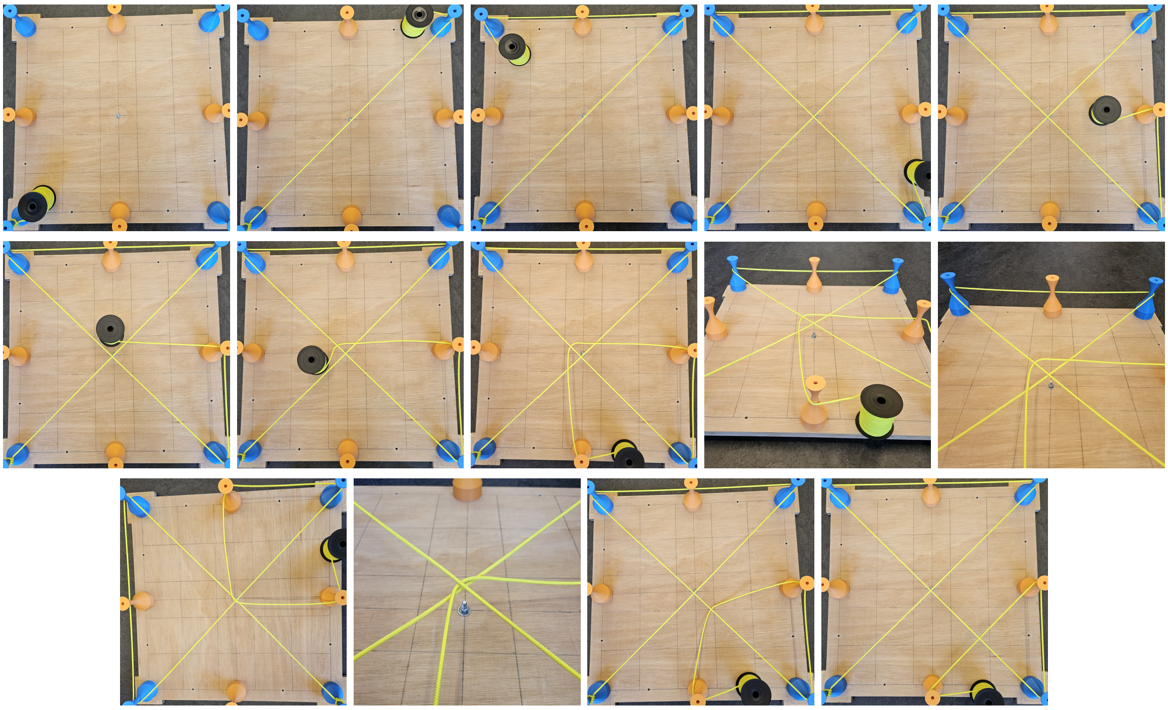

Figure 7.15: Actual example of Figure 7.14

In Sequence 1, the final connection is made to the lowest layer of the crossed ropes, ensuring the new line engages directly with all existing ropes. Sideview 1 in Figure 7.12 also shows that all lines intertwine with each other. In Sequence 2, the layering order causes the new line to connect in between both existing lines, reducing, or in this case eliminating physical interaction at the intended point as displayed in Figure 7.14. The second side view does not show any connection with the lowest (backside) rope layer.

In conclusion, although a rope may visually appear to intersect another, this does not necessarily mean it actually does. This is an important consideration when creating a interaction and choosing the most suitable connection method, in order to prevent the spanned rope from failing to interact with the other ropes. This could be prevented by using connections making sure all ropes are combined before interacting.

7.4. Knot Interactions

This chapter investigates how rope interactions can be used to replace fixed supports within a winding system. The main goal is to explore the behaviour of interaction points formed by these rope connections. When considering the force equilibrium stated in Section 4.4, it is expected that the formation of a stable node depends on the resulting force balance. For an equilibrium to be achieved, at least three unique directions (unit vectors) are required for stability. If only two directions are used, the rope will create a single straight line. It is also expected that adding more ropes will gradually reduce the movement of the connection point until it becomes negligible.

7.4.1. Sequences

Connections can be created through rope interactions. These interactions are shown in Subsection 5.3, where three possible connection types are presented. By using one of these methods to connect a rope, a specific geometry and its properties can be formed. To reduce the influence of the winding sequence, all connections are made from the robotic side of the winding plane due to the winding setup. This ensures the sequence becomes less influential. As a result, the "back and forth" and "loop around" methods penetrate the winding plane twice, while the fully looped connection goes through four times. This chapter evaluates these connections to understand the behaviour of the central connection point during winding and assess its stability once all ropes are in place. The primary aim is to identify which topologies are feasible to fabricate. To estimate the final location of the connection, the principle of force equilibrium is applied; for instance, adding another rope may cause the middle point to shift to a new equilibrium.

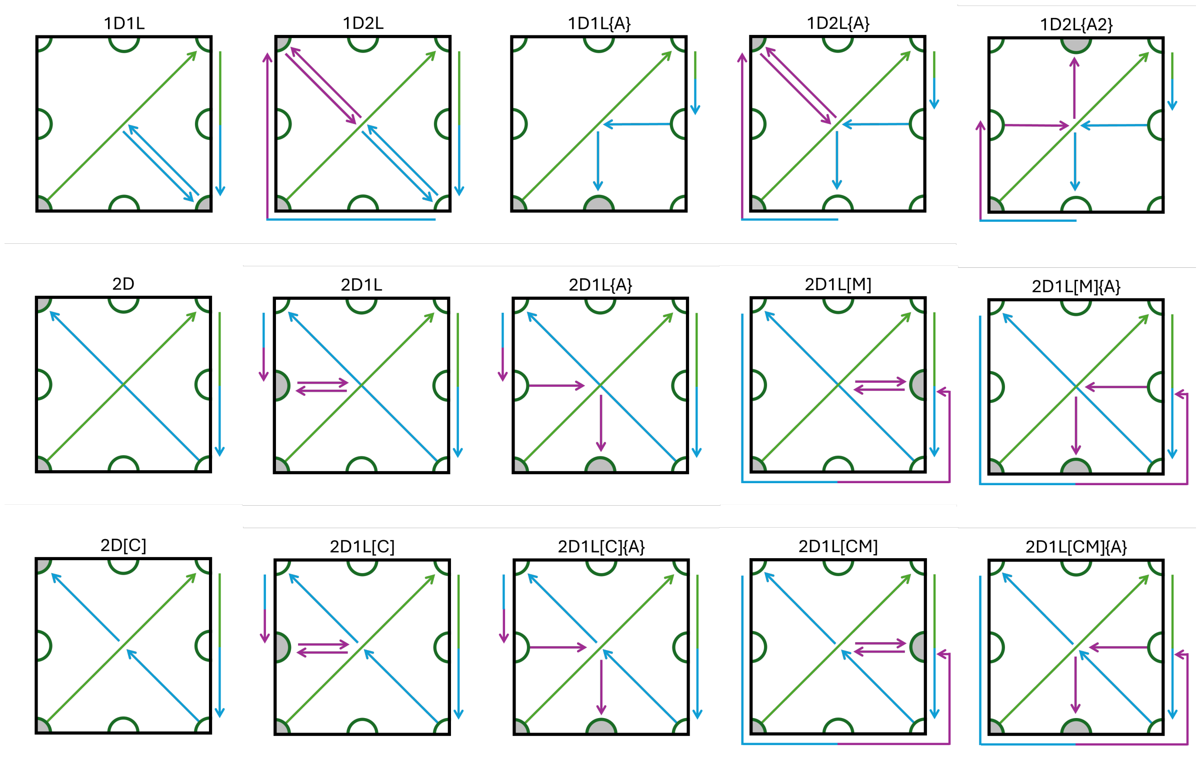

Figure 7.16: Winding sequences (path 1–15)

The desired topologies are illustrated in Figure 7.16 and 7.17. These show the spanned ropes along with their schematic winding paths. The positions of the support points are somewhat arbitrary and can vary without affecting the overall result. What matters are the conditions defined by the naming convention. In this system, the number before each letter indicates how many times that element occurs. Two main letters are used: "D" for diagonal lines between two fixed supports, and "L" for lines that connect one fixed support with a previously spanned rope. Additionally, three optional letters may be added. "C" stands for connection, indicating a loop around a previously spanned rope. "M" stands for more, indicating that a longer path is deliberately chosen instead of the shortest possible, which can increase resistance and prevent movement after tension is lost. Finally, "A" stands for angle, meaning that instead of returning to the same fixed support, the rope continues to another fixed support. This is intended to balance forces and reduce displacement of the middle knot. The starting point is at the bottom-left grey support, and the endpoint is the second grey-coloured circle. The robotic path begins and ends one support to the side of the points shown, to ensure the complete path is formed.

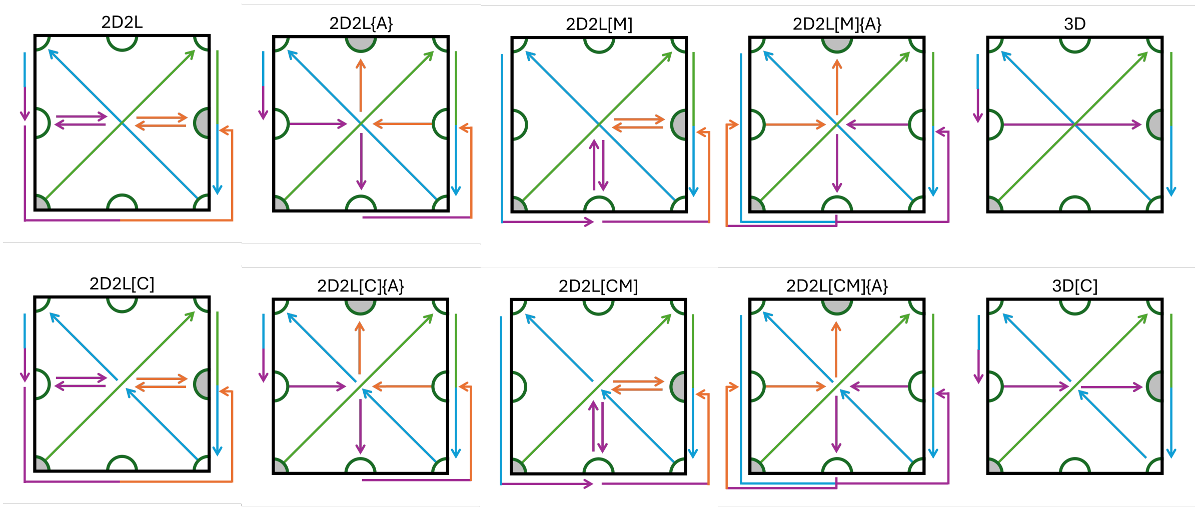

Figure 7.17: Winding sequences (path 16–25)

The experiment is structured as follows. Figure 7.17 and 7.17 display all 25 topologies that are tested. Each setup is evaluated based on several aspects. First, whether the path can be fabricated. In some cases, the rope may slide off due to loss of tension, making it too difficult to predict the required go-through points and thus unfeasible for large-scale use without manual adjustment. Second, how the central point behaves during winding (specifically whether it shifts significantly). Lastly, the stability of the central node is assessed. Once created and correctly positioned, can the knot resist displacement when additional ropes are added, or does it eventually stabilise after a certain number of windings?

To avoid damaging the winding head or disrupting the rope layout, collisions must be prevented. To identify suitable go-through locations, all ropes used in the structure are first simulated as a ground structure to determine the occupied and available positions. This provides an overview of which areas are occupied by ropes and therefore must not be penetrated. The remaining available positions (for example, marked with blue circles) are the closest to the centre point and are free of potential collisions. These positions must be determined prior to generating the robotic path, especially if go-through interactions are involved. This process is also illustrated in Figure 7.18, which compares the intended shape with the actual winding path. The two may differ slightly due to the available go-through

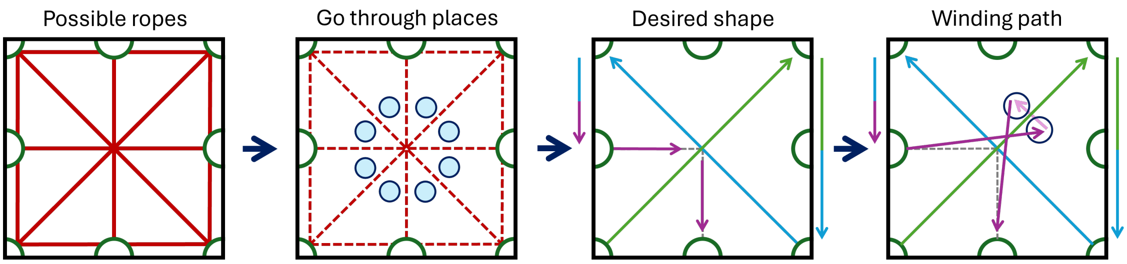

Figure 7.18: Go through limitations

locations. The sequence in which intersections are formed may depend on preferences related to the level of resistance desired during filament winding before hardening occurs. There are two main methods to form a rope interaction. The first is the slide-off angle. When only one rope is spanned, the second line should be spanned in a perpendicular direction. Otherwise, it might slide off to an undesired position. The second method involves routing the rope towards the opposite fixed point from where it started. When the rope changes direction halfway, as in Figure 7.18, the average of both go-through locations should approximately mirror the average of both (spanned) lines. Figure 7.19 illustrates the four used connections. The first is for connecting to a single line, which should be done perpendicularly, as noted in the slide-off angle test which is explained in section 7.2. The second connection is looped around another rope, creating more resistance than a simple crossing. Both angled connections are based on the idea of looping, but are adapted so the rope only penetrates the plane twice instead of four times. Green surfaces in the diagram indicate where and in what order the robotic head can move to the opposite side of the plane.

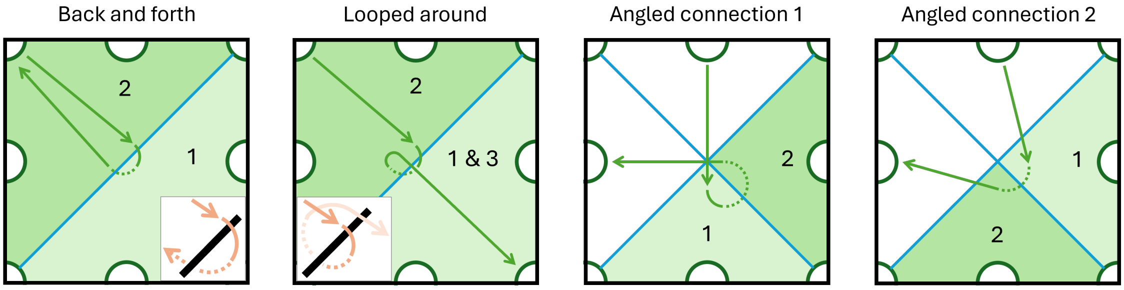

Figure 7.19: Used connections experiment

7.4.2. Topologies

The experiment begins by testing the topologies shown in Figures 7.16 and 7.17, with the goal of creating a stable middle point and observing its behaviour during the winding process. The winding sequence is created using the Grasshopper code and uses the prototypes described in Chapter 6. The setup consists of a 3×3 grid with 25 cm spacing, covering a total area of 0.5 × 0.5 metres. The winding head is positioned by the end of the robotic arm. Instead of the required conceptual second arm, the head penetrates the plane and pauses, allowing a person to manually reposition the rope. The winding head is then reattached to the robotic arm. These results are used to guide the winding of the final design. All outcomes are shown in Appendix C.

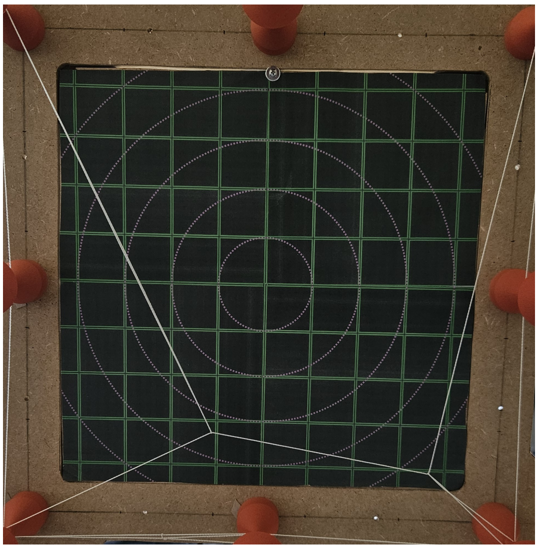

(a) Topology experiment: 1D2L.2 (Seperate side connection)

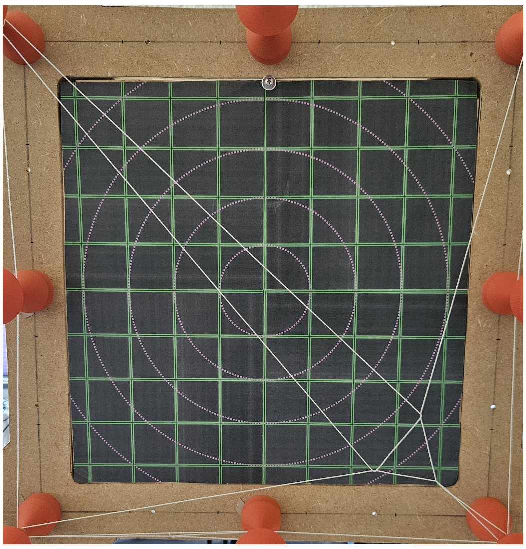

(b) Topology experiment: 1D2L (Integrated connection)

Figure 7.20: Difference in connections

The importance of the connection method is demonstrated in Figure 7.20a and Figure 7.20b, which compare two variants of topology 1D2L from Figure 7.16. The only difference lies in how the second rope is connected. The significance of the connection method is demonstrated in Figure 7.22, which compares two variants of topology 1D2L. In Figure 7.20a, the rope uses the back and forth winding next to one of the sides of the existing winding connection. This leads to the fact that the rope slides off. In contrast, Figure 7.20b uses an angled connection that secures the rope behind the existing one, preventing it from sliding away.

Analysis of the results reveals several patterns. Winding should ideally begin between fixed supports to establish tension and a consistent shape. This initial resistance helps to maintain the desired geometry when creating interactions. If the tension is lost during the formation of connections, the equilibrium point may shift and displace the centre node. Back-and-forth winding increases force in one direction, affecting the node's position.

The results of all tests are summarised in Table 7.1. It begins with the topology code referring to the selected structure and naming convention. The following columns show the horizontal and vertical deviations of the middle point from the centre of the grid. These values are expressed as a vector length (in cm), and the ratio relative to the 25 cm grid indicates displacement. A lower ratio signifies better alignment with the centre. This ratio is used to compare the performance across all experiments.

Table 7.1: Winding topologies deviation overview

Topology code	Horizontal deviation [cm]	Vertical deviation [cm]	Vector [cm]	Ratio [-]
1D1L	20	22	29.7	1.2
1D1LA	7	6	9.2	0.4
1D2L (Separate side connection)	No recognisable middle point			
1D2L2 (Integrated connection)	15	17	22.7	0.9
1D2LA	3	1	3.2	0.1
1D2LA.2	1	0	1.0	0.0
2D	1.5	0	1.5	0.1
2DC	0	0	0.0	0.0
2D1L	15	0	15.0	0.6
2D1LC	7	0	7.0	0.3
2D1LM	11	1	11.0	0.4
2D1LCM	9	2	9.2	0.4
2D1LA	5	4	6.4	0.3
2D1LCA	1	0	1.0	0.0
2D1LMA	4	4	5.7	0.2
2D1LCMA	3	5	5.8	0.2
2D2L	16	0	16.0	0.6
2D2LC	5	0	5.0	0.2
2D2LM	0	15	15.0	0.6
2D2LCM	0	11	11.0	0.4
2D2LA	3	5	5.8	0.2
2D2LCA	0	2	2.0	0.1
2D2LMA	3	4	5.0	0.2
2D2LCMA	2	1	2.2	0.1
3D	0	0	0.0	0.0
3DC	1	1	1.4	0.1

After analysing the data, particularly the vector to grid ratio, several conclusions can be drawn. First, resistance plays a significant role during the creation of these patterns, especially while forming the connections, when the tension in the rope temporarily decreases. This can cause the rope to shift its middle point closer to a new force equilibrium. Loop-around connections help counteract this effect by introducing additional friction, which provides resistance within the rope network. This friction reduces the impact of tension loss during winding. Figures 7.21a and 7.21b show the same dataset from different perspectives. Figure 7.21a compares topologies with and without looped connections, while Figure 7.21b examines longer rope paths and looped configurations.

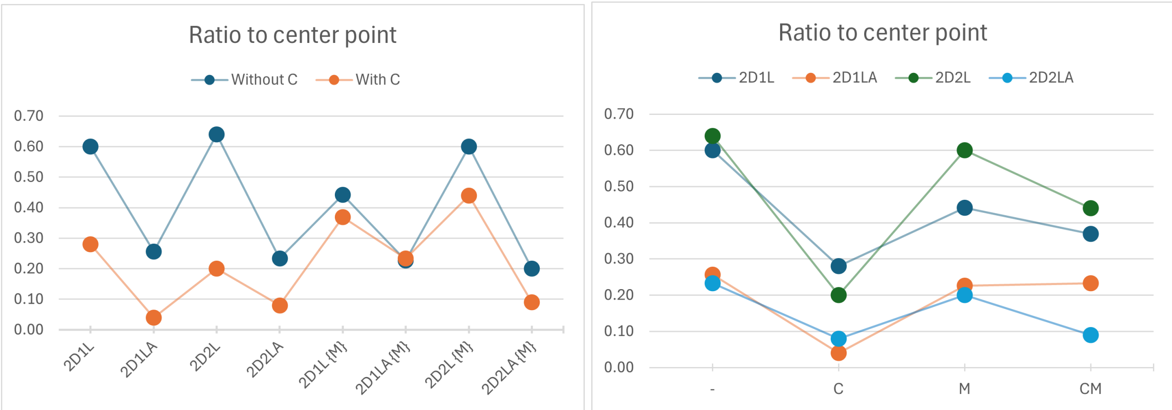

(a) Ratio difference of a connection

(b) Ratio difference between topologies

Figure 7.21: Comparing ratios of nodal deformation

This effect is further illustrated in Figure 7.22, which compares topologies 2D2L and 2D2LC (with a looped connection). In Figure 7.22a, the second diagonal passes through the centre without looping around the first diagonal, resulting in less friction. As soon as the third rope is added from the side, the middle point begins to deform. In contrast, Figure 7.22b shows that the looped connection maintains better centrality, thanks to increased resistance in the rope network.

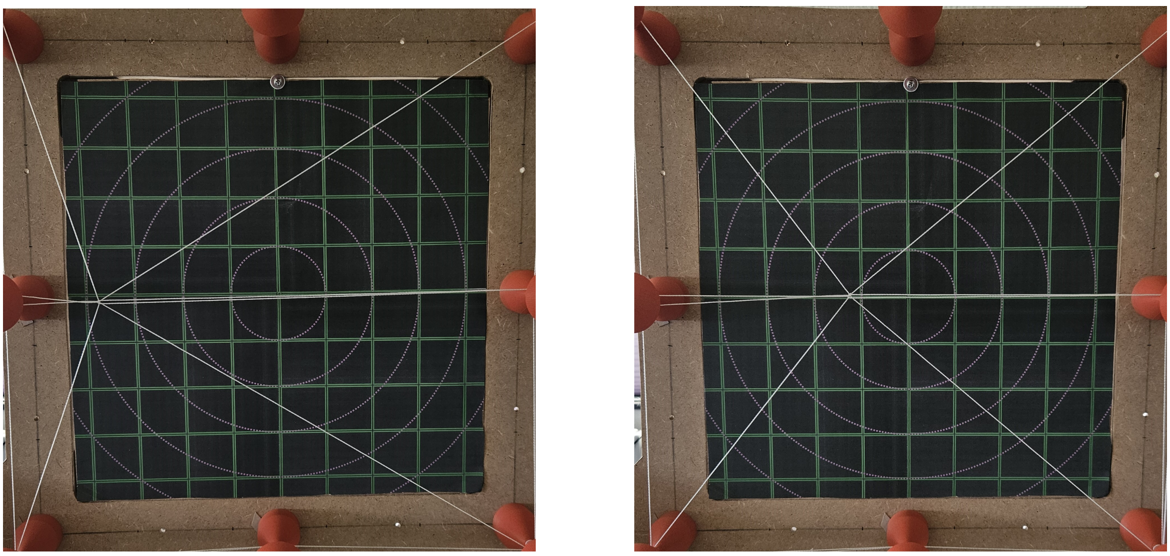

(a) Topology experiment: 2D2L

(b) Topology experiment: 2D2LC

Figure 7.22: Difference in connection

Furthermore, creating straight lines with a middle connection or introducing angled paths contributes to a more stable shape. These methods influence the force equilibrium less than winding back to the same fixed support. As a result, the middle point tends to remain more central. Figure 7.23a shows a looped connection between two diagonals, while Figure 7.23b includes an angled rope in the bottom-left corner. Note that each experiment is conducted from the start. Due to slight variations in robotic pathing and rope tension, small differences may occur between similar configurations.

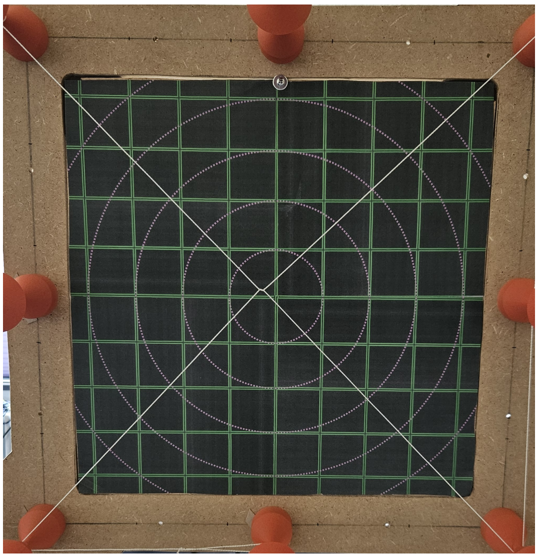

(a) Topology experiment: 2DC

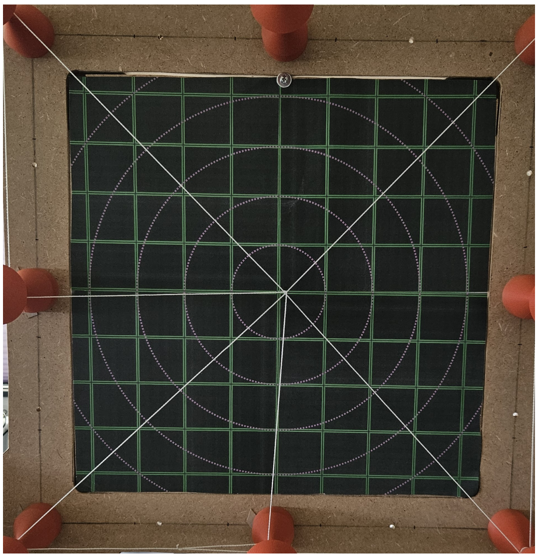

(b) Topology experiment: 2D1LCA

Figure 7.23: Angular line connection

To conclude the experiment, several recommendations can be made for the final design. Loop-around or angled connections are advised. Looping provides friction that prevents node displacement, while angled connections minimise directional force buildup.

Back-and-forth winding increases unidirectional force, shifting the equilibrium and affecting the node's position. These strategies contribute to maintaining a more stable point equilibrium throughout the winding process. Although longer rope paths were tested, they did not yield notably better results, especially when combined with looped connections, this remains a topic for further investigation.

Finally, it is recommended to begin with winding between fixed points before introducing interactions with non-fixed supports, as this helps to build up resistance in the system. These findings are relevant for the final design improving the reliability and scalability of filament-wound construction methods.

7.5. Weaving the Insights Together Towards a Final Design

This subchapter combines all the knowledge gained from the sub-experiments, offering further insight into how filaments can interact to create topologies without the need for fixed supports. These findings are used to inform the final design, in which the difference between using only fixed supports and also incorporating non-fixed supports is evaluated.

7.5.1. Setup of the Final Design

To evaluate differences in material use, the conventional method of winding around fixed supports is compared with the novel approach of using interaction points. For this comparison, a topology is chosen based on previous research [13]. Figure 7.24 shows three illustrations. It begins with the fixed support setup, including the lines that need to be fabricated (dotted lines). The middle image displays the desired topology, including node numbers, showing all the lines required in the final design. The final design consists of two diagonals (green), one diamond (purple), and one square (orange). The image on the right shows the setup using non-fixed supports. The difference becomes clear when observing the inner nodes, where a fixed support has been removed and must now be substituted with rope-based interactions.

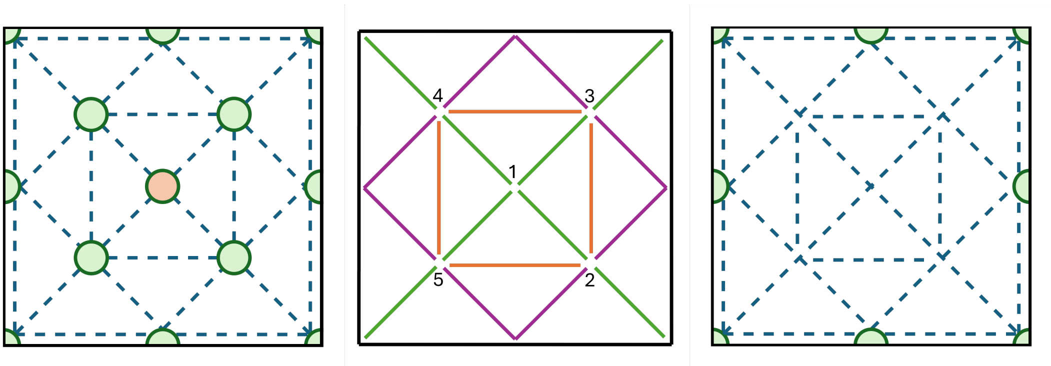

Figure 7.24: Final design setup

Several smaller experiments were performed to establish guidelines for creating the final design. Starting with the pulley effect, the slide off angle, the sequence ending with the knot interactions.

Table 7.2: Design guidelines

Experiment	Recommendation
Pulley effect	Avoid repeating patterns around a non fixed support point, as the stability of pulley points can be unpredictable. In addition, be aware of the increased force when winding in repeating patterns around a single point.
Slide-off angle	Wind the rope as close as possible to 90° when attaching it to a single line using a back-and-forth connection. This prevents the rope from sliding off and creating an undesired topology, due to the friction of the nylon rope.
Connection sequence	Use interaction-based connections to avoid dependency on winding sequence. Otherwise, not all ropes may be integrated into the interaction.
Knot interactions (1)	Prefer straight lines between fixed supports with a connection in the middle. If this is not desired in terms of topology, angled connections are prefered over back-and-forth windings due to their stability.
Knot interactions (2)	Start winding between fixed supports to build up resistance in the system. After that connect to non-fixed interaction points. This helps keep nodes in their intended positions.
General	Use generalised go-through zones instead of fixed coordinates to avoid collisions between the rope and the winding head. Additionally, only allow the winding head to penetrate the plane where strictly necessary.

7.5.2. Sequence

With these design guidelines in mind, a winding path can be developed. This begins with determining the sequence using an Eulerian circuit. The winding sequence for fixed supports (scaffolding points only) is shown in Figure 7.25, while the sequence for a mixed system using both supports and interactions is shown in Figure 7.26. In both figures, a dotted line indicates a second rope layer in a previously used location. This dotted line represents wasted material but is necessary to achieve the correct topology.

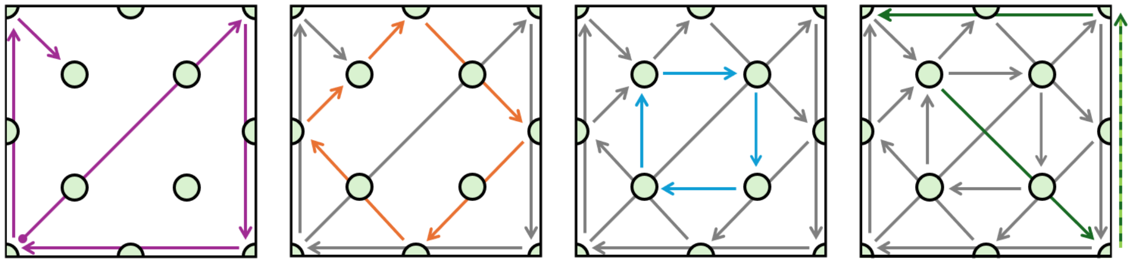

Figure 7.25: Winding sequence fixed supports

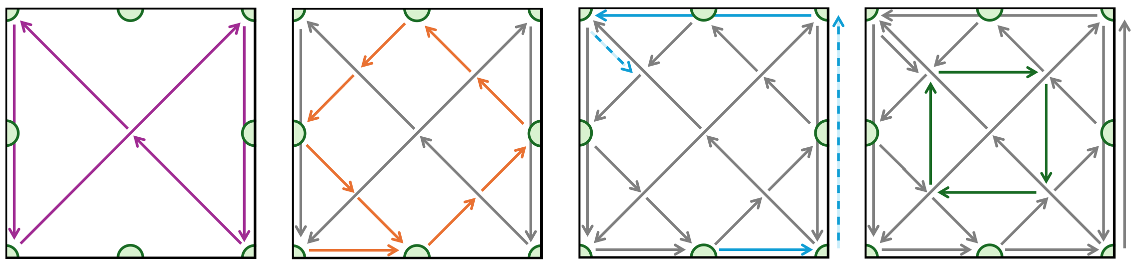

Figure 7.26: Winding sequence interaction based

Both sequences are shown again in Figure 7.27, where the centre image indicates the penetration points used in the final design. These locations provide the robotic arm with coordinates for generating the winding path.

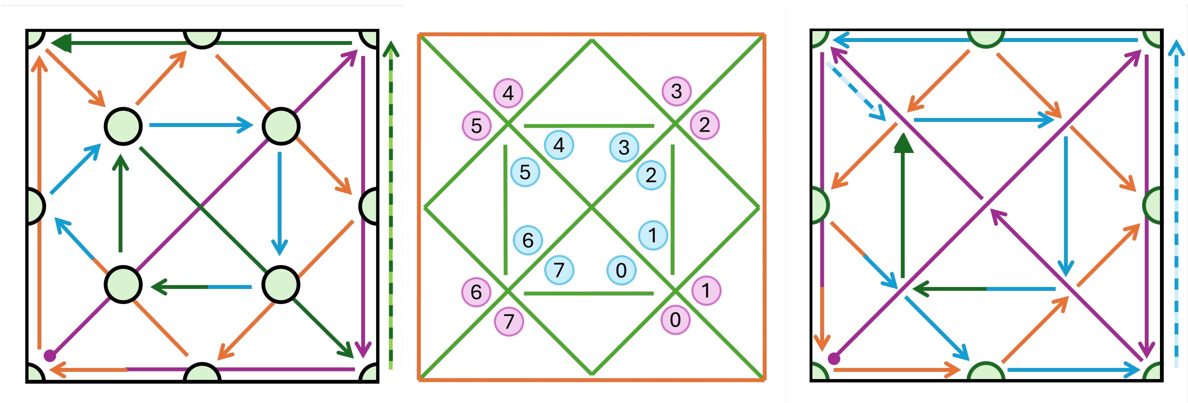

Figure 7.27: Final design sequence (both experiments)

In addition, an extra winding is applied on top of the existing winding. This creates a difference in rope per segment. It is done to evaluate the deviation in nodes when there is already resistance in the system, preventing this movement. Figure 7.28 shows the extra winding for both the the fixed support as the interaction-based system including the winding sequence. These connection points are assumed to behave (nearly) fixed in position due to the resistance built up in the system.

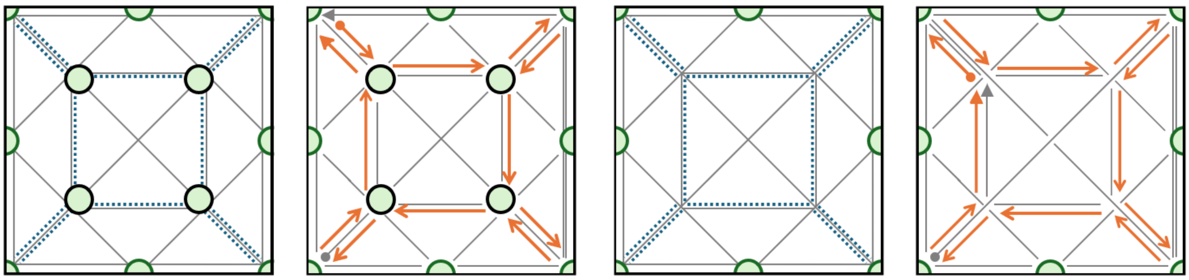

Figure 7.28: Final design sequence for the extra winding (both experiments)

7.5.3. Results

The winding path is generated by converting the sequence into coordinates while applying the design guidelines. The fixed-support experiment was performed only once, as the supports remain stationary and the rope lengths are not expected to vary. This is because the same pattern is used each time. The experiment using interaction points was performed four times to account for potential deviations. This is due to possible node displacement during the formation of interaction points, which can result in slight variations in topology even if the sequence remains the same.

Table 7.3: Experimental results

	Fixed support	**Non-fixed supports**
Number of supports	12	8
Theoretical length factor [-]	25.31	26.02
Theoretical length [m]	6.35	6.53
Actual length [m]	6.42	6.56 ± 0.03
Movement time [s]	108	150
Waiting time [s]	0	60 20 x 3 seconds break
Total time [s]	108	210

Material usage for both setups is compared in Table 7.3. First, the number of (fixed) supports is shown. Then, the theoretical length is stated in two ways: as a dimensionless factor (which can be multiplied by 0.25 m (the spacing between supports) to obtain the length in metres), and as a total theoretical length in metres. This calculation does not consider the diameter of the supports, assuming they are point-like. Finally, the actual lengths recorded during the experiment are shown, including standard deviation caused by variations in topology due to interaction-based connections.

To assess the resulting topology, the deviation between the intended and actual node locations is measured. This data is shown in Section D. The node numbering corresponds with Figure 7.24. Two stages are compared: first, the initial sequence is wound as shown in Figures 7.25 and 7.26; second, the inner square (orange) and outer diagonals (green) from Figure 7.24 receive an additional layer of winding, introducing variation in the number of strands per segment.

Table 7.4: Average displacement results: first windings

Normal winding	**∑ Vector lengths [cm]**	**Average vector length [cm]**	**Ratio [-]**
Test 1	8.9	1.8	0.07
Test 2	7.6	1.5	0.06
Test 3	9.0	1.8	0.07
Test 4	6.1	1.2	0.05
Average	**7.9** ± 1.0	**1.6** ± 0.2	**0.063** ± 0.008

Table 7.5: Average displacement results: extra windings

Extra winding	∑ Vector lengths [cm]	Average vector length [cm]	Ratio [-]
Test 1	8.9	1.8	0.07
Test 2	7.1	1.4	0.06
Test 3	9.7	1.9	0.08
Test 4	6.8	1.4	0.05
Average	**8.1** ± 1.2	**1.6** ± 0.2	**0.065** ± 0.009

Despite the differences in topology, other factors also influence the winding process. During fabrication, the robotic head must penetrate the plane at specific locations to create connections. Although no rope is intended to be present at these locations, minor displacements can cause collisions with the winding head. This usually occurs when the first interaction is made with a diagonally spanned rope. As the connection forms, tension may temporarily decrease, displacing the node until tension is restored, during which the winding head may collide with a rope. After a collision human intervention could be required to fix the stuck winding head, especially during the creation of early interaction points.

During later stages of the winding sequence, the spanned rope can occasionally be caught by the winding head, causing unintended movement. Additionally, forming interaction based connections is more time consuming. This because the path is more complex taking 38.9% more time comparing the interaction with the normal path (excluding the waiting time). The other differences is due to the waiting time which is chosen to make sure the coil can be loosened from the one and attached to the other robotic arm. This could be reduced drastically when automating the process. However, the time consumption is partially offset by the potential for automation, which reduces manual labour and the need for the fastest method of production. The result of the fixed support winding is shown in Figure 7.30, and Figure 7.31, 7.32 and 7.33 show three of the results when winding with the interaction based method.

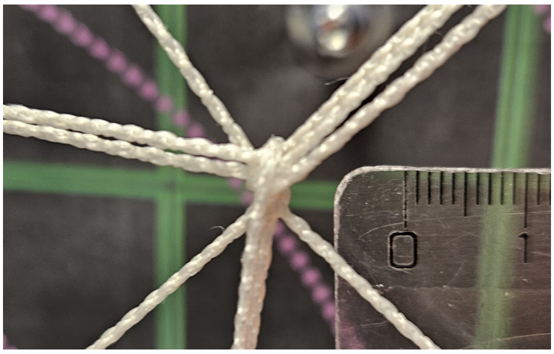

Figure 7.29: Knotted connection

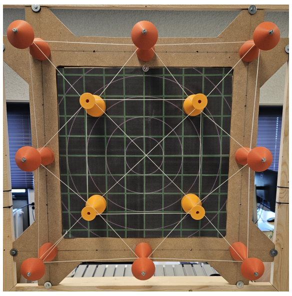

Figure 7.30: Fixed 1

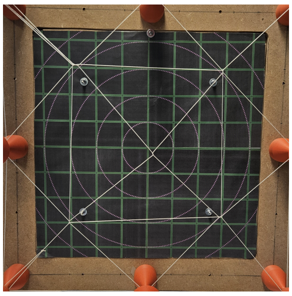

Figure 7.31: Non-fixed 1

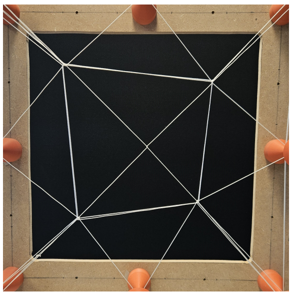

Figure 7.32: Non-fixed 2

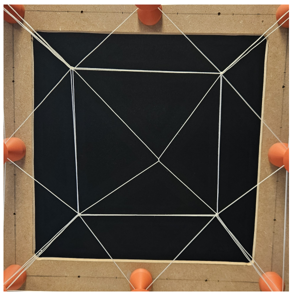

Figure 7.33: Non-fixed 3

8

Discussion

Although the work so far shows promising results, several limitations and practical observations emerged during prototyping. These should be considered to interpret the results or improve the hardware to reach its full potential.

To begin with, this research explores a novel approach to continuous filament winding, with a particular focus on interaction-based strategies, an area that has received little attention so far. The aim was to investigate the feasibility of this method by concentrating on approaches that were proven to work. As a result, some potentially more efficient topologies or methods may not have been explored in depth. Since the primary objective was to demonstrate the viability of interaction-based winding, the optimisation of topology was not a central focus. This leaves valuable opportunities for future research to optimise the design requirements and apply them within the winding strategy, especially when removing the internal support, thereby reducing the constraint when trying to find an optimal topology without collisions.

In terms of material, the scaffoldings have been reduced significantly, although the filament length increased slightly. In addition, the frame material is not considered, but attaching less scaffolding to the frame should also reduce the material used to build the frame, especially when comparing the volumes: a support uses more material compared to the filament winding. Therefore, manufacturing using the interaction-based methods helps to reduce the material. Nevertheless, when reusing all the scaffolding supports and the frame, winding around fixed supports only will likely result in the best option due to the more optimal rope length.

The setup occasionally required human intervention, particularly when the rope lost tension or became entangled with the robotic winding head. Due to these collisions, the results could be improved by making some changes in the hardware in combination with the code for the robotic path. For example, the rope got stuck behind the attachment part of the winding head. By improving the tool for creating connections, these entanglements could be reduced, striving to make it a fully automated process.

Although the geometric accuracy of the interaction-based setup approaches that of the system using only fixed supports, there is potential for further improvement. Two examples of these inaccuracies are shown in Figure 8.1. To reduce deviations, additional winding sequences could be tested. Currently, only a limited number of topologies and sequences have been explored, but varying these parameters could influence the resulting nodal displacements. Moreover, winding on the same side of a support introduces a systematic deviation equal to half the diameter of the support, since the rope cannot pass exactly through the centre of the support. Take into account that these deviations occur in both setups due to the diameter of the support. This inherent offset represents a minimum deviation that cannot be eliminated without altering the hardware setup.

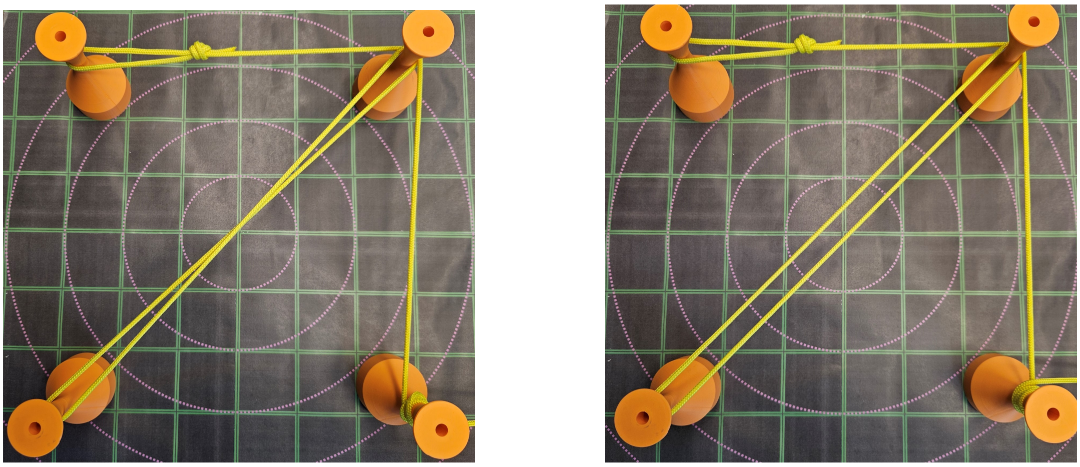

(a) Crossed winding

(b) Looped winding

Figure 8.1: Winding accuracy

Additionally, further investigation into the material properties would be beneficial. For safety reasons, these experiments were conducted using a nylon rope, which behaves somewhat similarly to carbon or glass fibres in terms of flexibility but lacks comparable structural properties. To perform these tests, the filament fibres need to be able to loop around themselves (small curvature), which could be achieved by using a small number of strands (diameter). In addition, the filament should have some resistance; otherwise, the rope would slide off immediately, which should result in a change of the winding path parameters or possibilities of the connections.

A promising direction would be to study the material behaviour during the hardening phase. This opens the possibility of a two-phase winding process: first winding the fibres between fixed supports and allowing them to harden to establish a resistant base structure, followed by the addition of interaction-based connections. This approach could improve geometric precision while maintaining structural stability. If combined with scaling strategies, this method may enable the complete removal of internal scaffolding, using hardened filaments to preserve the intended topology during subsequent winding steps, minimising displacements as shown in Figure 8.2. Besides this, it could also lead to greater accuracy because the deviation caused by the support's diameter will be reduced to the deviation caused by the connection.

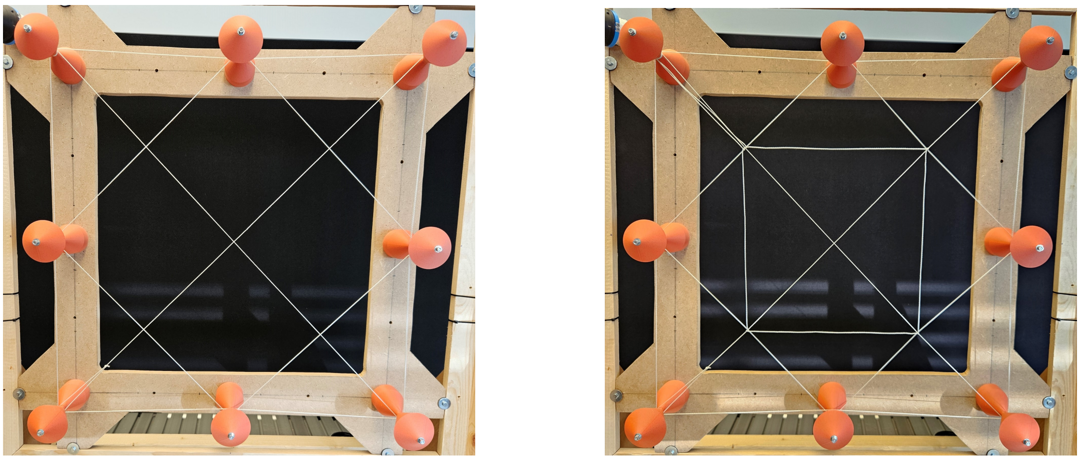

(a) Between scaffolding

(b) Interaction winding

Figure 8.2: 2-step winding process

9
Conclusion

This research explored the use of interactions with the goal of replacing the fixed supports in a filament-wound structure. By analysing the pulley effect, slide-off angles, connection sequences, and knot interactions, a set of design guidelines has been created to help produce the final design. The conclusion analyses the combination of both the research question and the final design, focusing on the difference between a traditional fixed-support setup and a partially non-fixed, interaction-based system.

To start with a method of reducing material usage by changing the way of filament winding. This currently occurs by winding fibres only around fixed supports, which should change towards a method of using the intersections of different filament windings. In this way, the scaffolding can be reduced for the coreless winding techniques. In existing structures, these interactions created from intersections have not been used yet, although they have huge potential in terms of both generating a wide range of possible topologies and reducing the need for scaffolding points, especially when scaling the winding setup. To make use of these intersections, an interaction between different sublayers needs to be created. These interactions can be created by using one of the connections based on the (adjusted) Reidemeister moves. These connections allow an interaction by penetrating the winding plane, which could replace the scaffolding within the process of manufacturing a filament-wound structure.

Secondly, the desired topology should not differ. Winding around fixed support points guarantees the same topology as the design path, whereas winding based on interactions has nodes that can move depending on the force equilibrium, resistance created by connections, and the sequence, which influences the moveability of a node. To provide some design guidelines, sub-experiments have been performed to determine the necessary considerations when creating interaction-based windings around non-fixed support points. When working with non-fixed support points, several design principles should be followed to ensure stability and manufacturability. First, repeating patterns should be avoided, as pulley-like arrangements can lead to unpredictable behaviour and instability in the connection points. The angle at which the rope is connected also plays a crucial role. When creating a back-and-forth connection to a single rope, it is essential to wind as close as possible to 90 degrees. This reduces the chance of the rope sliding off and altering the intended topology. Furthermore, to reduce dependency on the winding sequence, it is recommended to use interaction-based connections. Without this approach, there is a risk that certain ropes may not fully integrate into the node, weakening the structure.

Furthermore, the topology of the robotic path needs to be determined. It is generally preferable to create straight lines between fixed supports and place the interaction at the centre. If the desired layout does not allow for this, angled connections are more reliable than repeated back-and-forth windings, which are prone to instability. The winding process should always begin between fixed supports to build up resistance in the system. Once this tension is established, additional ropes can then connect to the non-fixed interaction points without disturbing the existing structure. Lastly, to prevent collisions between the winding head and the rope, go-through zones should be defined in generalised areas rather than with fixed coordinates. The winding head should only pass through the plane when absolutely necessary.

Finally, the final design was developed using all the design recommendations established throughout this research. This design serves to answer the central question: “How can material usage be reduced in both the filament and the scaffolding by using a construction process of continuous robotic winding?” The evaluation is based on the outcomes of the final design experiment stated in Section 7.5, incorporating both fixed and non-fixed supports to assess their impact on material efficiency and overall construction strategy.

To begin with the material use for scaffolding, the number of supports was reduced from 12 to just 8, representing a 33.3% reduction in support material. Besides that, the internal supports were removed, reducing the constraint when trying to find an optimal topology without collisions with supports. In contrast, the rope length increased by only 2.1%, from 6.42 m to 6.56 m. This difference equates to just 0.71 times the grid spacing, where each grid unit measures 25 cm.

Another key difference observed in the partially interaction-based winding system is the occurrence of nodal displacement. Across all five non-fixed support points, the combined average vector deviation amounted to 1.6 cm, which is 6.3% of the distance between supports. When an additional layer of winding was applied, thereby increasing the number of windings for some segments, it was observed that the interaction points began to behave similarly to fixed supports. The deviation ratio increased only slightly, from 6.3% to 6.5%, corresponding to an overall shift of just 0.2 cm across all five windings. This reflects a minor change of 3.1%, suggesting improved stability with the added layer. Because the system behaves more rigidly over the number of windings, this setup can be scaled easily, as the interactions tend to behave like fixed supports as the number of windings including connections increases. Although creating these connections requires more time than winding around scaffolding points, the goal of automating the process makes time a less critical factor compared to deviations in geometry.

Lastly, as pointed out in the discussion, it should be noted that the winding head occasionally collided with already spanned ropes, particularly when the rope tension was temporarily reduced to form a connection. In such instances, manual assistance was required to guide the winding head, preventing the system from operating fully autonomously. In addition, the long filament fibre material should be tested using the interaction-based methods to evaluate curvature and workability. This applies both to the impregnated carbon and glass fibre combination, as well as to the potential eco-friendly biofibre (flax fibre).

In conclusion, the use of interaction-based methods enables a reduction in scaffolding material by replacing internal supports with rope intersections. Although this approach results in a slight increase in filament length, the difference is minimal. Therefore, provided that the nodal displacement remains within acceptable limits and the autonomy of the robotic arm is further improved, the continuous filament winding method can be effectively applied to non-fixed support setups based on interactions.

10

Unwinding the Future

This chapter is intended to explore future possibilities that go beyond the direct recommendations of this research, offering a broader perspective on the potential of interaction-based filament winding.

When winding in a 2D plane, a 3D working environment is required to enable interactions between different sublayers. In this research, the chosen approach involved penetrating the plane and winding around a pre-spanned rope. Beyond improving the winding tools and setup, alternative techniques may offer new opportunities. The overarching vision for achieving automated interaction-based winding involves using multiple robotic arms. Reducing disturbances to the nodes during the creation of interactions can significantly improve accuracy. One promising concept is the development of a ring-based system, which could help maintain tension throughout the process and prevent the temporary tension loss that currently occurs when looping around a spanned rope.

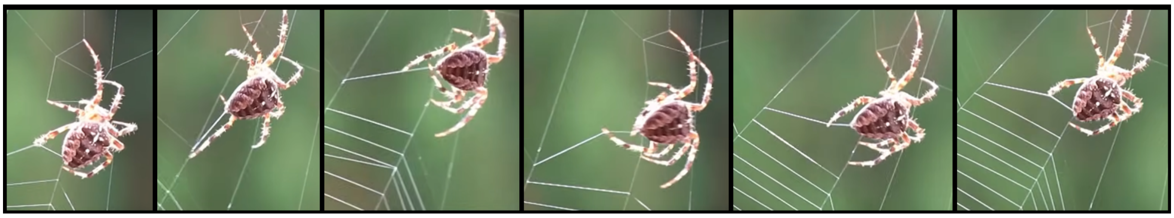

Figure 10.1: Spider web interaction [7]

The way of controlling the tension can be compared to how a spider creates its web, as illustrated in Figure 10.1. After the spider attaches a new strand to the web, it pulls out additional thread to move to the next location on the opposite side. Once there, the spider adjusts the thread to the exact required length, ensuring that the force equilibrium of the web remains unchanged. When the strand no longer introduces additional tension, the connection is secured, resulting in a balanced web with stable connections. Controlling the tension could help future research aim for even greater accuracy in nodal locations.

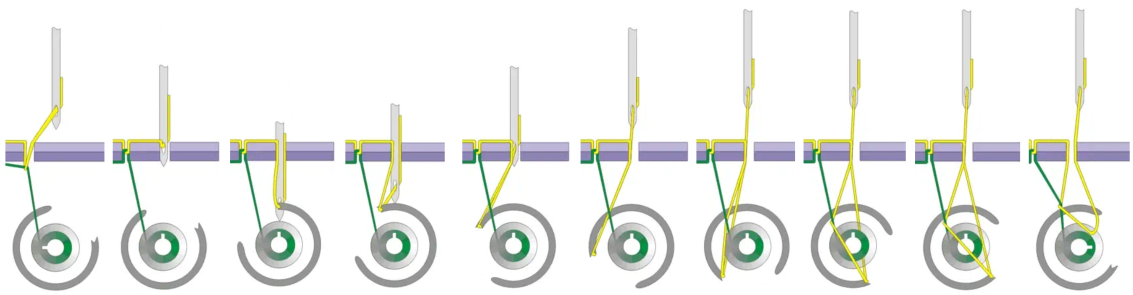

Figure 10.2: Bobbin sewing technique (stepwise) [19]

Another technique with significant potential is a knitting-based approach. The bobbin sewing technique, illustrated in Figure 10.2, serves as inspiration. In this method, collaboration between two robotic arms is required. One acts as the needle, representing the current winding head, while the other functions like the spinning wheel, facilitating the formation of connections. This setup would resolve sequence-related challenges, as the new winding is formed at the outermost layer on both sides of the plane. Moreover, tension can be preserved more effectively, enhancing precision. Since a knitted connection can be made both before and after the spanned rope, this method holds promise for improving both stability and automation.

Due to the unpredictability of nodal positions, exploring methods to accurately locate these points could be of great interest. One potential approach is the development of a predictive model that estimates the current position of a node by taking all winding steps into account. For instance, when a rope is first spanned without any additional connections, the midpoint lies centrally between the supports. However, as further connections are added, the node will gradually shift towards a new equilibrium point governed by the resulting force balance. This process continues until the node accumulates sufficient resistance from surrounding fibres, effectively becoming a stable node. From that moment, it may be considered to behave as a fixed support, with minimal further displacement.

Another promising direction is to combine a predictive model with a camera or digital scanning tool to monitor the position of nodes in real time. By doing so, connections can be made closer to the actual location of the spanned rope, reducing the temporary loss of tension and improving the accuracy of the final topology. Moreover, this approach could help avoid collisions, as the robotic winding head would be able to detect when its path might intersect with an existing rope. Increasing spatial awareness during winding would enhance the reliability of interaction-based methods and reduce the need for human intervention, thereby making the process more scalable and suitable for larger applications.

In terms of materials, carbon and glass fibres are the most commonly used in filament winding processes due to their high tensile strength and stiffness. However, from an environmental perspective, bio-based fibres such as flax fibre offer significant potential. The production of flax fibres typically results in considerably lower carbon emissions compared to conventional synthetic fibres, making them a more sustainable alternative. This could be assessed with a life cycle assessment, which combines several possible designs with the choice of materials.

Furthermore, the feasibility of implementing the interaction-based method at a larger scale warrants further investigation, particularly when considering a two-step winding process. This approach begins with the creation of a rigid framework by winding between fixed supports. Once these fibres have fully hardened and provide structural integrity, a second winding phase can take place, in which new fibres are added based on interaction points established with the hardened framework. This staged method, shown in Figure 10.3, illustrates the topology: the first step creates the rigid frameworks, and the second step establishes the interactions. This can significantly improve the geometric accuracy of nodal positions, as the pre-tensioned first layer offers additional resistance against nodal displacement.

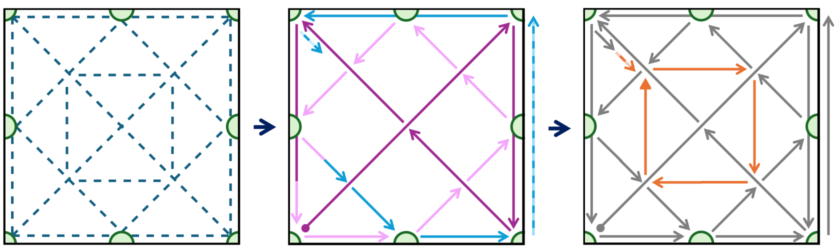

Figure 10.3: 2-step filament winding

Moreover, scaling up such setups could enhance the utility of interaction points within filament winding systems. Figure 10.4 illustrates two commonly used grid layouts: one composed of horizontal and vertical lines, and another incorporating only diagonal elements. These configurations are prevalent in structural applications, especially in reinforcement strategies for concrete elements. Notably, when the density of scaffolding points increases, the number of potential interaction points rises substantially. This expanded network of intersections opens new possibilities for structurally efficient, material-saving designs that make better use of the interaction-based method.

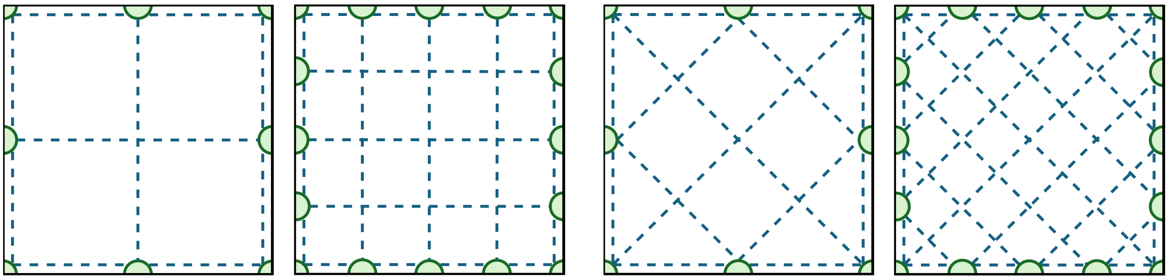

Figure 10.4: Scaling example

Using the novel approach of filament winding, this technique could be applied to improve concrete reinforcement. This is illustrated in Figure 10.5. The figure starts with a concrete wall containing a reinforcement mesh. When a window opening is introduced, the uniform reinforcement pattern is interrupted, preventing the reinforcement net from continuing its path. To maintain the structural integrity of the wall, additional reinforcement must be added. Figure 10.5b shows a conventional steel-reinforced design based on Figure 1.1a, where extra steel rebars, including their anchorage lengths, are placed around the opening. Figure 10.5c instead applies filament winding using continuous long filament fibres, which allows for optimisation in several ways. This example is displayed to show the differences for a reinforcement net without any calculations used. Firstly, it is no longer constrained to a grid layout, enabling the creation of reinforcement paths that better follow the actual force flow within the element. Secondly, the standardised bar sizes are no longer required. The effective diameter of the reinforcement can be defined by the thickness of a single filament strand multiplied by the number of windings. The wound filaments form a reinforcement network that can be applied in a similar manner to a conventional steel mesh.

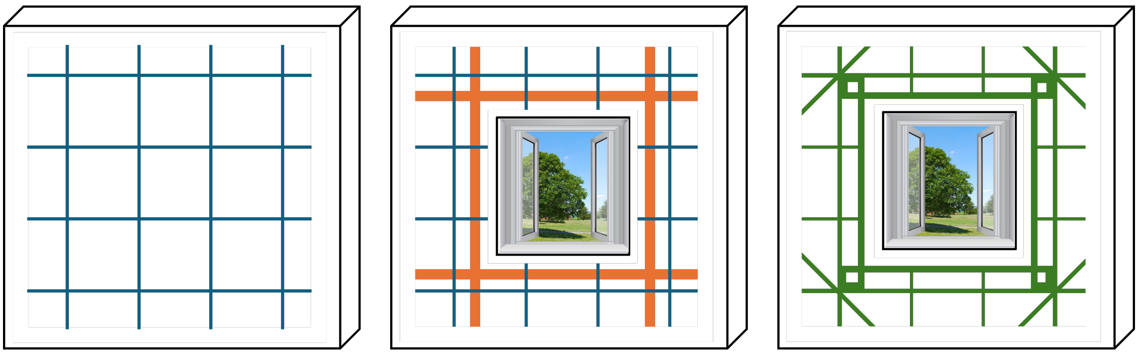

(a) Reinforced wall mesh

(b) Steel reinforcement

(c) Filament wound reinforcement

Figure 10.5: Window placement within a wall

Finally, the robotic fabrication process minimises inaccuracies by following a programmed path that can be validated step by step. Moreover, using filament winding can significantly reduce material waste, aligning with sustainable construction goals. The robotic winding process can also be easily adapted for custom geometries without increasing labour costs, making it particularly suitable for prefabricated production. However, the flexibility of the process also allows for potential in-situ applications, such as creating reinforcement nets. Beyond reinforcement applications, this method of winding continuous filament fibres has significant potential for creating lightweight structures such as canopies, trusses, and other coreless frameworks.

Ultimately, interaction-based filament winding has strong potential to become a novel approach in the automated winding industry, offering the opportunity to reduce material waste and incorporate more environmentally friendly materials into the production process of reinforced concrete. While challenges remain within the process of continuous coreless robotic filament winding, it is time to continue exploring its possibilities and unravel its full potential.

References

[1] Milad Abolfazli et al. “Residual compressive strength of filament wound hybrid glass/carbon fibre reinforced polymer tubes after exposure to elevated temperature”. In: *Composite Structures* 316 (Apr. 2023), p. 117050. DOI: 10.1016/j.compstruct.2023.117050.

[2] Addcomposites. *Winding the Future: An Exploration of Filament Winding Applications*. URL: https://www.addcomposites.com/post/winding-the-future-an-exploration-of-filament-winding-applications.

[3] Marcio S. V. De Souza and Ruy M. O. Pauletti. “A computational framework for the design of tensile structures”. In: *Advances in Computational Science and Engineering* 2.1 (Jan. 2024), pp. 37–72. DOI: 10.3934/acse.2024005. URL: https://doi.org/10.3934/acse.2024005.

[4] Luke Fiederer. *AD Classics: Olympiastadion (Munich Olympic Stadium) Behnisch and Partners, Frei Otto*. Dec. 2022. URL: https://www.archdaily.com/109136/ad-classics-munich-olympic-stadium-frei-otto-gunther-behnisch.

[5] Marta Gil Pérez et al. *Coreless filament-wound structures: toward performative long- span and sustainable building systems*. Sept. 2022.

[6] Tristan Gobin et al. “HAL Robotics Framework”. In: *Proceedings of the 38th International Symposium on Automation and Robotics in Construction (ISARC)*. Ed. by Chen Feng et al. Dubai, UAE: International Association for Automation and Robotics in Construction (IAARC), Nov. 2021, pp. 733–740. ISBN: 978-952-69524-1-3. DOI: 10.22260/ISARC2021/0099.

[7] hikeart. *Spider spinning its web - Close-Up*. Oct. 2015. URL: https://www.youtube.com/watch?v=4J5kArP5gAE.

[8] D Kallan. *Steel Fiber Reinforced Concrete for Tunnel Linings*. 2023. URL: https://resolver.tudelft.nl/uuid:b961dc90-423c-424f-a2d2-fdd3e1fe16c8.

[9] Charles Livingston. “Knot theory”. In: *Washington, DC : Mathematical Association of America* (1993), p. 240. DOI: https://doi.org/10.1016/j.jcomc.2024.100547. URL: WorldCat.org.

[10] Pascal Mindermann et al. “Material Monitoring of a Composite Dome Pavilion Made by Robotic Coreless Filament Winding”. In: *Materials* 14 (Sept. 2021), p. 5509. DOI: 10.3390/ma14195509.

[11] *Munich Olympic Stadium Data Photos and Plans WikiArquitectura*. Sept. 2020. URL: https://en.wikiarquitectura.com/building/Munich-Olympic-Stadium/.

[12] John Orr et al. “Design methods for flexibly formed concrete beams”. In: (Jan. 2014). DOI: 10.17863/CAM.17612.

[13] Robin Oval, John Orr, and Paul Shepherd. “Structural design and fabrication of concrete reinforcement with layout optimisation and robotic filament winding”. In: *Automation in Construction* 170 (2025), p. 105952. ISSN: 0926-5805. DOI: https://doi.org/10.1016/j.autcon.2024.105952. URL: https://www.sciencedirect.com/science/article/pii/S0926580524006885.

[14] Robin Oval et al. “Automated Framework for the Optimisation of Spatial Layouts for Concrete Structures Reinforced with Robotic Filament Winding”. In: *Proceedings of the ... ISARC* (Oct. 2020). DOI: 10.22260/isarc2020/0214. URL: https://doi.org/10.22260/isarc2020/0214.

[15] Surya Pandita et al. “Clean wet-filament winding “ Part 1: design concept and simulations”. In: *Journal of Composite Materials* 47 (Feb. 2013), pp. 379–390. DOI: 10.1177/0021998312440474.

[16] Michael Purton. *Cement is a big problem for the environment. Here’s how to make it more sustainable*. Sept. 13, 2024. URL: https://www.weforum.org/stories/2024/09/cement-production-sustainable-concrete-co2-emissions/.

[17] R. Pandia Raj and Simon D. Guest. “USING SYMMETRY FOR TENSEGRITY FORM-FINDING”. In: *Journal- International Association for Shell and Spatial Structures* 47 (2006), pp. 245–252. URL: https://api.semanticscholar.org/CorpusID:35593582.

[18] Steffen Reichert et al. "Fibrous structures: An integrative approach to design computation, simulation and fabrication for lightweight, glass and carbon fibre composite structures in architecture based on biomimetic design principles". In: *Computer-Aided Design* 52 (2014), pp. 27–39. ISSN: 0010-4485. DOI: https://doi.org/10.1016/j.cad.2014.02.005. URL: https://www.sciencedirect.com/science/article/pii/S0010448514000293.

[19] Sarah. *Beginner's Guide to Sewing: Sewing Machine Parts Reference Guide*. July 2014. URL: https://www.sewingpartsonline.com/blogs/education/beginners-guide-sewing-sewing-machine-parts-reference-guide.

[20] International Association for Shell and Spatial Structures (IASS). *Innovation in festival architecture from design to construction: Ingenta Connect*. 2017. URL: https://www.ingentaconnect.com/content/iass/piass/2017/00002017/00000004/art00013#.

[21] Saverio Spadea et al. "Wound FRP Shear Reinforcement for Concrete Structures". In: *Journal of Composites for Construction* 21.5 (Mar. 2017). DOI: 10.1061/(asce)cc.1943-5614.0000807. URL: https://doi.org/10.1061/(asce)cc.1943-5614.0000807.

[22] Hynek Stekbauer. "The Pulley Element". In: *Transactions of the VAB - Technical University of Ostrava Civil Engineering Series* 16 (Dec. 2016). DOI: 10.1515/tvsb-2016-0027.

[23] University of Stuttgart. *livMatS Pavilion: Institute for Computational Design and Construction | University of Stuttgart*. URL: https://www.icd.uni-stuttgart.de/projects/livMatS-Pavilion/.

[24] University of Stuttgart. *Maison Fibre: Institute for Computational Design and Construction | University of Stuttgart*. URL: https://www.icd.uni-stuttgart.de/projects/maison-fibre/.

[25] Daniel Tapia. *BUGA Fibre Pavilion ICD/ITKE University of Stuttgart*. July 2024. URL: https://www.archdaily.com/916650/buga-fibre-pavilion-icd-itke-university-of-stuttgart.

[26] Boathous Team. *The definitive guide to nautical knots: 10 basic knots every sailor should master*. Apr. 2025. URL: https://www.boathous.com/nl/blog/the-definitive-guide-to-nautical-knots-10-basic-knots-every-sailor-should-master/90.

[27] Gunnar Tibert and Sergio Pellegrino. "Review of Form-Finding Methods for Tensegrity Structures". In: *International Journal of Space Structures* 18 (Dec. 2003), pp. 209–223. DOI: 10.1260/026635103322987940.

[28] UKGBC. *ESTIMATING THE AMOUNT OF CO2 EMISSIONS THAT THE CONSTRUCTION INDUSTRY CAN INFLUENCE*. 2010. URL: https://assets.publishing.service.gov.uk/media/5a79dc1040f0b670a8025f44/10-1316-estimating-co2-emissions-supporting-low-carbon-igt-report.pdf.

[29] D. Veenendaal and P. Block. "An overview and comparison of structural form finding methods for general networks". In: *International Journal of Solids and Structures* 49.26 (2012), pp. 3741–3753. ISSN: 0020-7683. DOI: https://doi.org/10.1016/j.ijsolstr.2012.08.008. URL: https://www.sciencedirect.com/science/article/pii/S002076831200337X.

[30] *What is Filament Winding Process?* URL: https://www.addcomposites.com/post/filament-winding.

[31] Wikipedia-bijdragers. *Olympiastadion (München)*. Jan. 2025. URL: https://nl.wikipedia.org/wiki/Olympiastadion_%28M%C3%BCnchen%29.

[32] Nixon Wonoto and Vincent Blouin. "Integrating Grasshopper and Matlab for Shape Optimization and Structural Form-Finding of Buildings". In: *Computer-Aided Design and Applications* 16 (Aug. 2018), pp. 1–12. DOI: 10.14733/cadaps.2019.1-12.

A

Designs and Prototypes

Extra pictures and designs of all prototypes will be shown in this appendix

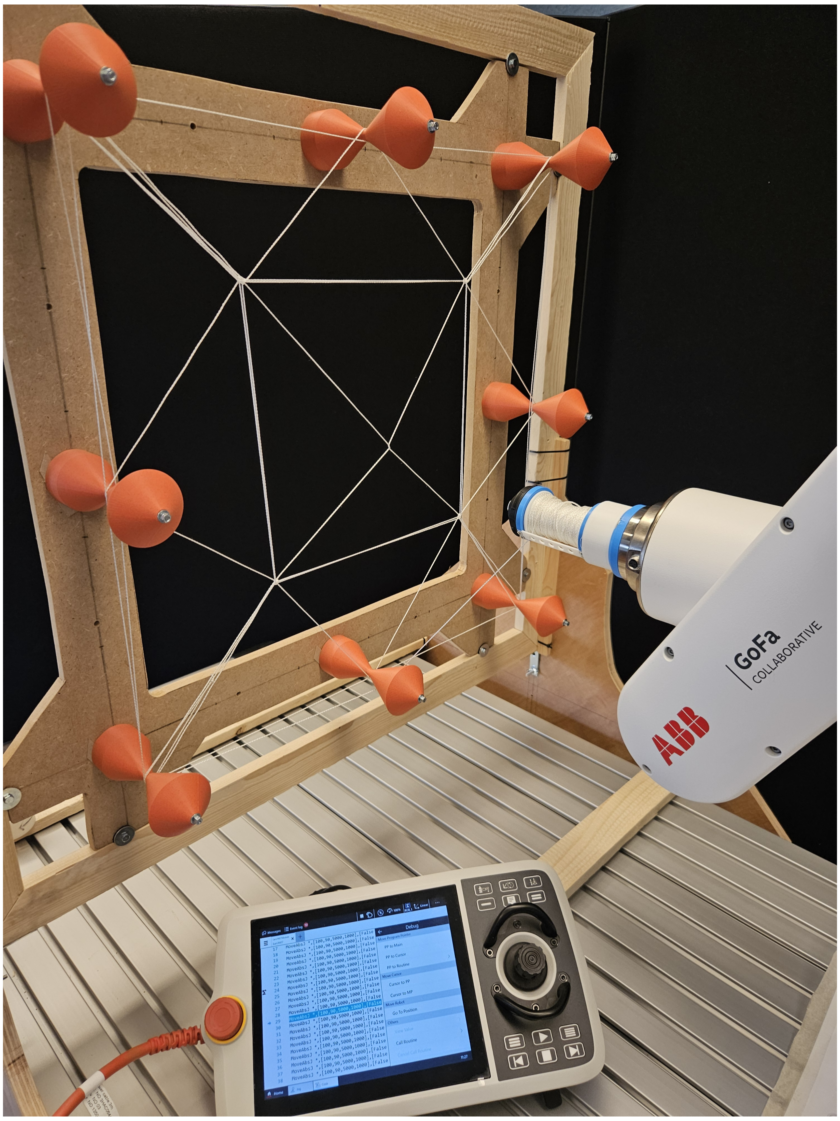

Figure A.1: Final setup 1

Figure A.2: The Board (bottom side)

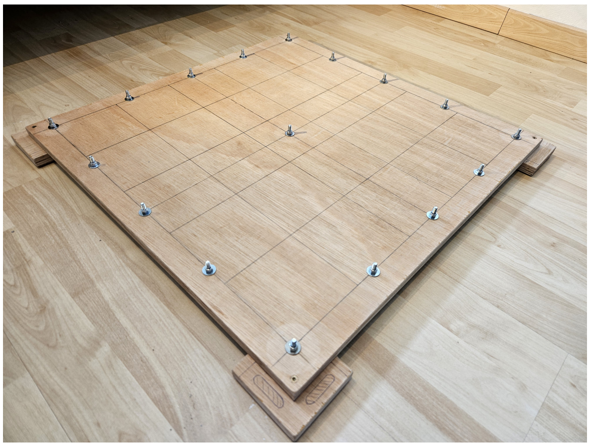

Figure A.3: The Board (3D view)

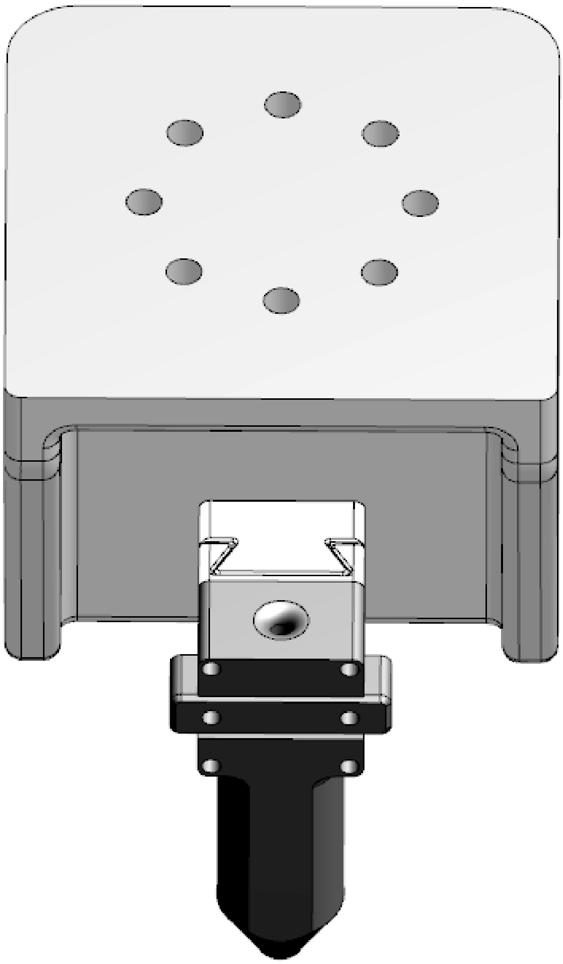

Figure A.4: Dispenser Head (3D view)

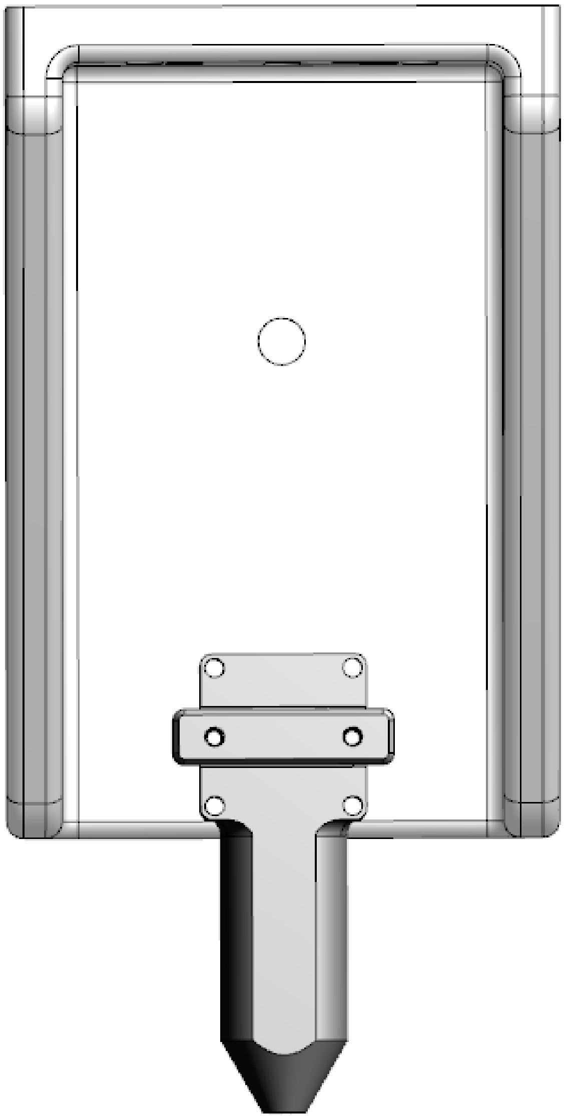

Figure A.5: Dispenser Head (sideview)

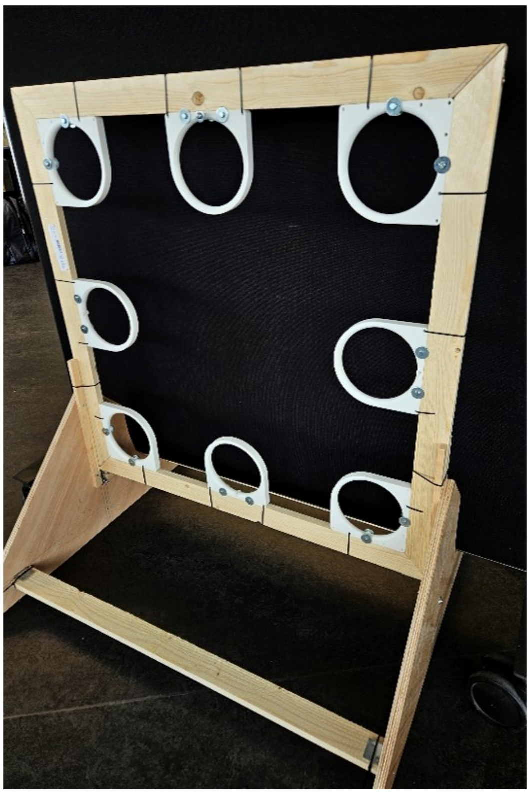

Figure A.6: Standing setup rings 2

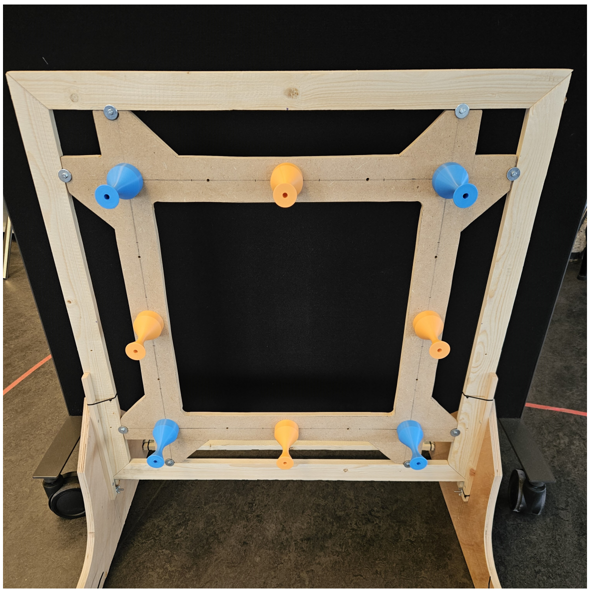

Figure A.7: Standing setup support 2

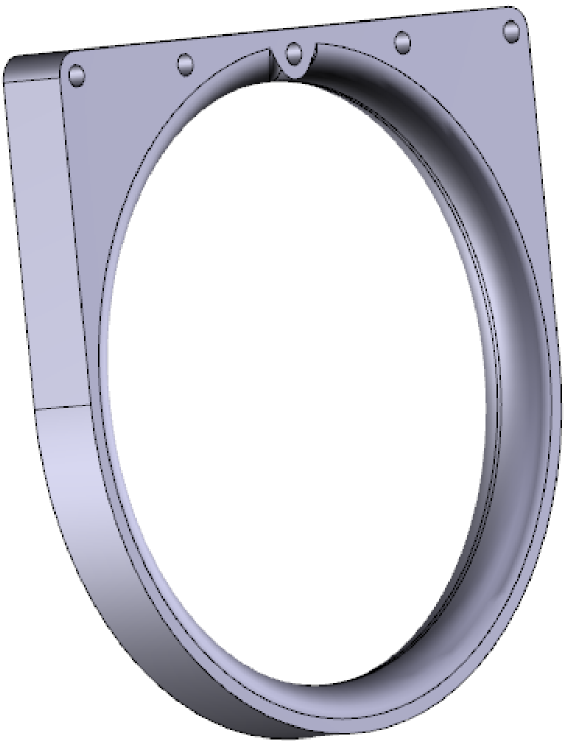

Figure A.8: Ring support side (3D view)

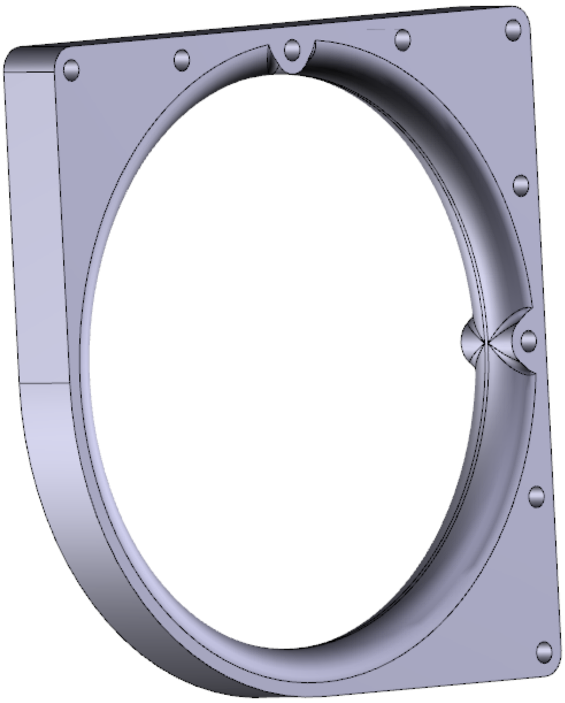

Figure A.9: Ring support corner (3D view)

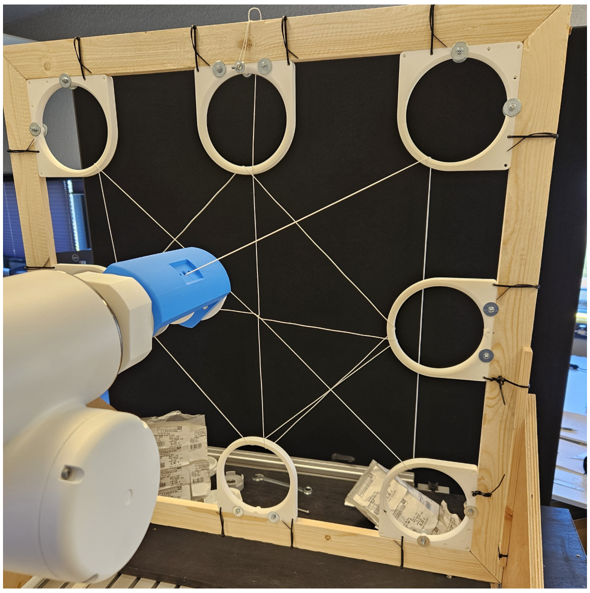

Figure A.10: Slide Through Head setup

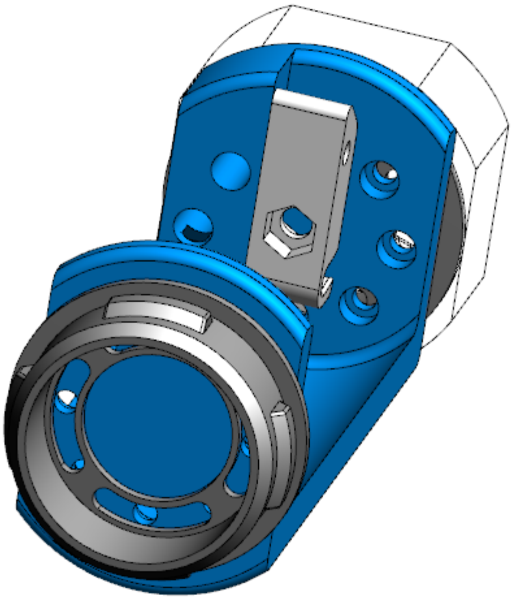

Figure A.11: Go through head (3D view)

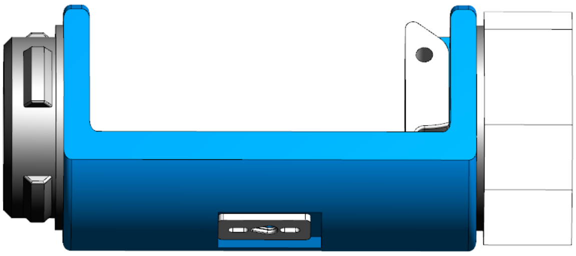

Figure A.12: Slide Through Head (sideview)

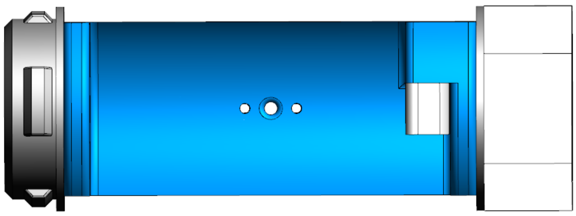

Figure A.13: Slide Through Head (topview)

The supports had the following dimensions (from left to right) with a height of 100, 100, 135, 140, 140 and 130 mm and diameters of 34, 34, 70, 52, 60 and 58 mm, respectively. These supports are shown in Figure A.14.

Figure A.14: Standing support modifications

Figure A.15: Standing support improvements

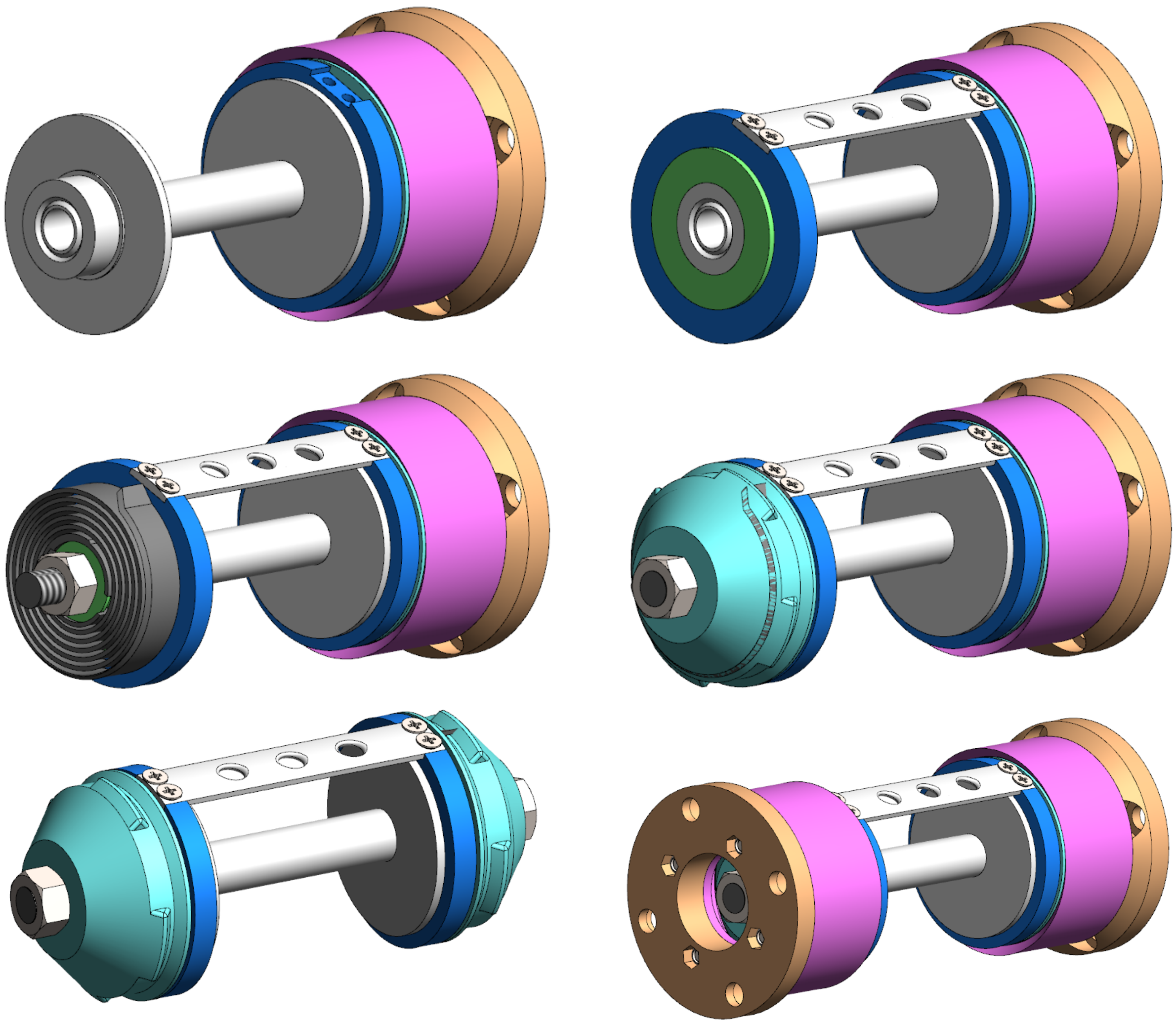

Figure A.16: Penetrating Head (stepwise 3D views) and rope winding examples

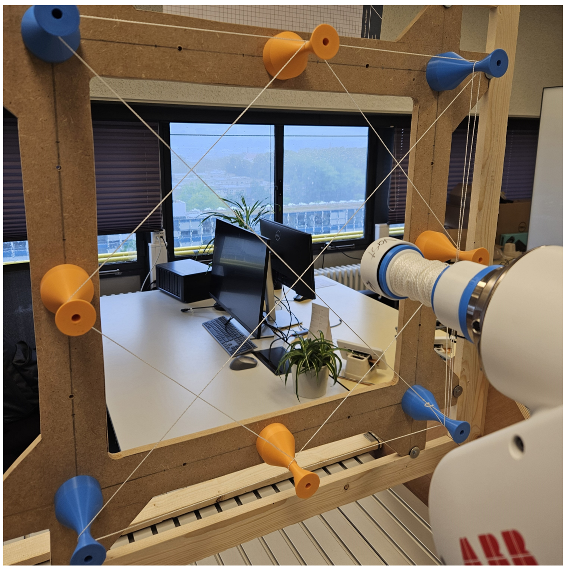

Figure A.17: Rope winding example 1

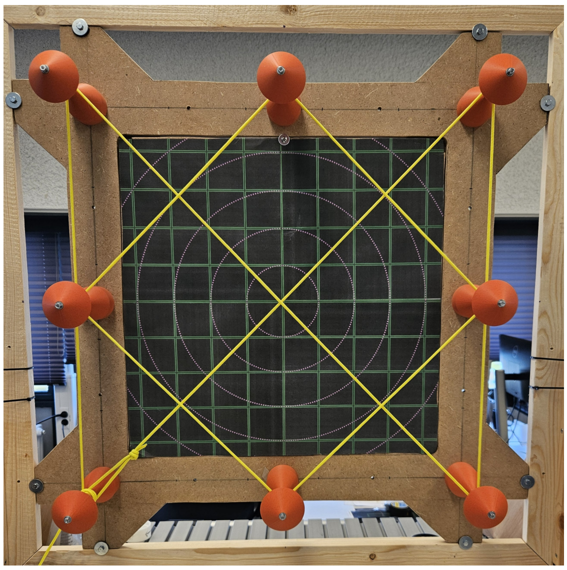

Figure A.18: Rope winding example 2

B

Grasshopper code

The code is systematically explained in Chapter 6. The appendix shows the complete grasshopper code used for this project. It combines all steps required to generate the robotic arm's movements. The process starts with defining all parameters and creating the start and end coordinates. This is followed by generating both the (standing) support path and the ring path (purple boxes). Once these are defined, they are combined into a single path (green boxes), concluding with the robotic arm settings and control properties (light blue boxes).

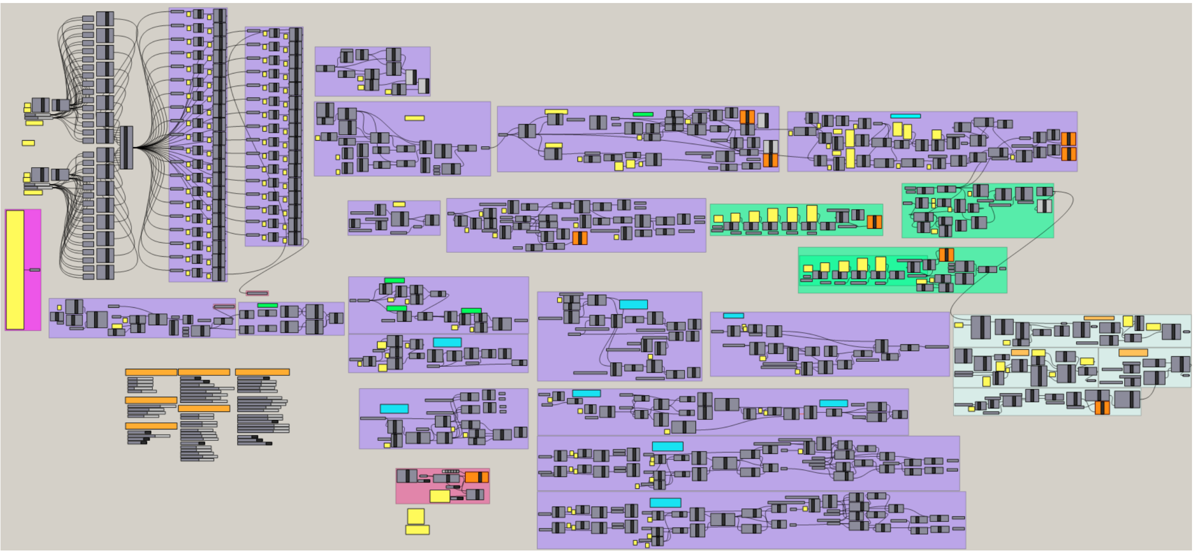

Figure B.1: All code combines

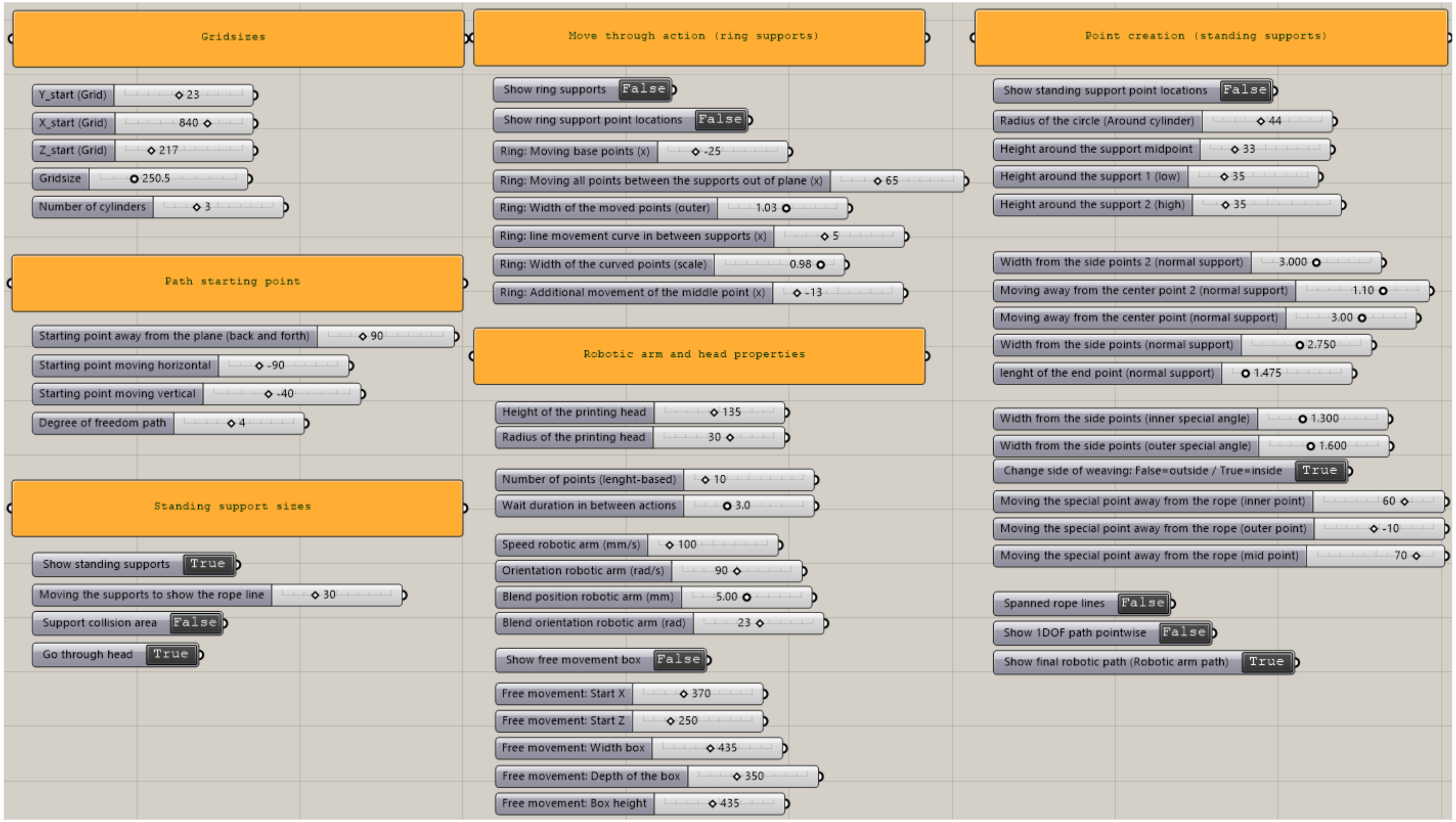

Figure B.2: All parameters used

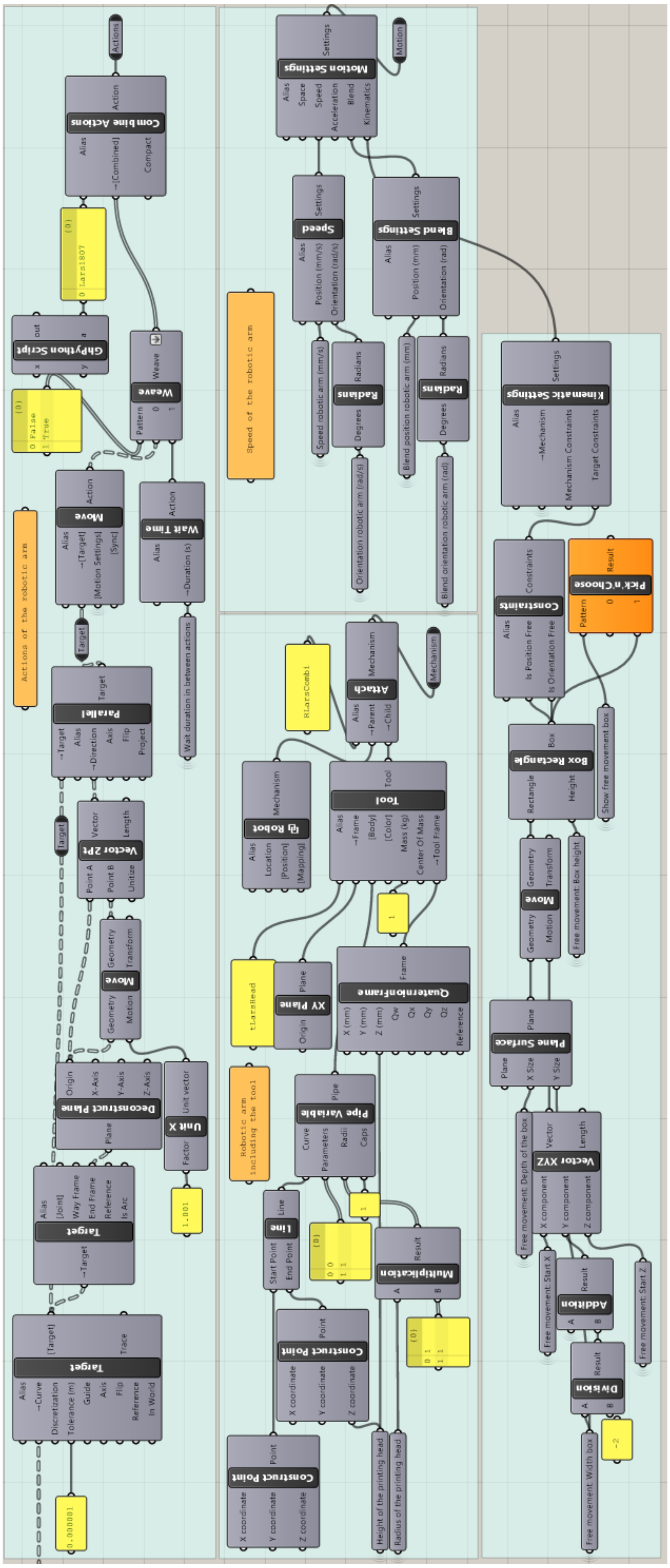

Figure B.3: Robotic code

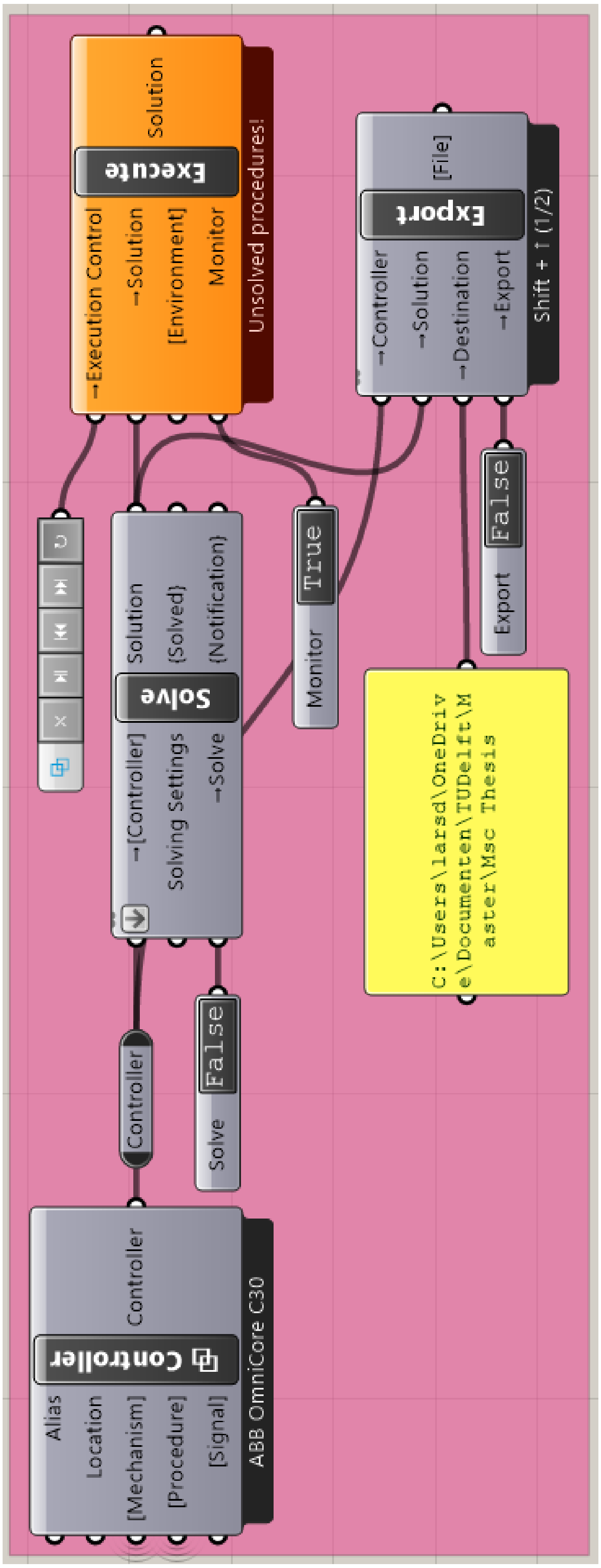

Figure B.4: Robotic control centre

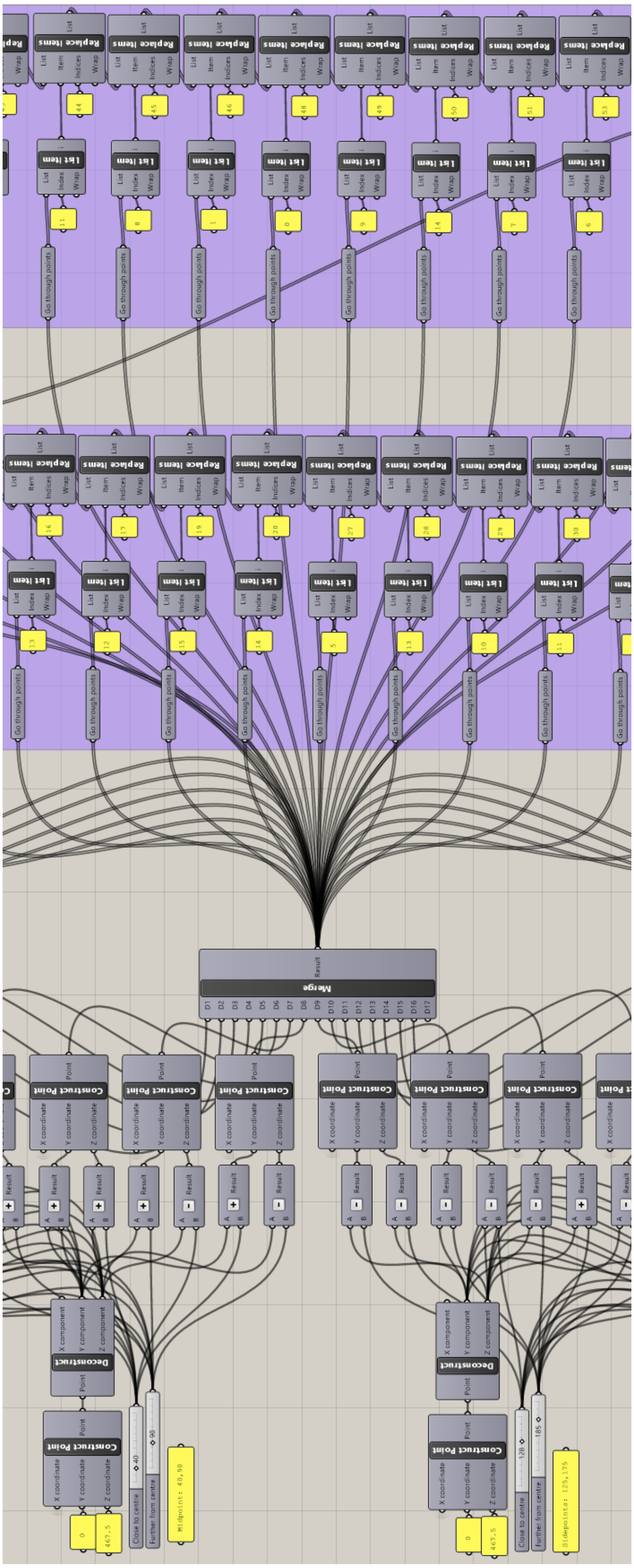

Figure B.5: Go through locations

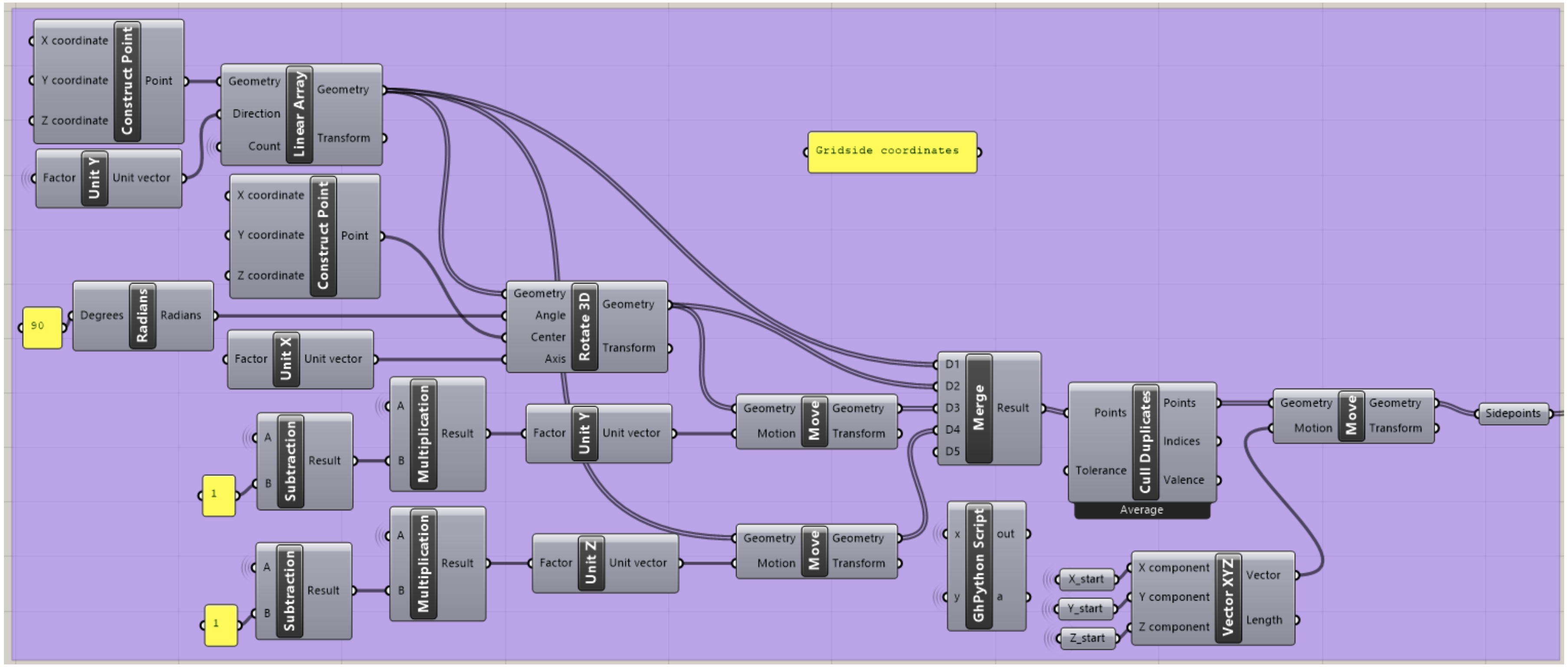

Figure B.6: Creating gridside coordinates

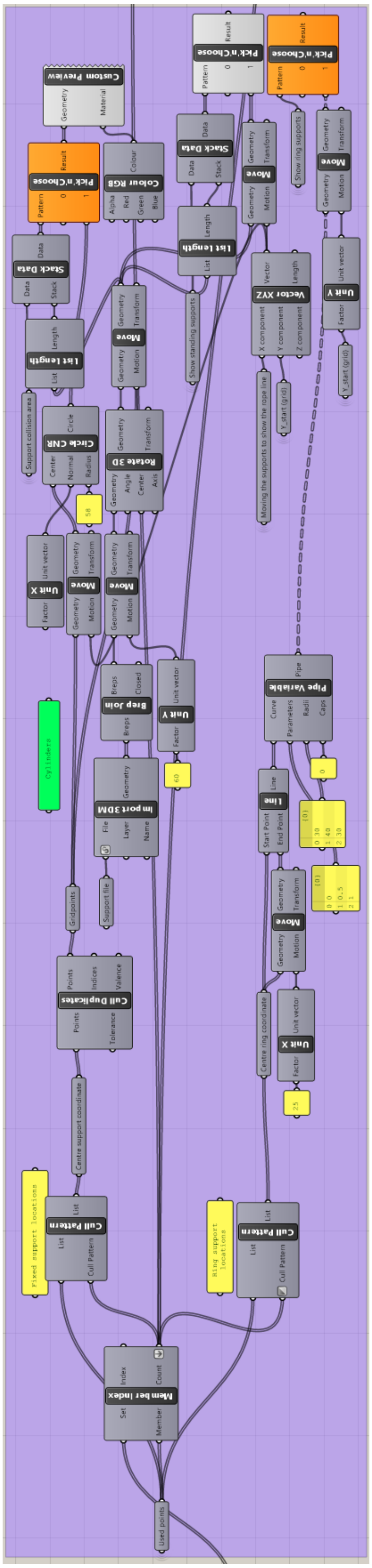

Figure B.7: Creating supports

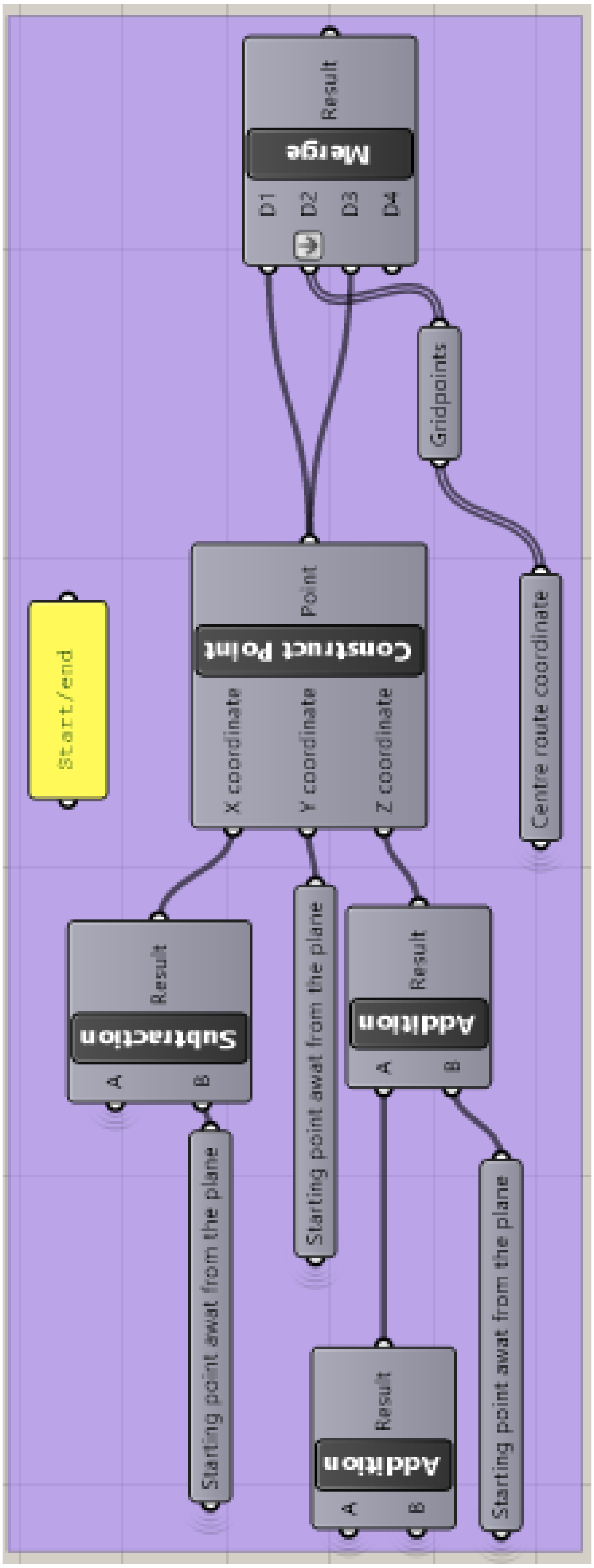

Figure B.8: Start and end coordinates

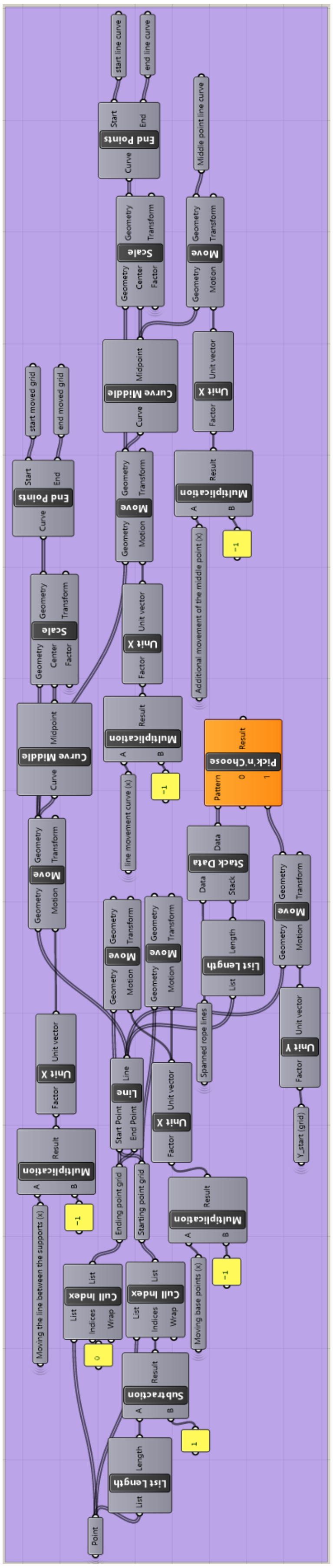

Figure B.9: Ring path 1

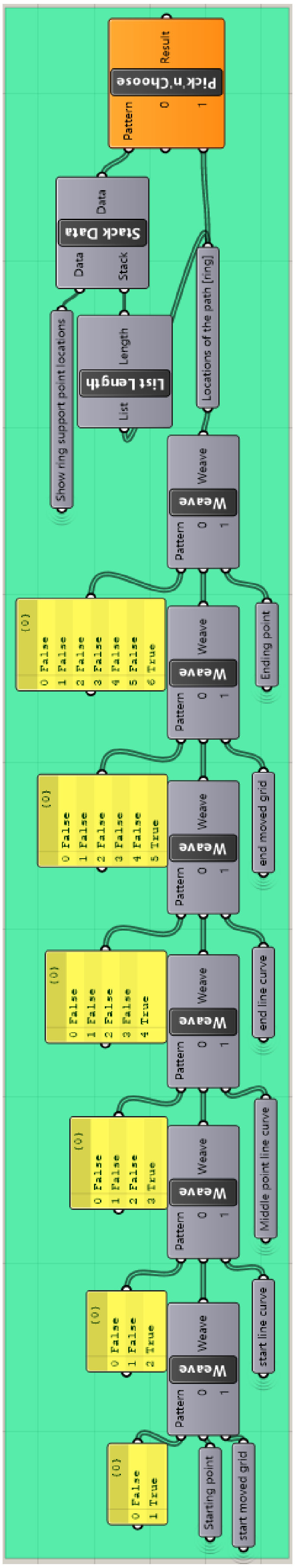

Figure B.10: Ring path combining

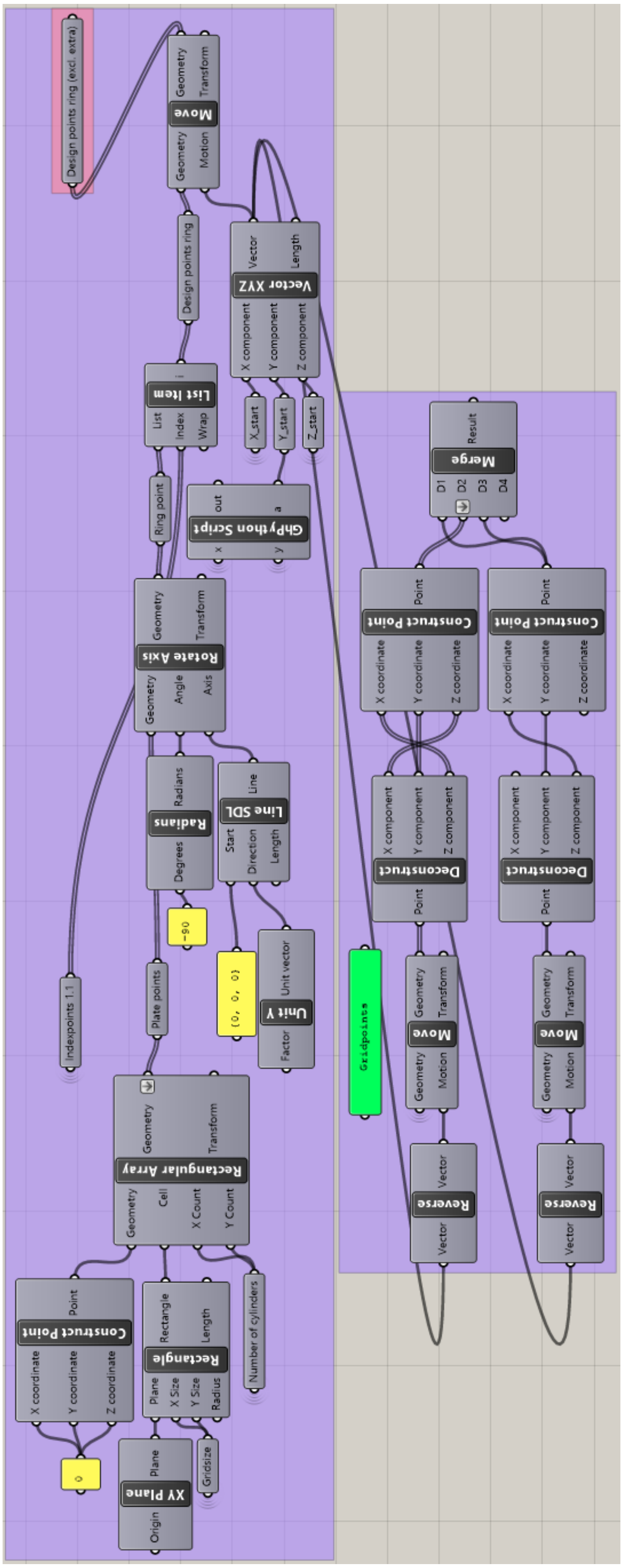

Figure B.11: Grid and points support

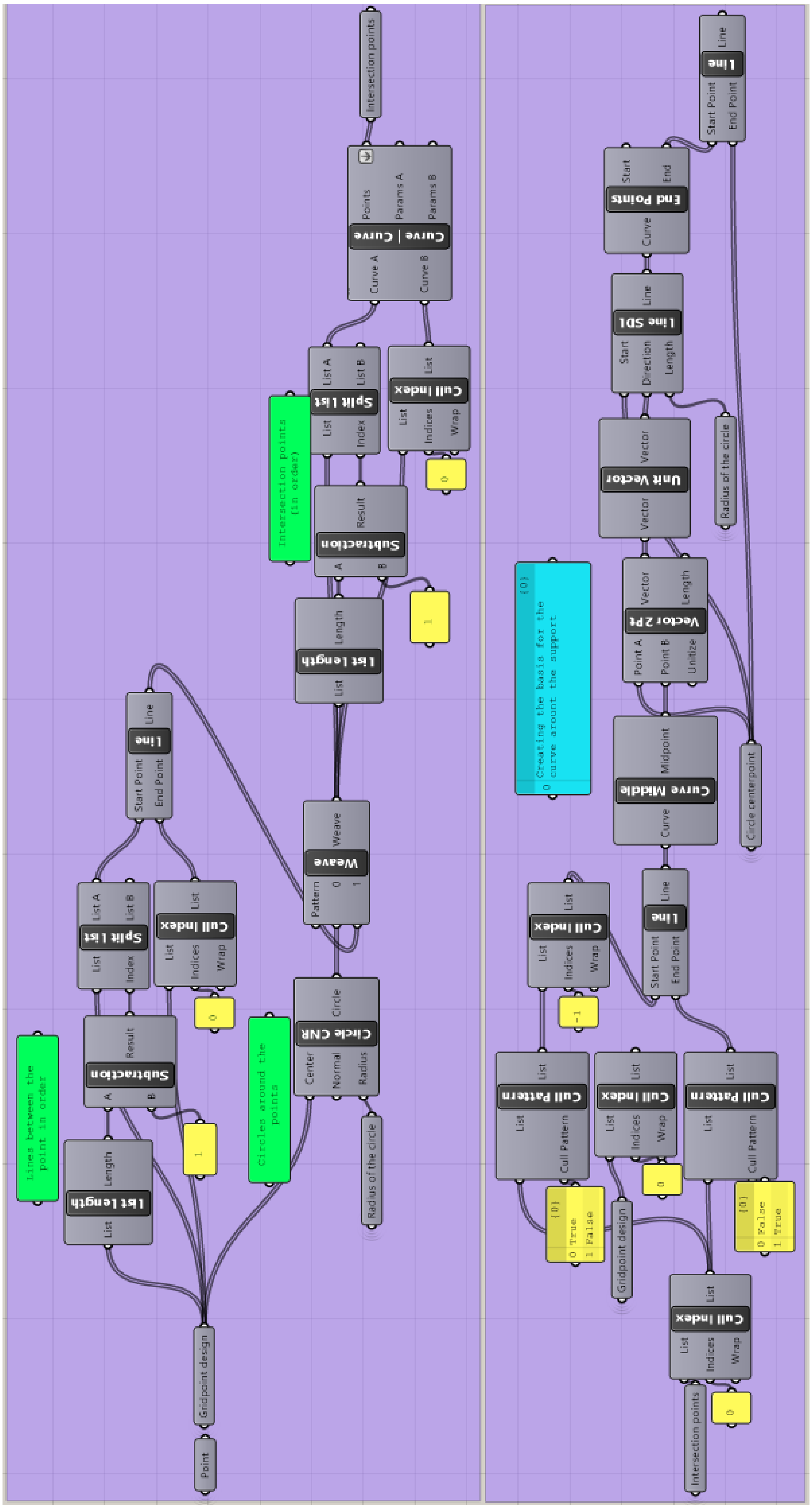

Figure B.12: Support path 1

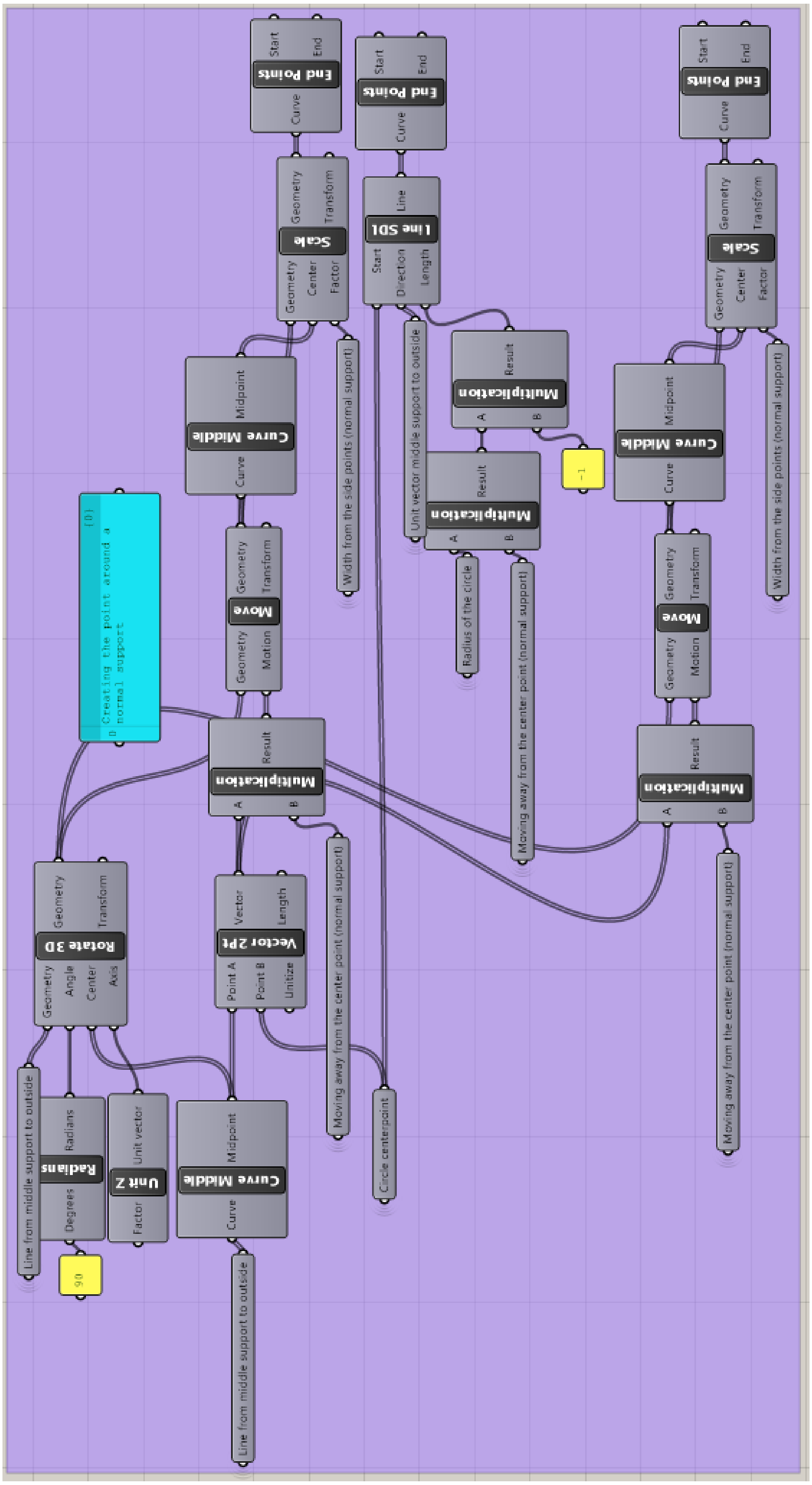

Figure B.13: Support path 2

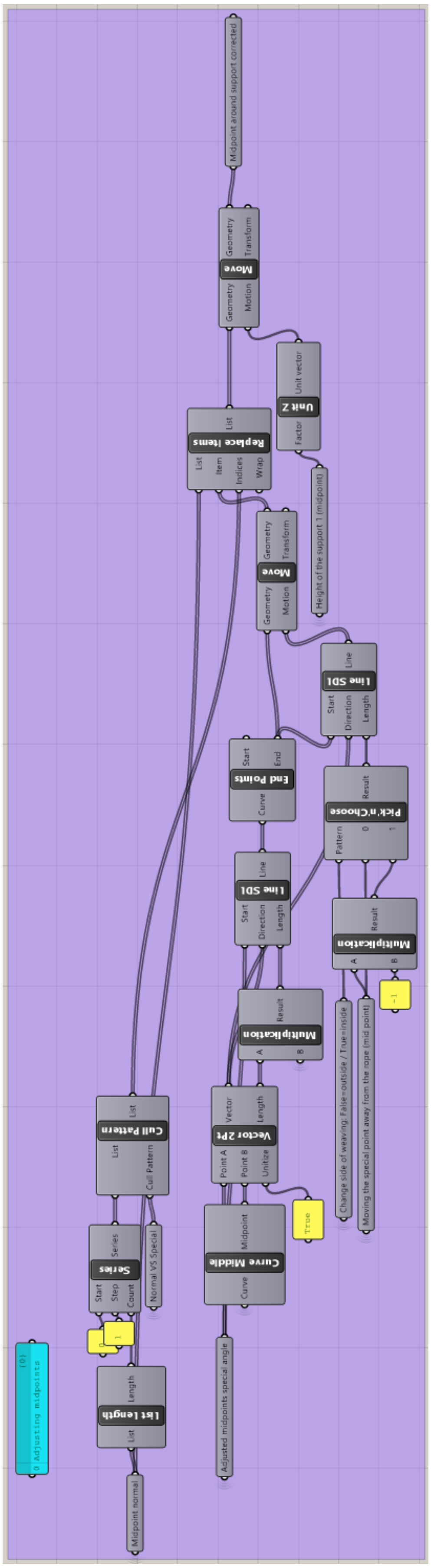

Figure B.14: Support path 3

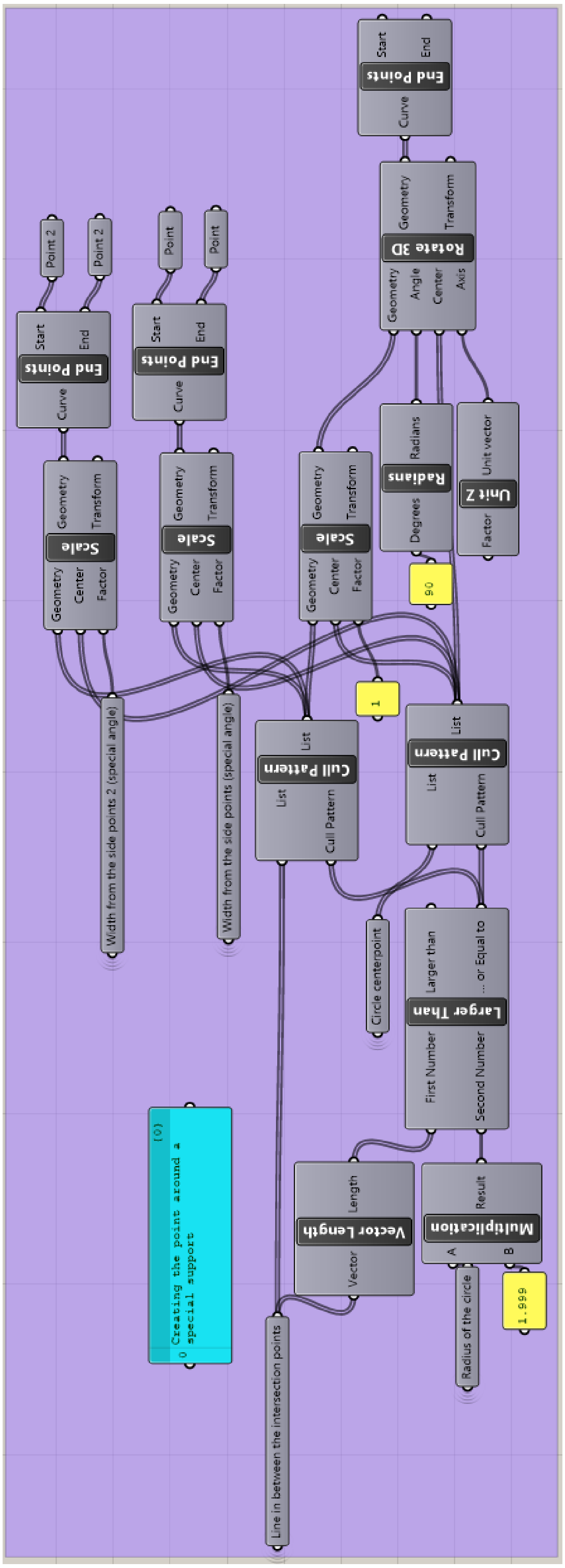

Figure B.15: Support path 4

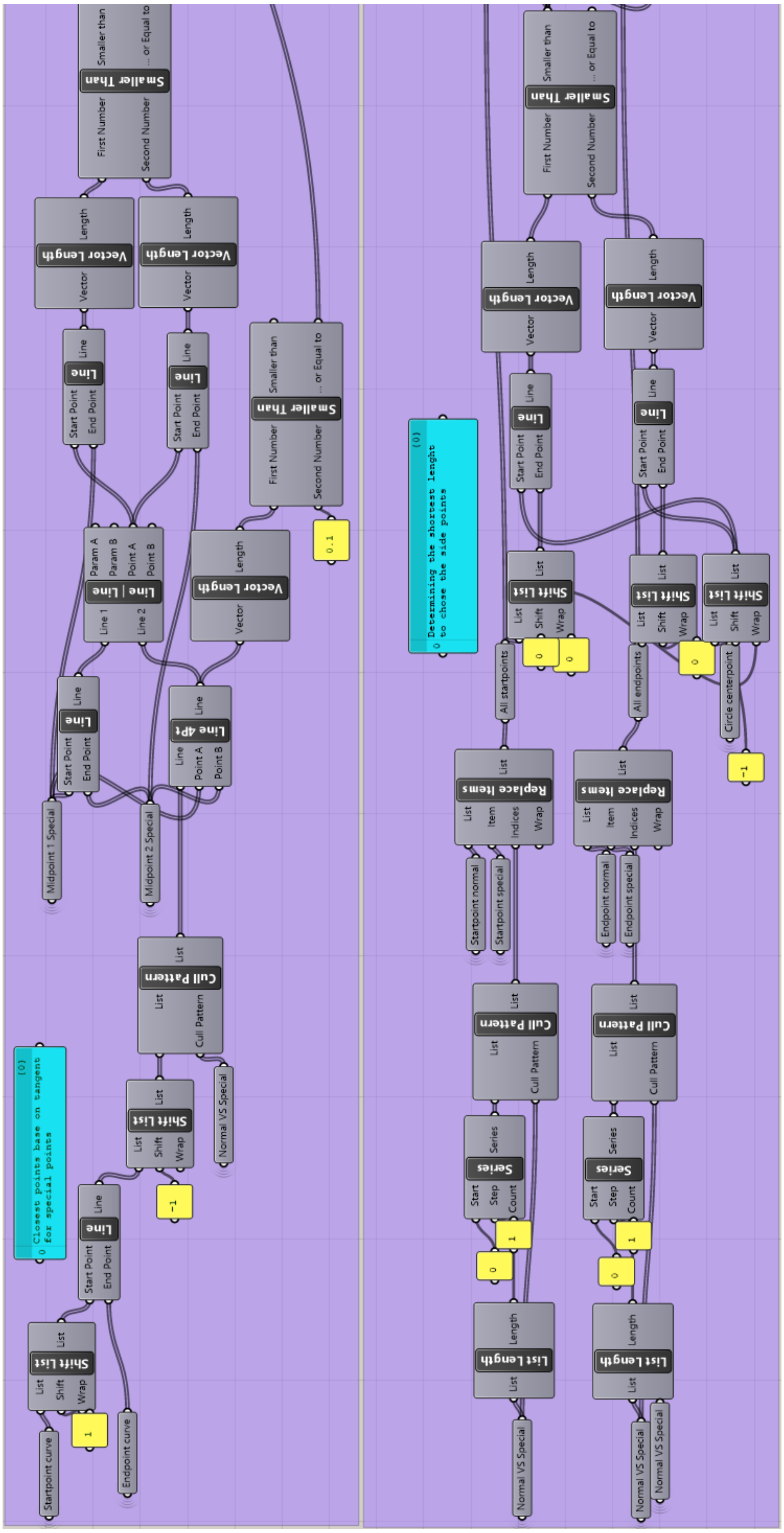

Figure B.16: Support path 5

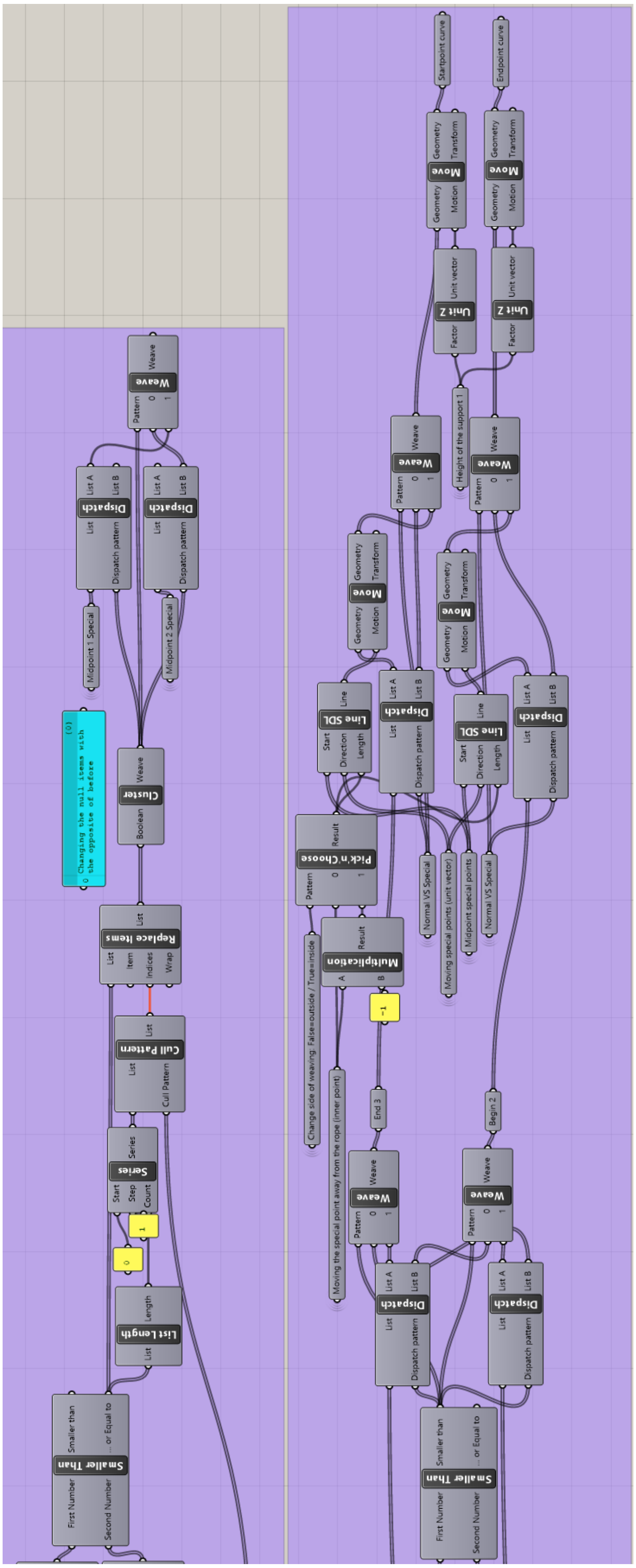

Figure B.17: Support path 6

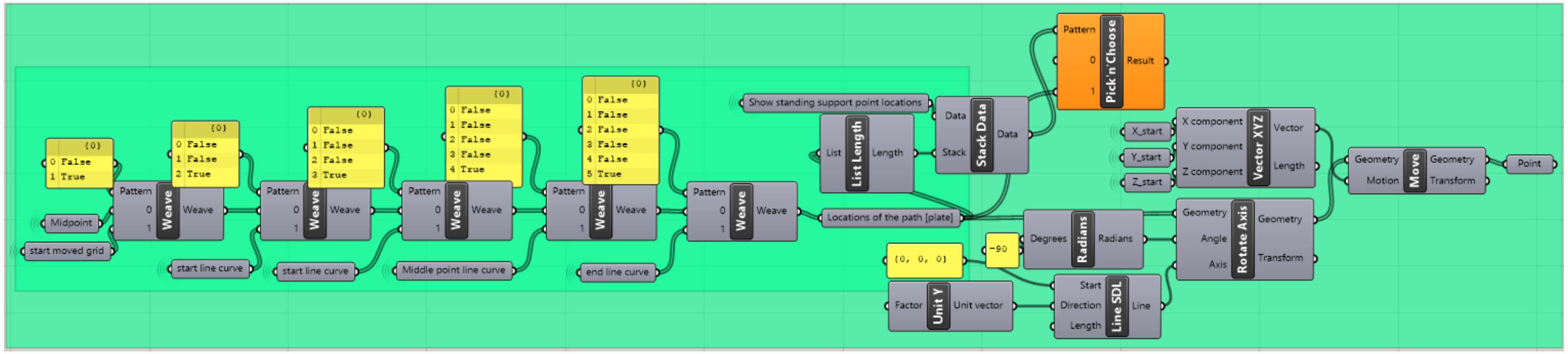

Figure B.18: Support path combining

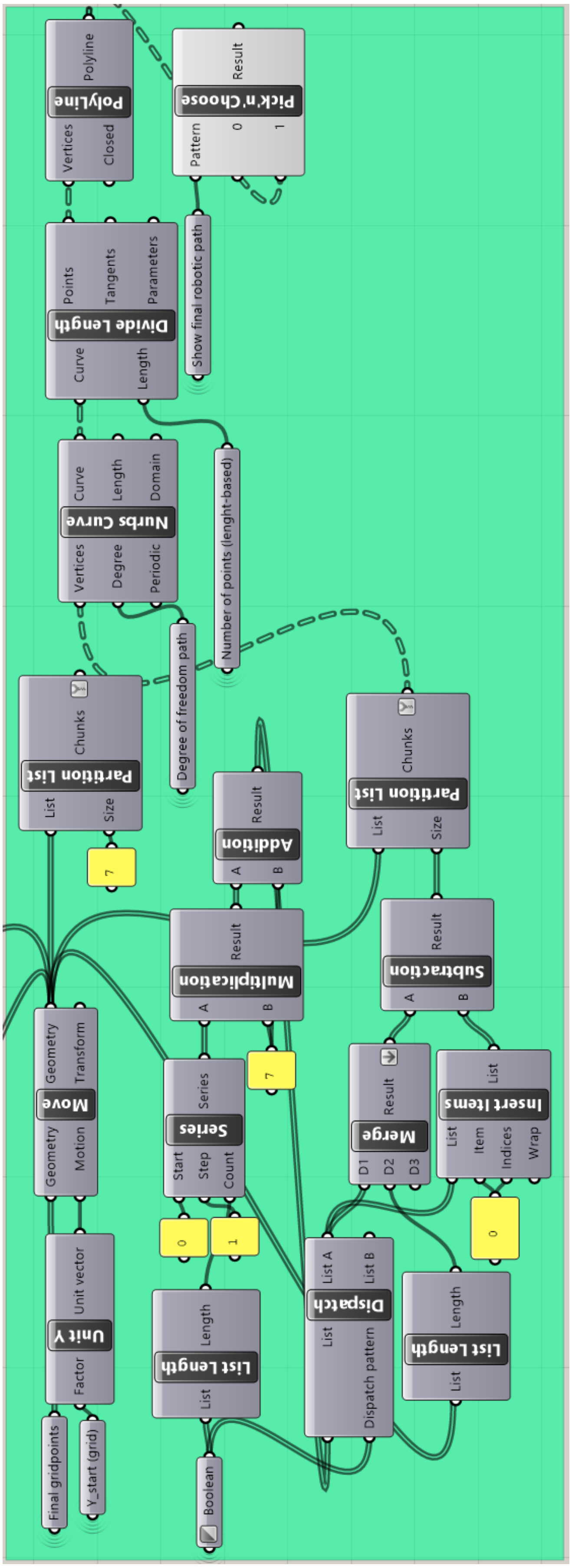

Figure B.19: Weaving the paths

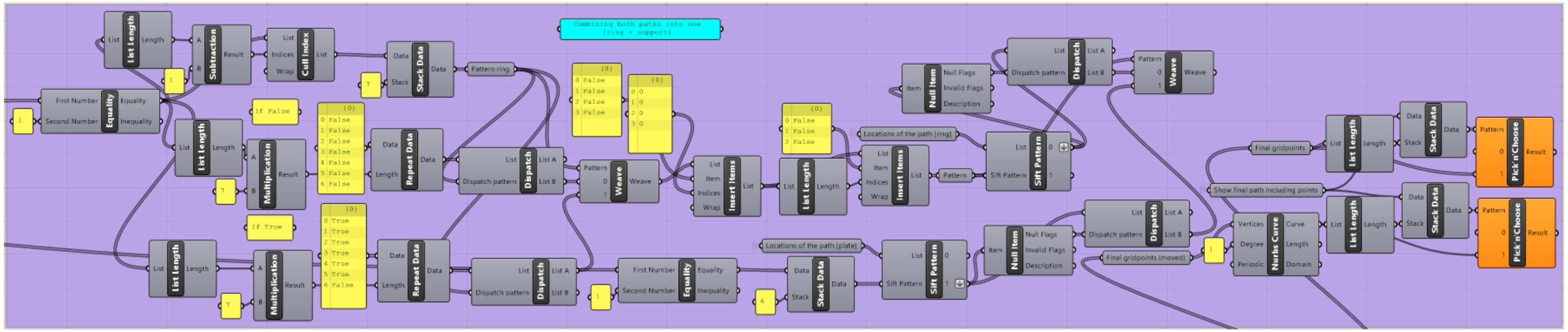

Figure B.20: Combining the paths

C

Knot Interaction Figures appendix

This appendix shows the results of all performed topology tests. The green grids are 5 by 5 centimeter and the purple circles have diameters raising by 10 centimeters. The rope is spanned according the the desired topology and these are the actual results.

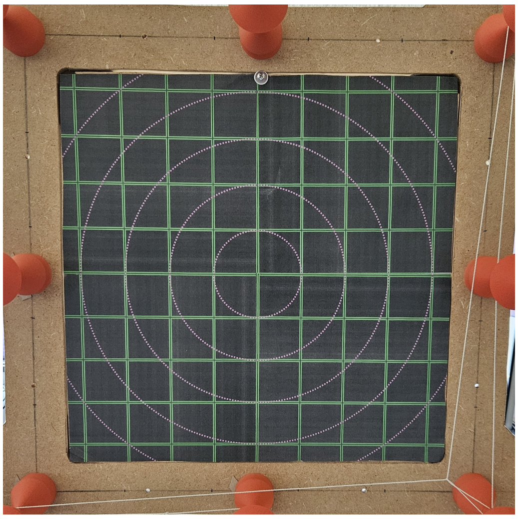

(a) Topology experiment: 1D1L

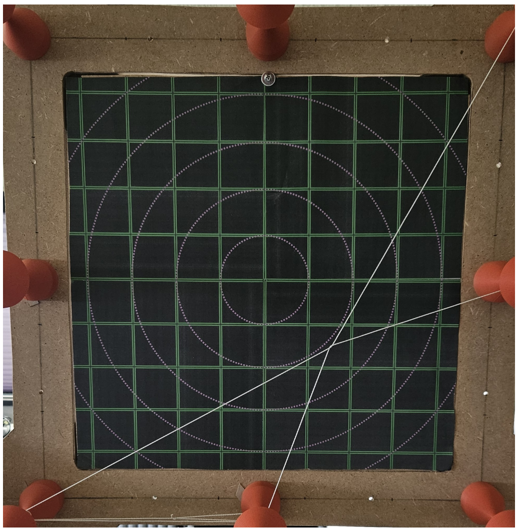

(b) Topology experiment: 1D1LA

Figure C.1: Topology experiments

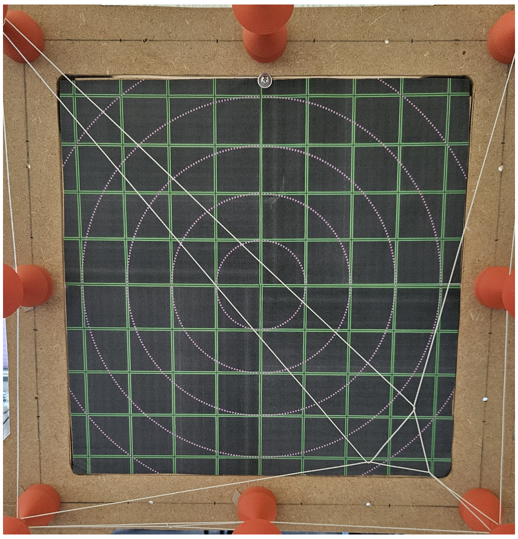

(c) Topology experiment: 1D2L

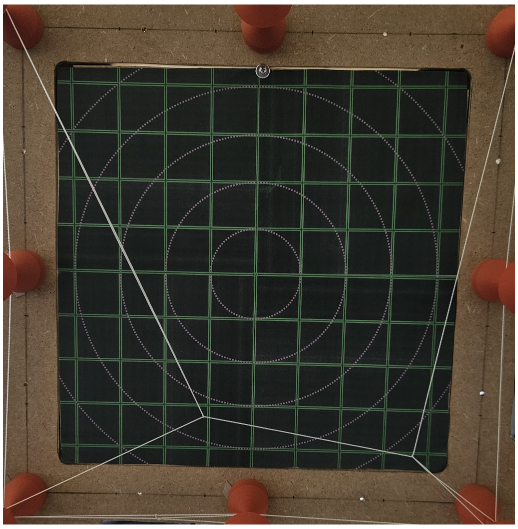

(d) Topology experiment: 1D2L.2

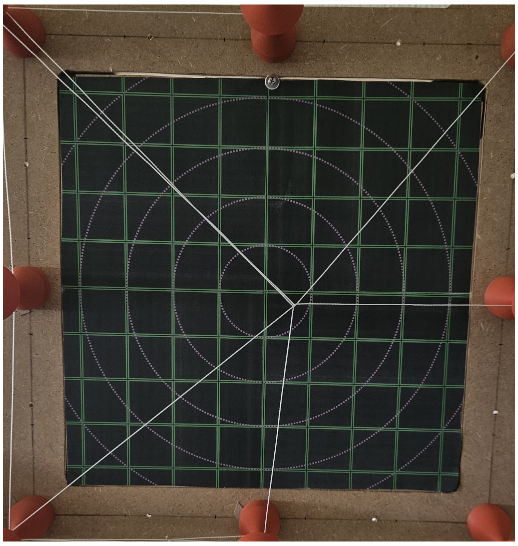

(e) Topology experiment: 1D2LA

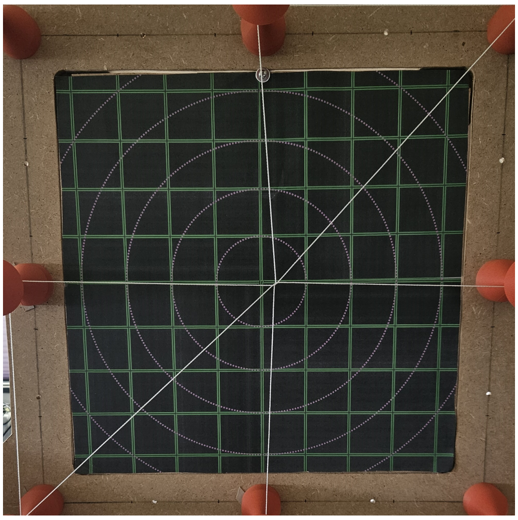

(f) Topology experiment: 1D2LA.2

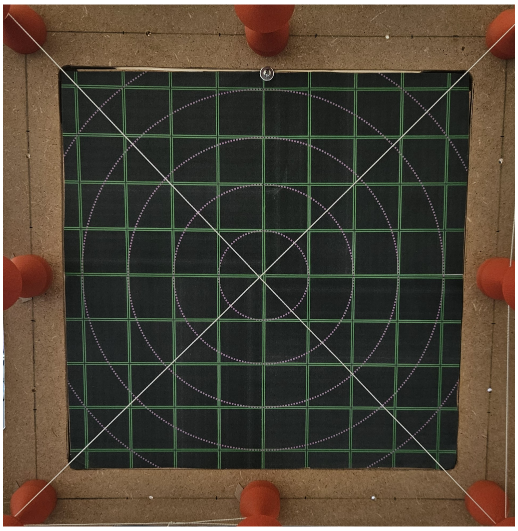

(g) Topology experiment: 2D

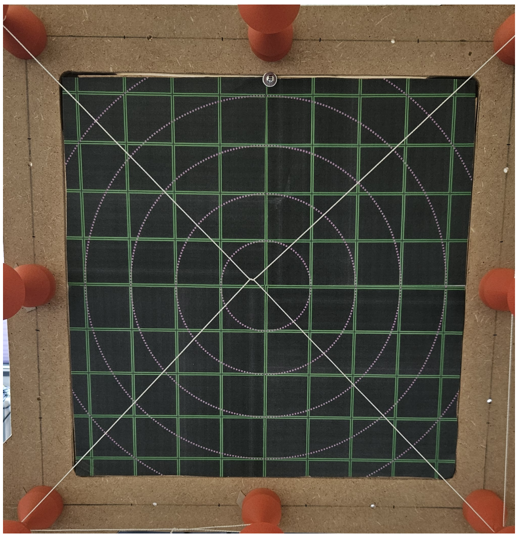

(h) Topology experiment: 2DC

Figure C.1: Topology experiments (continued)

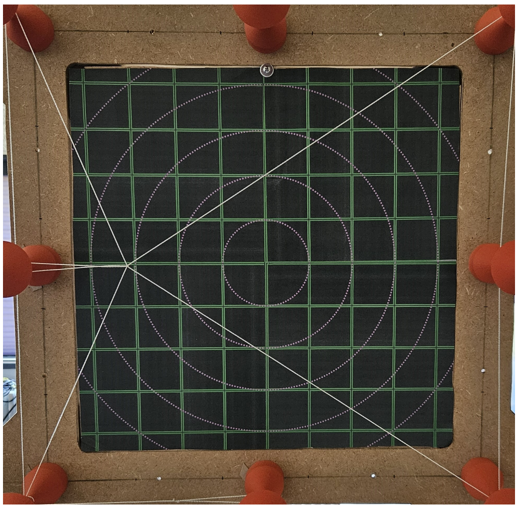

(i) Topology experiment: 2D1L

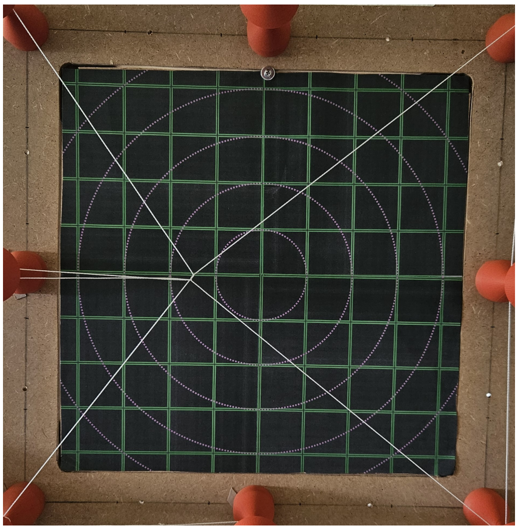

(j) Topology experiment: 2D1LC

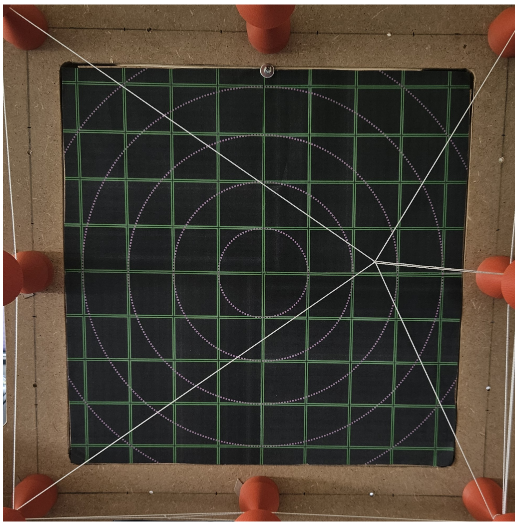

(k) Topology experiment: 2D1LM

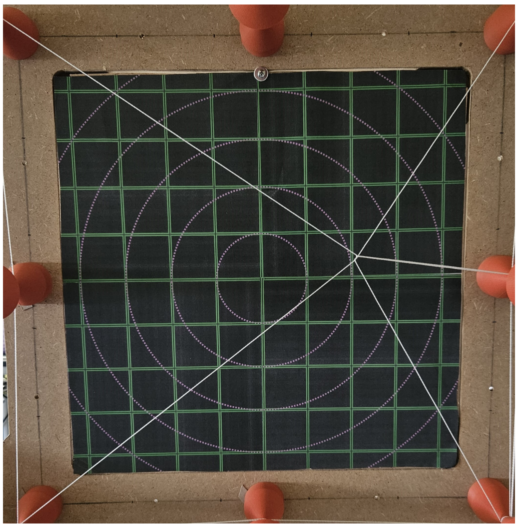

(l) Topology experiment: 2D1LCM

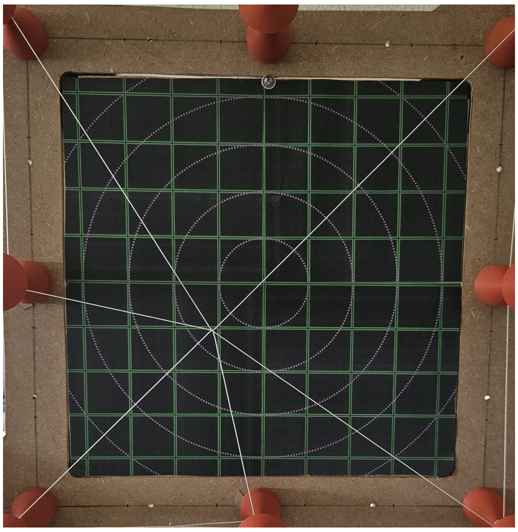

(m) Topology experiment: 2D1LA

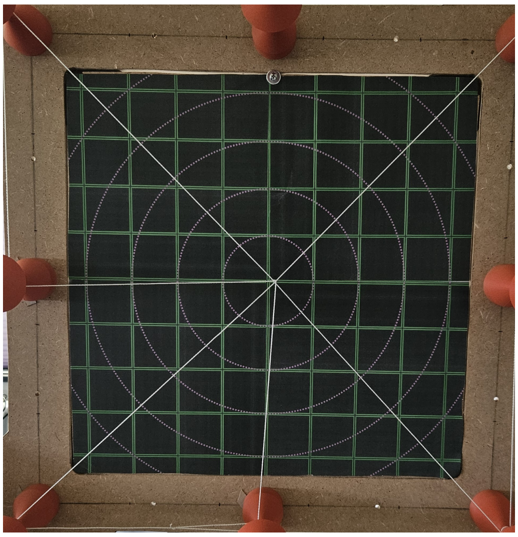

(n) Topology experiment: 2D1LCA

Figure C.1: Topology experiments (continued)

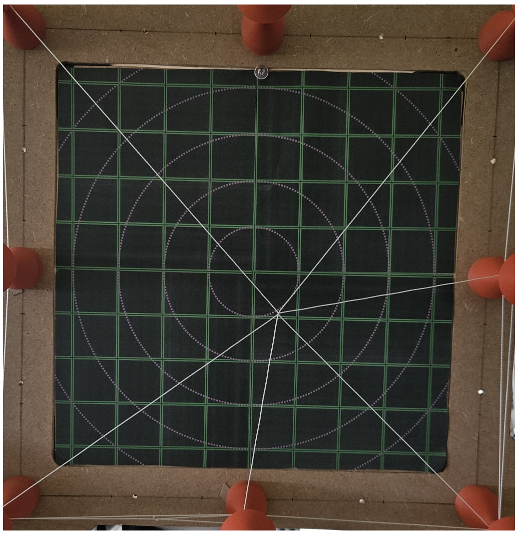

(o) Topology experiment: 2D1LMA

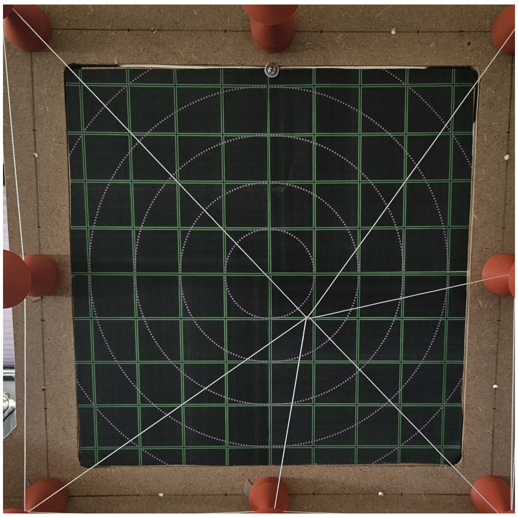

(p) Topology experiment: 2D1LCMA

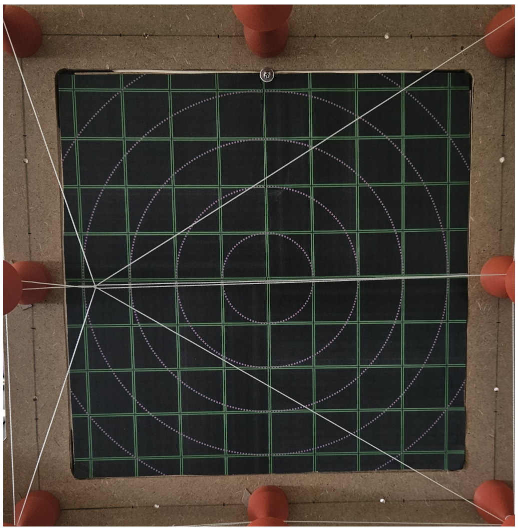

(q) Topology experiment: 2D2L

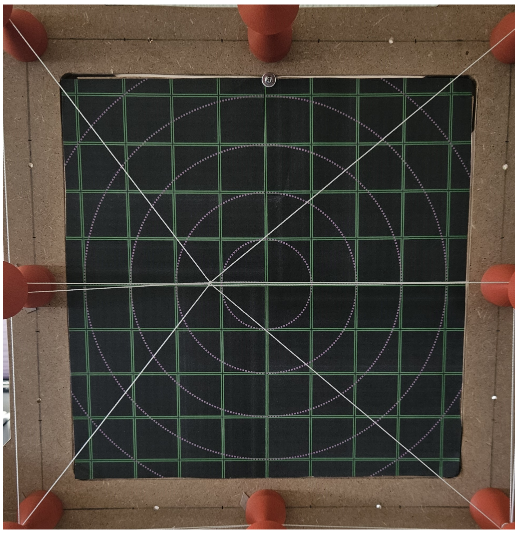

(r) Topology experiment: 2D2LC

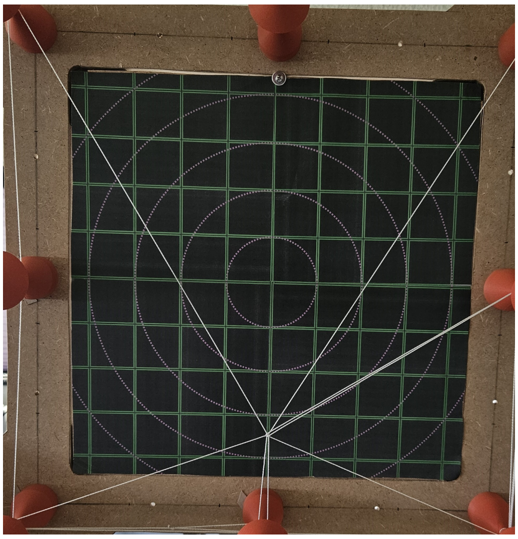

(s) Topology experiment: 2D2LM

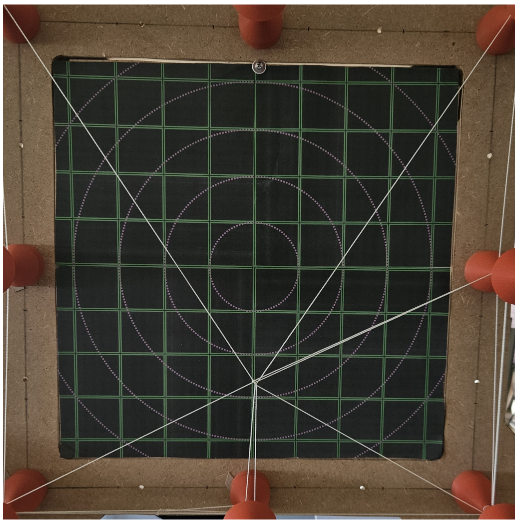

(t) Topology experiment: 2D2LCM

Figure C.1: Topology experiments (continued)

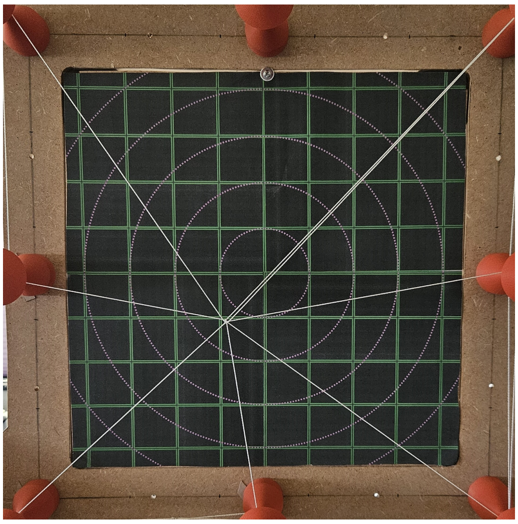

(u) Topology experiment: 2D2LA

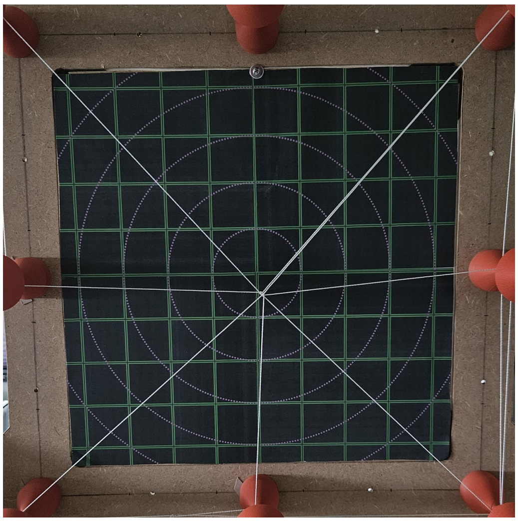

(v) Topology experiment: 2D2LCA

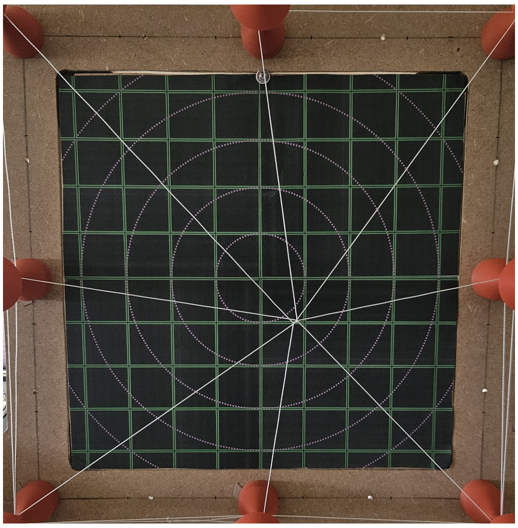

(w) Topology experiment: 2D2LMA

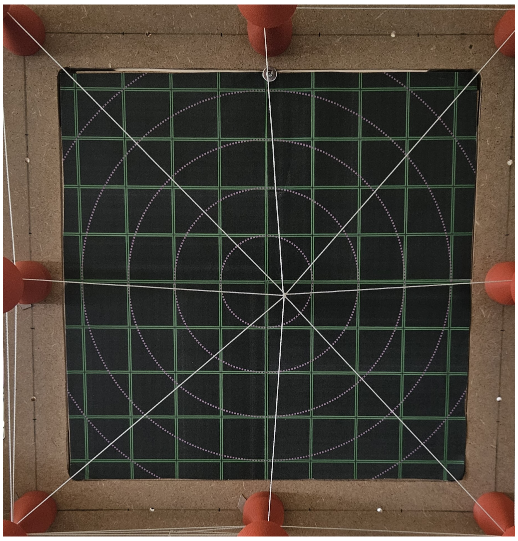

(x) Topology experiment: 2D2LCMA

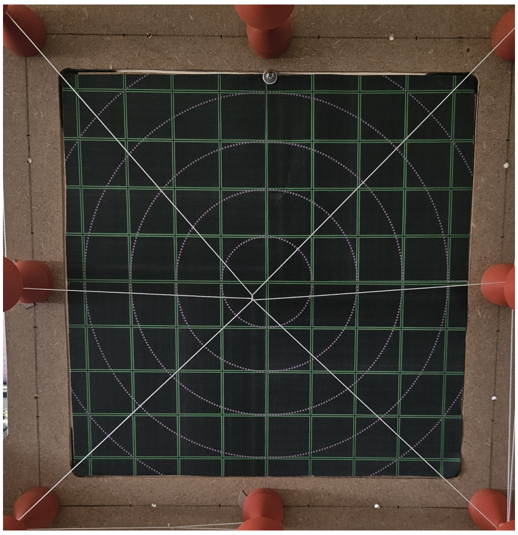

(y) Topology experiment: 3D

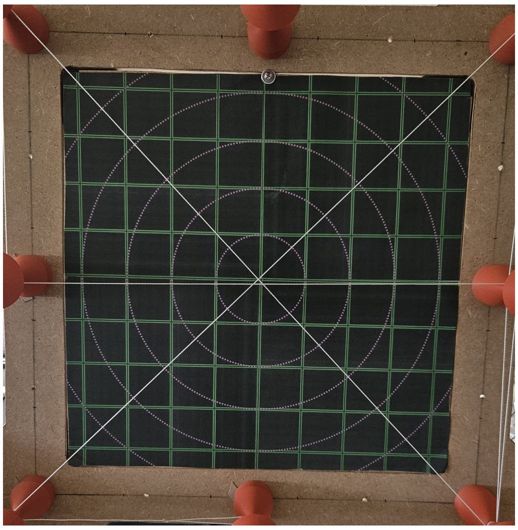

(z) Topology experiment: 3DC

Figure C.1: Topology experiments (continued)

D

Nodal displacement results

This chapter presents the results of nodal displacement for all four tests. It includes data from both the initial winding and the additional windings, which vary the number of strings across the design. All tables include the following data: each node is numbered and corresponds to a specific location as shown in Section 7.5. The horizontal deviation, vertical deviation, and vector length are given in centimetres. The relative vector is calculated by dividing the vector length by the distance between the supports.

Table D.1: Node deviation results – Experiment 1

Node	**Horizontal deviation [cm]**	**Vertical deviation [cm]**	**Vector length [cm]**	**Relative vector [-]**
1	3	1	3.2	0.13
2	0.5	1.5	1.6	0.06
3	0.5	1	1.1	0.04
4	0.5	1.5	1.6	0.06
5	1	1	1.4	0.06
Extra winding	**Horizontal deviation [cm]**	**Vertical deviation [cm]**	**Vector length [cm]**	**Relative vector [-]**
1	3	1	3.2	0.13
2	0.5	1.5	1.6	0.06
3	0.5	1	1.1	0.04
4	0.5	1.5	1.6	0.06
5	1	1	1.4	0.06

Table D.2: Node deviation results – Experiment 2

Node	Horizontal deviation [cm]	Vertical deviation [cm]	Vector length [cm]	Relative vector [-]
1	1	0	1.0	0.04
2	2	2	2.8	0.11
3	0	0.5	0.5	0.02
4	1	2	2.2	0.09
5	1	0	1.0	0.04
Extra winding	**Horizontal deviation [cm]**	**Vertical deviation [cm]**	**Vector length [cm]**	**Relative vector [-]**
1	1	0	1.0	0.04
2	2	2	2.8	0.11
3	0	0.5	0.5	0.02
4	1	1.5	1.8	0.07
5	1	0	1.0	0.04

Table D.3: Node deviation results – Experiment 3

Node	Horizontal deviation [cm]	Vertical deviation [cm]	Vector length [cm]	Relative vector [-]
1	0	0	0.0	0.00
2	1	2	2.2	0.09
3	1	1	1.4	0.06
4	0	2.5	2.5	0.10
5	2	2	2.8	0.11
Extra winding	**Horizontal deviation [cm]**	**Vertical deviation [cm]**	**Vector length [cm]**	**Relative vector [-]**
1	0	0	0.0	0.00
2	1	2	2.2	0.09
3	1.5	0.5	1.6	0.06
4	1	2.5	2.7	0.11
5	2	2.5	3.2	0.13

Table D.4: Node deviation results – Experiment 4

Node	Horizontal deviation [cm]	Vertical deviation [cm]	Vector length [cm]	Relative vector [-]
1	1	1	1.4	0.06
2	1	0	1.0	0.04
3	0.5	1	1.1	0.04
4	0.5	1.5	1.6	0.06
5	1	0	1.0	0.04
Node	**Horizontal deviation [cm]**	**Vertical deviation [cm]**	**Vector length [cm]**	**Relative vector [-]**
1	1	0	1.0	0.04
2	1	0	1.0	0.04
3	1	1.5	1.8	0.07
4	0	2	2.0	0.08
5	1	0	1.0	0.04